5-2015

Characterizing groundwater CH4 and 222Rn in relation to hydraulic fracturing and other environmental processes in Letcher County, KY

St. Thomas Majeau LeDoux
University of Tennessee - Knoxville, sledoux@vols.utk.edu

To the Graduate Council:

I am submitting herewith a thesis written by St. Thomas Majeau LeDoux entitled "Characterizing groundwater CH4 and 222Rn in relation to hydraulic fracturing and other environmental processes in Letcher County, KY." I have examined the final electronic copy of this thesis for form and content and recommend that it be accepted in partial fulfillment of the requirements for the degree of Master of Science, with a major in Geology.

Anna Szynkiewicz, Michael L. McKinney, Major Professor

We have read this thesis and recommend its acceptance:

Melanie A. Mayes

Accepted for the Council:
Carolyn R. Hodges

Vice Provost and Dean of the Graduate School

(Original signatures are on file with official student records.)

Characterizing groundwater CH_4 and ^{222}Rn in relation to hydraulic fracturing and other environmental processes in Letcher County, KY.

A Thesis Presented for the
Master of Science
Degree
The University of Tennessee, Knoxville

St. Thomas Majeau LeDoux
May 2015

ACKNOWLEDGEMENTS

Special thanks to my advisors, Drs. Anna Szynkiewicz and Michael McKinney, as well as the members of my committee, Drs. Melanie Mayes and Gray Dean for all their mentoring, guidance, and patience throughout the entirety of this project. Additional thanks to Drs. Anthony Faiia for his logistical support in the Stable Isotope Geochemistry Laboratory, as well as Dr. Annette Engel and Audrey Patterson for their logistical support in the Aqueous Environmental Geochemistry and Microbiology Laboratory, both in the EPS Dept. at UTK. Finally, I extend the utmost gratitude to the many field and laboratory assistants that worked alongside me through various portions of this project, including Justin Coleman, Andre Merino, Jessica Welch, and Caleb Smith.

Financial and material support for this project was provided by the 2014 Ralph E. Powe Junior Faculty Enhancement Award from Oak Ridge Associated Universities awarded to Drs. Anna Szynkiewicz and Melanie Mayes. Thanks to Kenneth Lowe and Alex Patton for their logistical support in the Hydrochemical Dynamics Group Laboratory of the Environmental Sciences Division at ORNL. Additional financial support was also provided by both the EPS Dept. and the Graduate Student Senate at UTK.

ABSTRACT

Hydraulic fracturing of shale deposits has greatly increased the productivity of the natural gas industry by allowing it to exploit previously inaccessible reservoirs. However, previous research has demonstrated that this practice can contaminate shallow aquifers with CH_4 [methane] from deeper formations. This study compares concentrations and isotope compositions of CH_4 sampled from domestic groundwater wells in Letcher County, Kentucky in order to characterize its occurrence and origins in relation to neighboring hydraulically fractured natural gas wells. Additionally, this study tests the reliability of ^{222}Rn [radon] as an alternative tracer to CH_4 in identifying processes of gas migration from Devonian shale. Other chemical and isotopic tracers – including isotope compositions of H_2O [water] and dissolved SO_4 [sulfate], as well as concentrations of major dissolved ions – were also compared in order to characterize groundwater in relation to other environmental processes.

Approximately half of the 59 households sampled in Letcher County showed elevated CH_4 concentrations (> 1 mg/L). CH_4 concentrations measured in groundwater ranged from < 0.05 mg/L to 10 mg/L (mean: 4.92 mg/L). $\delta^{13}C$ [delta-13 of carbon] values of CH_4 ranged from -66 ‰ [per mil] to -16 ‰ (mean: -46 ‰), and $\delta^{2}H$ [deuterium] values ranged from -286 ‰ to -86 ‰ (mean -204 ‰). The isotope composition of observed CH_4 was characteristic of an immature thermogenic or mixed biogenic/thermogenic origin, similar to that of coalbed CH_4 sampled from shallower, Pennsylvanian deposits. The occurrence of ^{222}Rn was rare, and determined not to be linked to the occurrence of CH_4. CH_4 and ^{222}Rn occurrences were not correlated with proximity to hydraulically fractured natural gas wells. Instead, CH_4 occurrence corresponded with groundwater abundant in Na^+ [sodium], Cl^- [chloride], and HCO_3^- [bicarbonate], and CH_4 concentrations were best predicted by the oxidation/reduction potential of the aquifer sampled. These results suggest that hydraulic fracturing has had a negligible impact on processes of stray gas migration in Letcher County. Furthermore, CH_4 found in shallow groundwater likely originated from shallower depositional and/or microbial processes unrelated to gas migration from Devonian shale.

TABLE OF CONTENTS

LIST OF TABLES

LIST OF FIGURES

1. INTRODUCTION

1.1. Impacts and tracers of groundwater contamination by hydraulic fracturing

Hydraulic fracturing – the process of fracturing rocks with pressurized fluid to release hydrocarbons trapped in their pore spaces – has garnered a great deal of controversy over the past decade due to its potential to impact groundwater quality. This controversy stems in part from the general lack of empirical information about these impacts. Research about the potential environmental impacts of hydraulic fracturing on the environment is still in its infancy. Nevertheless, a number of cases have been able to characterize the environmental impacts of shale gas drilling operations by at least three major mechanisms: 1) stray gas migration from hydraulically fractured wells (Jackson et al, 2013; Osborn et al, 2011, Vengosh et al, 2014), 2) improper treatment and disposal of produced wastewater from hydraulically fractured wells (Warner et al, 2013), and 3) induced seismicity from the fracturing process itself (Holland, 2011; de Pater & Baisch, 2011; Friberg et al, 2014).

Attempts to characterize the migration of stray methane (CH_4) have perhaps generated the most controversy in the literature. CH_4 in shallow groundwater can originate from multiple sources simultaneously and can be subsequently altered by a variety of processes, making its occurrence difficult to characterize. The greatest success so far in understanding stray gas migration has been accomplished by examining the stable carbon and hydrogen isotope composition ($\delta^{13}C$ and $\delta^{2}H$) of CH_4 dissolved in groundwater near hydraulically fractured wells (Osborn et al, 2011). Specifically, CH_4 from deep, thermogenic shale gas reservoirs is generally enriched in lighter ^{12}C and ^{1}H isotopes ($\delta^{13}C > -50$ ‰ VPDB, $\delta^{2}H > -175$ ‰ VSMOW), while shallower CH_4 of biogenic origin is conversely enriched in heavier ^{13}C and ^{2}H isotopes ($\delta^{13}C < -60$ ‰ VPDB, $\delta^{2}H < -175$ ‰ VSMOW) (Schoell, 1980). Furthermore, stray CH_4 from Devonian shales (the primary formations from which shale gas is extracted by hydraulic fracturing in Southern Appalachia) is accompanied by lower concentrations of noble gases (i.e., helium) and higher concentrations of higher-chain hydrocarbons (i.e., ethane, butane, etc.) (Hunt et al, 2012, Tilley et al, 2011).

Using these parameters, previous studies were able to demonstrate that in certain contexts groundwater CH_4 increases with proximity to hydraulically fractured natural gas wells, and its chemical and isotope composition is unique to Devonian shale gas (Jackson et al, 2013; Osborn et al, 2011, Vengosh et al, 2014). Conversely, these studies were also able to demonstrate that produced waters, fracturing fluids, and formation brines do not accompany stray thermogenic CH_4 in these waters. This suggests that CH_4 primarily migrates by advection to the surface via the buoyant displacement of water (a process exclusive to gases and non-aqueous phase liquids lighter than water), rather than by pressure-driven flow or molecular diffusion (processes utilized by aqueous phase liquids) (Vengosh et al, 2014). As a result, groundwater CH_4 related to stray gas migration is not correlated with concentrations of Na^{+} and Cl^{-}, or waters with distinctly brackish isotopic signatures (mean $\delta^{2}H = -41$‰ VSMOW, mean $\delta^{18}O = -5$ ‰ VSMOW) (Osborn et al, 2011).

However, relying on concentration and isotope composition of CH_4 as the primary tracers of local contamination of drinking water by hydraulic fracturing is problematic. CH_4 is often unstable in shallow, oxidizing environments, where various microbial processes are able to metabolize CH_4 as a source of carbon and oxidize it to CO_2 or HCO_3^{-} (Barker and Fritz, 1981). In addition, there are multiple sources of CH_4 in groundwater with different isotopic signatures throughout Appalachia (e.g., shale, coal, and biogenic processes), making it difficult to differentiate between various gas sources. For instance, mixed thermogenic/biogenic CH_4 is

known to occur in Pennsylvanian coal deposits (Strapoc et al, 2007), and thermogenic CH_4 has been shown to occur within shallow deposits characterized by higher abundances of Na^+ and Cl^- (> 100 mg/L), possibly due to interaction with Appalachian Basin Brine (Molofsky et al, 2011). These formation brines are thought to originate within Devonian shale, gradually diffusing upward to depths as shallow as 500 m (Dresel and Rose, 2010).

1.2. Radon as an alternative tracer to CH_4

Radon (^{222}Rn) gas is a naturally occurring radioactive material (NORM) that originates from ^{238}U decay in fractured carbonate deposits and crystalline, sialic igneous and metamorphic rocks, and specifically the Chattanooga shale Letcher County (Wood et al., 2004). Its occurrence is common throughout Appalachia, and ^{222}Rn signatures in bedrock are frequently used by oil and gas companies to identify the location of prospective shale plays in this region (Nicoll, 2012). Being carcinogenic, ^{222}Rn occurrence is of particular concern to health officials in the context of gas drilling because it is able to migrate very quickly to the ground surface from deep reservoirs and ingress into homes. This process occurs when ^{222}Rn attaches to buoyant, lighter-than-water carrier gases (e.g., CO_2) as they advect through faults and weathered fractures in bedrock (Etiope & Lombardi, 1995).

In the context of hydraulic fracturing, CH_4 may facilitate the transport of ^{222}Rn because, similar to CO_2, it readily displaces groundwater due to its buoyancy. Multiple authors have demonstrated that CH_4 can migrate to the soil surface from deep, thermogenic basins and storage reservoirs by the same mechanisms as those documented for CO_2 and Rn^{222} (Annunziatellis et al, 2008; Etiope and Martinelli, 2002; Gurevich et al, 1993). This suggests that ^{222}Rn and CH_4 may be likely to co-occur in instances of stray gas migration from shale formations undergoing hydraulic fracturing.

Given the possible co-occurrence of CH_4 and ^{222}Rn in proximity to shale gas drilling, ^{222}Rn may be a reliable alternative tracer for stray gas migration and contamination of shallow groundwater by hydraulic fracturing. Unlike CH_4, ^{222}Rn is not susceptible to alteration by oxidation or mixing with confounding sources in shallow environments (Flohr and Appelman, 1968). Additionally, because of its rapid rate of decay, the presence of ^{222}Rn can be attributed to mechanisms of rapid, continuous fluid migration from its source deposit. This is not the case with CH_4, which can linger in aquifers more or less indefinitely in the absence of oxidizing microbes (Valentine, 2002).

1.3. Goals and Hypotheses

Letcher County, Kentucky has been a hotbed of recent natural gas development in Kentucky, hosting the majority of the state's hydraulically fractured wells drilled after 1980.The major goal of this study was to investigate sources of CH_4 and ^{222}Rn in groundwater from domestic wells in Letcher County, and to determine if these gases occurred as a result of stray gas migration from hydraulically fractured natural gas wells.

If groundwater quality in Letcher County has been significantly impacted by stray gas migration due to hydraulic fracturing of Devonian shale, the following chemical processes should be observable in groundwater sampled with varying proximity to hydraulic fracturing operations:

1) Concentrations of dissolved CH_4 and ^{222}Rn in groundwater should increase with closer proximity to hydraulically fractured natural gas wells – in this case, proximity is defined as the distance (in meters) from each sample site to the nearest hydraulically fractured natural gas well.

2) The occurrence of CH_4 and ^{222}Rn should be positively correlated.
3) The C and H isotope composition of CH_4 should be characteristic of a deep, Devonian, thermogenic origin.
4) The occurrence of CH_4 and waters mixed with deeper formation brines – characterized by elevated total dissolved solids (TDS) and higher Na^+ and Cl^- concentrations – should not be positively correlated.

To investigate these hypotheses, this study measured the concentration and isotope composition of CH_4, as well as concentrations of ^{222}Rn, in groundwater throughout Letcher County. The occurrence of these tracers was subsequently characterized by their proximity to neighboring hydraulically fractured natural gas wells. Additionally, other geochemical tracers, including the composition of major dissolved ions, the sulfur (S) and oxygen (O) isotope composition of sulfate (SO_4), and the H and O isotope composition of water, were used to characterize sources of groundwater across the study area in relation to other environmental/geological processes (e.g., surface mining, water-rock interaction, etc.). For a conceptual model summarizing the geologic and environmental context of this study, as well as the potential sources and migration pathways of groundwater CH_4, ^{222}Rn, and other soluble compounds discussed in **Chapter 2**, see **Figure A.1**.

2. BACKGROUND

2.1. Mechanisms of stray CH_4 migration

Gas phase hydrocarbons that are lighter than water, buoyant, and able to accumulate in great enough density to overcome the capillary pressure of the surrounding rock matrix are predisposed to upward migration in the water table. This migration can occur in two ways: 1) diffusion through the primary porosity of the source rock, or 2) continuous-phase flow through open conduit structures, such as faults, fractures, wellbores, etc. The rate at which gases diffuse through pore spaces is generally very slow (cm per day), and is controlled by a number of factors such as permeability, capillary pressure, sorption, etc. (Gurevich et al, 1993).

Although pore space diffusion is the primary process by which all gas migration begins, the rate at which gases migrate to the surface increases by orders of magnitude upon encountering some continuous macropore structure (Gurevich et al, 1993). In the cases of dissolved gases, this phenomenon allows for the formation of larger, continuous-phase gas bodies within these larger spaces (i.e., fractures, well bores, etc.) that are able to displace water much more rapidly than similar bodies in porous media (Gurevich et al, 1993).

Within the context of hydraulic fracturing, there are essentially four types of continuous macropore structures that these gas bodies are able to use during their upward migration from shale basins: 1) the hydraulically induced fractures stemming from the wellbore, 2) the casing/annulus of the wellbore, 3) any faults intersecting the casing/annulus of the wellbore or its corresponding fractures, and 4) the wellbore itself (Gurevich et al, 1993). In their work, in which they modeled fracture dispersion during drilling, Fisher and Warpinski (2012) suggested that bedrock fractures induced hydraulically are unlikely to propagate far enough upward to reach shallow aquifers. These structures are therefore not likely a significant means by which stray gas reaches shallow groundwater. This may be different in cases where hydraulically induced fractures intersect neighboring faults or other tectonic fractures that do extend the ground surface (Gurevich et al, 1993), though the occurrence of this phenomenon is not widely documented.

Additionally, some investigators suggested that the wellbore itself is generally the most likely structure through which gas losses from oil and gas reservoirs are likely to occur (Gurevich et al, 1993; Vengosh et al, 2014). This is especially true for abandoned and compromised wells that have been improperly maintained. Weathering of the concrete annuluses encasing these wellbores creates fracturing (William Carey et al, 2010) that serves as a convenient pathway for accumulated gases to begin their escape to the surface.

These structures, however, are not similarly conductive to the rapid migration of formation brines because their dissolved, non-gaseous constituents cannot take advantage of the same physical mechanisms (i.e., buoyant advection) to assist their upward motion. Any significant upward migration of brines would have to occur as a result of direct fluid pressure induced by the fracturing process itself, or by chemical diffusion (Jackson et al, 2013; Warner et al, 2012).

2.2. Mechanisms of ^{222}Rn formation and migration

Rn^{222} is the radioactive decay product of radium (^{226}Rd), which is a prior decay product of uranium (^{238}U) formed during the deposition of marine deposits (Scott, 1994). ^{222}Rn formation is dependent on the physical migration and chemical alteration of its parent materials, ^{238}U and ^{226}Rd. Wood et al. (2004) showed that in the presence of salt water ^{238}U dissolves and eventually decays into ^{226}Rd, which then diffuses through the primary porosity of its source rock. This diffusion ceases upon encountering open fractures in bedrock or other macropore structures,

where ^{226}Rd sorbs and is incorporated into weathering products forming along the fracture surface (Etiope and Lombardi, 1995).

Once present in the fracture, dissolved ^{226}Rd dissipates within the fracture. This process creates an increasing activity gradient toward the fracture by removing dissolved radionuclides from the pore spaces adjacent to the surface of that fracture. This creates a zone within the pore space of the rock along such a fracture that is continually deficient in dissolved ^{226}Rd. As a result, radionuclides further embedded in the rock readily diffuse towards this zone in order to replace ^{226}Rd as it is lost from the system. The long half-life of ^{226}Rd (~1600 years) allows it to gradually accumulate along faults and other fractures in bedrock at concentrations well above the background level (2 to 3 ppm) of its parent material, ^{238}U (Gall et al, 1995). The precipitated ^{226}Rd eventually decays into ^{222}Rn gas, which becomes considerably more mobile in hydrological systems. Within source deposits, the concentrations of daughter-to-parent material have been shown to increase at each stage of decay from U^{238} to Rd^{226} to Rn^{222} (Scott, 1994; Wood et al., 2004); thus, the final end products of this decay cycle most commonly occur as ^{222}Rn.

Being a gas, ^{222}Rn preferentially flows through macropore structures (i.e., fractures, wellbores, etc.) with high hydraulic conductivity (Gall et al., 1995; Scott, 1994). The permeability of these fractures has been demonstrated to be multiple orders of magnitude greater than that of the corresponding matrix rock (Aydin, 2000; Gurevich et al., 1993). Additionally, there are a great number of studies correlating radionuclide presence with fault zones (Gall et al., 1995; Choubey & Ramola, 1997; Etiope & Lombardi, 1995; Cook et al., 1999; Scott, 1994). This is also true for other gases such as CO_2 and CH_4 (Etiope & Martinelli, 2002; Annunziatellis et al., 2008). In relation to groundwater quality, advecting ^{222}Rn has also been shown to infiltrate intersecting aquifers, although ^{222}Rn concentrations within these aquifers remain highest at the point of intersection with the conducting faults (Gall et al., 1995).

Nevertheless, ^{222}Rn migration does not occur by itself. ^{222}Rn has an extremely short half-life (< 4 days) and must move very quickly through hundreds to thousands of meters of overlying rock formations to reach the atmosphere before it decays. Etiope and Lombardi (1995) addressed several hypotheses for ^{222}Rn transport, suggesting that ^{222}Rn attaches to larger, lighter-than-water gas bodies such as CO_2 and CH_4 that are able to displace water in order to advect upwards to the surface (Etiope & Lombardi, 1995; Etiope & Martinelli, 2002; Annunziatellis et al., 2008). Generally, ^{222}Rn is thought to attach itself to bubbles of CO_2 moving through groundwater. These larger quantities of CO_2 gas then make their way to the surface via buoyant flow. This hypothesis is supported by positive correlations between ^{222}Rn and CO_2 degassing along fault zones (Etiope & Lombardi, 1995).

Hypothetically, ^{222}Rn should migrate the same way in the presence of CH_4 as it would in the presence of CO_2. CH_4 migration is likely to take place within the same pathways as CO_2 – pathways in which ^{222}Rn is also most likely to occur. Gurevich et al. (1993) modeled multiple mechanisms of CH_4 transport to account for the observed accumulation of volatile CH_4 in soil near oil and gas drilling sites. Their findings suggest that, similar to CO_2 and ^{222}Rn, the upward migration of CH_4 is primarily driven by preferential flow through faults and weathered fractures emanating from or intersecting hydrocarbon reservoirs.

The rate of ^{222}Rn formation may also be affected by anthropogenic activity such as hydraulic fracturing of its source deposits. It is already known that fluids produced during the fracturing process (gases, brines, fracturing fluids, etc.) contain elevated levels of naturally occurring radioactive materials (NORM), referred to by the oil and gas industry as "technologically enhanced naturally occurring radioactive materials" (TENORM, the activities

of which can range from ~ 5,000 to 16,000 pCi/L) upon retrieval from a well (Vengosh et al, 2014; Nicoll, 2012). In addition, hydraulically induced fractures in shales may actually increase radionuclide production in deep basins because they maximize the flow of fluids (and subsequently the activity of ^{238}U and ^{226}Rd) in these formations. In order to fracture a shale deposit, a well is pumped with millions of gallons of water and proppant fluid, physically breaking apart the rock to release any CH_4 trapped in its pore spaces. Generally, this proppant includes large amounts of sand (or other insoluble grains) meant to hold new fractures open during withdrawal from the reservoir. According to the mechanisms outlined by Wood et al. (2004), such processes may increase radionuclide formation and migration rates in two major ways:

1) Influx of fracturing fluid under high pressure creates new fractures in the rock, which are permanently held open by infiltrating proppant. This, in turn, increases the secondary permeability of the matrix rock and decreases the distance (and time) required for Rd^{226} to diffuse toward, precipitate into, and dissolve from the nearest fracture surface.
2) Well pumping increases the rate of fluid flow within and gas escape/removal from these formations, thereby further increasing the dissolution rates of naturally occurring gases, salts, and radionuclides within newly formed fractures.

3. GEOLOGICAL SETTING

3.1. Bedrock geology: Overview

Letcher County covers an area of 878 km^2 in the southeast corner of the state of Kentucky, and is comprised of rolling Appalachian Mountains between 360 and 670 m in elevation. This area is encompassed by the US Environmental Protection Agency's (USEPA) Eco-region 69 (Central Appalachians), subunits 69d (Dissected Appalachian Plateau) and 69e (Cumberland Mountain Thrust Block). Letcher County and nearby areas have been a hotbed of fossil fuel development for more than a century, and contain a significant portion of the state's coal and natural gas resources (unconventional shale deposits in particular).

The geology of Letcher County is uniformly composed of five major rock units: 1) the Chattanooga Shale, 2) the Pennington Formation, 3) the Lee Formation, 4) the Lower Breathitt Formation, and 5) the Middle Breathitt Formation (**Figures A.2** and **A.3**). These strata are Devonian to Pennsylvanian in age, respectively, and reflect a waxing/waning fluvial depositional history characteristic of the Appalachian basin prior to its upheaval during the Paleozoic. The distribution and composition of these formations throughout this region of Kentucky are structurally heterogeneous. Two formations, the Middle and Lower Breathitt, dominate the surface geology throughout most of Letcher County. Within these formations, all of the same rock types are present from site to site; however, the continuity, thickness, and relative proportions of these rock units differ between sites significantly. Those formations that underlie the Breathitt are only exposed along the northern base of the Pine Mountain Ridge (PMR) along Kentucky's southeastern border with Virginia.

The following descriptions of each major geologic unit were adopted from survey reports compiled by the United States Geological Survey's (USGS) Mineralogical Resources Data System (Noger, 1988).

3.1.1. Chattanooga Shale

This is the thickest and most productive formation from which unconventional shale gas is extracted in Letcher County by hydraulic fracturing and horizontal drilling. Devonian in age, this formation is less than 15 m thick at its exposure along the base of PMR, which is the only place at which it has been described in Letcher County, specifically. Other accounts of its extent and thickness from other regions have reported similar values throughout (Conant and Swanson, 1961)

The Chattanooga Shale is brownish-black to almost black and weathers yellowish gray into thin chips with planar surfaces. Bedding planes in this unit are thinly laminated and fissile. Rock fragments from this unit are fine-grained or silty and locally fossiliferous; they also contain inclusions of organic matter (~ 2 % to 12 %), and are pyritic, bituminous, and carbonaceous. Secondary minerals present in this unit include melanterite ($FeSO_4 \cdot 7H_2O$), copiapite ($Fe^{2+}Fe^{3+}_4(SO_4)_6(OH)_2 \cdot 20H_2O$), and halotrichite ($FeAl_2(SO_4)_4 \cdot 22H_2O$), which are the products of sulfide weathering.

This unit is also abundant in uranium ore (~ 0.02 %) relative to overlying formations (< 0.005 %), specifically in the form of carnotite ($K_2(UO_2)_2(VO_4) \cdot 3H_2O$) (Kaiser et al, 1983). The radioactivity of the Chattanooga Shale is considered average relative to other uranium-rich shales and other major uranium deposits across the US (Kaiser et al, 1983).

3.1.2. Pennington Formation and Newman Limestone

These two, intermixed formations are dominated primarily by limestone (75 %) and dolostone (15 %), with localized occurrences of shale (5 %) and sandstone (5 %). Together, these two units represent the Mississippian following the deposition of previous Devonian shale. Their thickness ranges from 50 to 200 m along PMR.

Limestone units are argillaceous and locally dolomitic. Their color is medium- to dark-gray and they weather yellowish brown. These strata are medium- to micro-grained, fossiliferous, and occur in discontinuous lenses as much as 5 m thick in the middle and lower parts of this unit. These strata also intergrade with overlying shale beds.

Siltstone and shale units are interbedded and integraded with sandstone. Both units can be greenish gray, reddish brown, or dark gray in color. Red and green shales commonly occur with siltstone and sandstone in the upper and lower parts of the Pennington Formation. Both siltstone and shale units can locally contain several thin coal beds in their uppermost and lowermost parts.

Sandstone units are usually silty, fine- to medium-grained, and slightly micaceous. They are light- to medium-gray or olive-gray to yellowish-brown in color. Strata in these units are commonly ripple-bedded, locally crossbedded, and intergrade with siltstones and shales eastward.

3.1.3. Lee Formation

Mississippian to Pennsylvanian in age, the Lee Formation is composed of mixed conglomerate (35 %), sandstone (30 %), siltstone (25 %), shale (10 %), and coal (< 1 %). Its thickness varies from 260 to 610 m where it is exposed at the surface along PMR. The Lee Formation and its underlying formations (the Pennington Formation and the Chattanooga Shale) are poorly exposed on the surface. The descriptions of rock types in these units, therefore, vary depending on the outcrop exposure from which they were derived.

The conglomerate units of the Lee Formation are angular to sub-rounded fragments of firmly cemented, iron-stained shale and siltstone. These conglomerates occur at the base of cross-bedded sandstones.

Sandstone units are quartzose, locally argillaceous and micaceous, and commonly conglomeratic with quartz pebbles. These units are white- to light-gray in color, fine- to coarse-grained, and cross-bedded.

Siltstone and shale units are medium- to dark-gray, micaceous, and carbonaceous, although outcrops of these rock types are often poorly exposed on the surface.

Coal units of the Lee Formation, though poorly prospected, are underlain by interstratified clay-rich shale and siltstone. They commonly contain plant fragments and siderite concretions, and can be as thick as 10 m in the upper part of the unit.

3.1.4. Lower Breathitt Formation

The Lower Breathitt is also Pennsylvanian in age, ranging from 680 to 800 m in thickness on the south side of Letcher County, and ~500 m thick or more on the north side of the county. The interbedded strata of this unit are dominated by shale (45 %) and siltstone (40 %), with occasional occurrences of sandstone (15 %), coal (5 %), and conglomerate (< 1 %).

Sandstone units are light- to medium-gray, very fine to fine-grained, locally coarse-grained, and calcareous. Similar to the Middle Breathitt Formation, these sandstones are intergraded with siltstone and shale, and locally contain abundant carbonaceous plant fragments.

Siltstone and shale units are medium-dark to dark-gray in color and are locally interbedded with sandstone in the middle and lower parts of each unit. Sideritic nodules and abundant carbonaceous plant fossils are also common in these siltstones.

Together with the Middle Breathitt, the Lower Breathitt is the other major surface unit from which coal is extracted in Letcher County. The lowermost coal unit of the Lower Breathitt is continuous throughout most of Letcher County, ranging in thickness from 1 to 20 m. This unit is underlain by sandstone. The uppermost coal bed in this formation, however, is discontinuous, similar to the coal beds of the overlying Middle Breathitt Formation.

3.1.5. Middle Breathitt Formation

The Middle Breathitt is the youngest strata in the area. It is Pennsylvanian in age and occurs at the uppermost elevations in the county. This formation ranges from ~350 m in thickness at the southernmost part of Letcher County along PMR to anywhere from 0 to 200 m at the northern border of the county. It is composed of alternating cross-beds of sandstone (40 %), shale (35 %), siltstone (15 %), coal (10 %), and limestone (5 %). The Middle Breathitt is the most prevalent unit into which groundwater wells are drilled throughout the county. This is also one of the two primary units from which coal is currently extracted via surface mining.

Sandstone units in Breathitt Formation are fine- to medium-grained. They weather to yellowish gray and are locally micaceous and lenticular. The bedding planes of this unit are generally interstratified with siltstone and shale. Stream channel fills located at the formation's base are composed of coarse grained and cross-bedded sandstone.

Shale units are light to medium-gray, weather to dark greenish gray and light brown, and are carbonaceous in intervals of 1 to 5 m. Some surface outcrops contain plant and invertebrate fossils between bedding planes. These outcrops are subjected to weathering and, thus, poorly exposed.

Siltstone units are medium- to dark-gray, weather to yellowish orange to yellowish brown, and are generally thinly or ripple-laminated. In surface outcrops, siltstone strata are locally interbedded with sandstone and shale.

Coal units of the Middle Breathitt Formation are separated into three discontinuous beds of variable thickness. These beds are interstratified with thin beds of sandstone and carbonaceous shale, and various strata contain sideritic nodules and limestone concretions.

3.1.6. Pine Mountain Thrust Fault

The southern border of Letcher County runs adjacent to the Pine Mountain thrust fault (PMTF), which is located along the crest of PMR (**Figures A.1** and **A.2**). Both features are part of the larger Cumberland Overthrust Block (McGrain, 1983) and were formed as a result of mountain building during the Alleghanian Orogeny (Chestnut et al, 1998). The PMTF is bounded to southwest by the Jacksboro fault and to the northeast by the Russel Fork fault. The PMTF is the westernmost major thrust in the Appalachian thrust belt system separating the Valley and Ridge and the Appalachian plateau provinces (Mitra, 1988). Across most of its aerial extent, the PMTF is a bedding plane fault, dipping to the southeast (Miller, 1973). The underlying strata exposed by this fault are located along the northern side of PMR. This means that along a transect beginning at the top of PMR and moving downward in elevation towards the northwest, the previously defined strata (i.e., the Breathitt, Lee, and Pennington Formations and the Chattanooga Shale) occur from top to bottom (i.e., Pennsylvanian Sandstone at the top of the ridge to Mississippian limestone at the middle to Devonian shale at the base of the ridge.

Additionally, in which strata north of the PMTF dip underneath, the Chattanooga Shale is in direct contact with various portions of the Breathitt Formation along the northern margin of the fault. This creates a setting in which formation brines, dissolved gases, or other contaminants from the Chattanooga Shale may be able to directly migrate northward into younger, shallower formations, independent of (or possibly worsened by) hydraulic fracturing practices.

3.1.7. Hydrogeology

Letcher County is divided between the greater Kentucky River and Upper Cumberland River watersheds. The headwaters of these rivers are located in the northeastern side of the county, receiving nearly 115 cm (~100 million m^3) of precipitation per year (Kentucky Mesonet, 2014). Runoff and stream flows are highest in early spring and lowest in early autumn (NWIS, 2014). The USGS classifies stream discharge and groundwater flux for this area as normal (i.e., not excessively high or low) relative to neighboring watersheds (NWIS, 2014). The geologic and topographic heterogeneity of the area's mountainous terrain dictates the depth of the water table, which can be extremely variable within a few square kilometers, ranging from less than 10 m near streambeds to as high as 500 m atop nearby ridges.

Major aquifers are primarily composed of sandstone at depths of anywhere from 10 to 100 m within the Lower Breathitt Formation. These aquifers are usually less than 10 m in thickness and are horizontally discontinuous. The hydraulic conductivity of these aquifers is variable within several orders of magnitude, ranging from 1×10^{-7} ft/min to 1×10^{-3} ft/min in more fractured bedrock (Minns, 1993). Groundwater flow within this region is differentiated between two primary zones. The first zone exists from depths of 0 m to 20 m, is composed of more heavily fractured bedrock, and has generally high hydraulic conductivity. Flow direction within this shallow fracture zone has been shown to mirror topography towards first order streams (Minns, 1993). The second zone exists at depths below 20 m, is considerably less fractured, and has generally lower hydraulic conductivity. At these depths, groundwater flow is instead directed towards third order streams.

Alternatively, groundwater chemistry in Letcher County can also differentiated between two zones existing above and below the Magoffin Member of the Breathitt Formation (Minns, 1993). Above the Magoffin Member, water chemistry has been previously characterized as being abundant in Ca^{2+}, Mg^{2+}, HCO_3^-, and SO_4^{2-}. Below the Magoffin Member, water chemistry has been previously characterized as being abundant in Na^+, Cl^-, and HCO_3^-, and deficient in Ca^{2+} and Mg^{2+} (Wunsch, 1992).

Domestic wells drilled into either hydraulic/chemical zone commonly intersect multiple conducting strata to increase their longevity, often passing through adjacent coal and shale seams, uncased (KGS, 2014). While most wells remain hydrologically active throughout the year, some shallower wells < 15 m deep become seasonally dry during periods of summer drought, based on anecdotal reports from residents in this area.

3.2 Water quality in Letcher County

Access to municipal water is rather sparse across the county. The only municipal water provider in the county, the Letcher County Water and Sewer District, serves approximately 2,600 households (Lewis, 2013). The majority of wastewater is treated by individual, private septic systems, or in some cases wastewater is piped directly into local streams. Few houses outside the immediate vicinity of urban centers, such as the towns of Whitesburg and Fleming-Neon, have access to municipal water and sewer services. However, the number of homes serviced by the Letcher County Water and Sewer District has greatly increased over the past decade, primarily to

mitigate the negative impacts from surface coal mining and inadequately maintained septic systems in the eastern half of the county (Lewis, 2013). The two most prevalent surface water contaminants across the county are *E. coli* and silt (Ormsbee & Zechman, 2001).

The majority of people surveyed for this project – both those served by the county water district and those with private wells – reported a heavy reliance on bottled water for drinking, citing poor taste, discoloration, and health concerns as reasons for avoiding the consumption of household groundwater. This factor likely reduces residents' exposure to waterborne contaminants via direct consumption. However, it does not preclude them from ambient exposure to dissolved gases in air (e.g., radon degassing from a house's plumbing, underlying soil, etc.) or from direct physical contact with contaminants capable of entering the body through dermal adsorption (e.g., from showering, washing clothes, etc.). Additionally, some households with access to municipal water services still use private wells for other needs such as cooking, washing clothes, showering, and flushing toilets. In these cases, residents may still be significantly exposed to groundwater-borne contaminants.

There are a number of geologic and anthropogenic processes affecting water quality in Letcher County, mostly tied to processes of fossil fuel extraction (e.g., coal mining, gas and oil drilling, etc.). Coal mining, in particular, has a long documented history of impacting surface and groundwater quality in this area as a result of acid mine drainage (e.g., stream acidification) from sulfide oxidation of excavated coal beds (Carey et al, 1993). The negative effects of oil and gas drilling on groundwater quality in Letcher County are not yet well understood. Prior to the widespread implementation of hydraulic fracturing in Letcher County, most documented complaints were in response to isolated instances of hydrocarbon combustion or dissolved gases leaking into groundwater from faulty or compromised gas wells and pipelines, and were not common (Carey et al, 1993).

3.3. Natural gas drilling in Letcher County

This study is geographically distinct from its predecessors in that it is the first comprehensive, public investigation of the environmental impacts of hydraulic fracturing in Southern Appalachia. Most previous work on hydraulic fracturing and its effects on water quality has been done in the northeastern US, focusing exclusively on the more northern Marcellus Shale. However, the more southern Chattanooga Shale is unique since it resides at shallower depths (~1000 to 1500 m; KGS 2014) compared to its northern counterpart Marcellus Shale (depth ~2000 to 3000 m; Jackson et al, 2013). Due to the excessive depth and overbearing weight of the Marcellus shale, immense amounts of fresh water have to be pumped under high pressure into these deposits in order for them to successfully fracture and produce. Conversely, the shallower Chattanooga Shale requires far less pressure to be fractured, and so nitrogen foam is alternatively used to induce hydraulic fracturing. This latter process is less hydraulically intensive and generates considerably less wastewater.

Similar to other fracturing fluid mixtures, the specific chemical content of nitrogen foam is largely proprietary, unregulated, and unknown to the public. As a result, little is known about how this process may affect water quality because previous studies pertain only to traditional, freshwater fracturing of deeper reservoirs. By focusing on the Chattanooga Shale, this study seeks to contribute information from a new study area to the existing body of research about hydraulic fracturing, providing a much needed point of comparison between different regional, technical, and commercial contexts in which this process is taking place.

Aside from hydraulic fracturing, conventional (i.e., non-fractured, vertical) oil and gas drilling is also ubiquitous throughout eastern Kentucky, with over 165,000 wells drilled across

the state since 1900 (Nuttall, 2013). Hydraulic fracturing is not new to this region, even in the context of conventional drilling, because oil and gas companies have been utilizing hydraulic fracturing to increase production in conventional deposits more or less ubiquitously since the onset of the 1980's (KGS, 2014). These same companies also began vertical fracturing of more unconventional deposits (i.e., the Chattanooga Shale) as early as 1990.

Horizontal (or "deviated" as it is referred to by KGS, 2014) drilling/fracturing was not introduced to Letcher County until 2006, and has been more or less dominated by a single contractor, EQT Corporation (Nuttall, 2013). Between 2006 and 2012, EQT permitted and drilled nearly 1,400 horizontal shale gas wells across Kentucky, producing more than 2.8 billion m^3 of natural gas in Letcher County since 2002. For a map illustrating all of the hydraulic fracturing activity in Letcher County, see **Figure A.4**.

3.4. Coal mining in Letcher County, KY

Over the past century, the more dominant form of resource extraction in Letcher County has been coal mining, taking place throughout Appalachia since the late 1800's. In total, Letcher County has been the third most productive mining county in Kentucky, producing more than 500 million tons of coal throughout its history (Carey et al, 2009).

The coal industry in Kentucky saw most of its growth between about 1930 to 1960. However, this industry's productivity has been on the decline since about 1980. Surface mining began as early as 1940 and had become the most prevalent means of coal mining in Kentucky by 1970 (Carey et al, 2009). In comparison to the natural gas industry, ~120 million tons (2.21×10^{11} kWh) of coal were extracted from Kentucky in 2006, compared to ~5 million tons (~ 50 million barrels, or 2.67×10^{10} kWh) of natural gas in 2009 (Nuttall, 2013). For a map illustrating all of the surface mining activity in Letcher County, see **Figure A.5**.

There are a number of ways that surface mining can affect shallow groundwater. For instance, bedrock excavation oxidizes pyrite and other metal-sulfides present in coal and its adjacent strata. This process releases sulfate (SO_4), iron (Fe^{2+}), and hydrogen (H) ions and significantly lowers the pH of water discharging from mining sites (Blodau, 2006). Therefore, drastic decreases in pH are commonly observed in surface water receiving untreated discharge from coal mine sites. Nevertheless, underlying aquifers with high limestone ($CaCO_3$) or dolostone ($CaMg(CO_3)_2$) contents are less vulnerable to acid mine drainage due to the high degree of buffering controlled by the dissolution of these carbonate minerals (Blodau, 2006). Very often, $CaCO_3$ is added to the internment ponds of coal mines to buffer the pH of acid mine drainage.

Even when buffered by carbonates, both surface water and shallow aquifers are vulnerable to intrusion by dissolved sulfate SO_4^{2-} and Fe^{2+} from pyrite oxidation. While not toxic, these contaminants can render groundwater unusable for most domestic purposes. For example, when affected waters are pumped to the surface and exposed to the atmosphere, the oxidation of dissolved Fe^{2+} to Fe^{3+} in groundwater causes the precipitation of iron-oxide (rust, Fe_2O_3) (Blodau, 2006). This Fe-rich water is noticeably discolored and turbid, with an unpleasant taste – commonly described as metallic, rusty, or blood-like. Additionally, dissolved SO_4^{2-} that has leached into more anoxic waters with high organic matter (or any source of carbon that can behave as an electron donor) is readily reduced to hydrogen sulfide (H_2S) gas by microbial processes (Blodau, 2006). Aside from having a characteristically unpleasant, egg-like odor, H_2S is also toxic to most aquatic life, and can be dangerous to people in elevated concentrations (Beauchamp et al, 1984).

Because coal mining has the potential to oxidize shallow groundwater, it also has the

potential to obfuscate the observable impacts of stray gas migration by rendering aquifers unstable with respect to CH_4. That is, CH_4 is more likely to oxidize (and be removed from the system as either HCO_3^- or CO_2) under more oxic conditions (E_H > -150 mV) (Head et al, 2003). While the effects of coal mining on the occurrence of ^{222}Rn are not well understood, ^{238}U does occur in trace amounts in coal (Kolker and Finkelman, 1998). U-bearing minerals in coal may also be soluble under acidic conditions (Quispe et al, 2011). Mine sites demonstrating especially heavy amounts of oxidation and subsequent acidification may, therefore, be more likely to affect neighboring aquifers with elevated ^{222}Rn produced from dissolved ^{238}U. In these cases, though, ^{222}Rn is likely to migrate by different mechanisms and pathways than ^{222}Rn produced at greater depths, and so the probability of its occurrence correlating with that of CO_2, CH_4, or faults is uncertain.

3.5. Summary

Though geologically uniform at a broad scale, the bedrock composition and hydrogeology of Letcher County is a considerably heterogeneous at the local level. Furthermore, the region's long history of fossil fuel extraction and drastic anthropogenic alternation of the landscape has created a scenario in which groundwater quality may be impacted simultaneously or in succession by multiple, confounding processes. This is made worse by the region's widespread shortcomings in terms of public water infrastructure and civic planning. To account for and make sense of any potential, conflicting interactions among various geologic and anthropogenic processes in this study area, it was therefore necessary to collect a large variety of chemical, isotope, and spatial information. In additional to investigating the occurrence of stray gas migration with proximity to hydraulic fracturing, this supplemental information made it possible to more thoroughly characterize groundwater types, origins, and subsequent processes of physical, chemical, and microbial alteration.

4. METHODS

4.1. Field protocols

4.1.1. Selection of sampling sites

Groundwater samples were collected from domestic wells at consenting households across Letcher County. Based on anecdotal reports from homeowners, most of these wells were drilled into the Lower Breathitt Formation at depths ranging from ~ 10 m to 100 m, intersecting multiple layers of siltstone, shale, sandstone, and coal where they are uncased. Water sampling took place at regular, bi-weekly intervals over two seasons (winter and summer, 2014), alternating between areas of high and low natural gas drilling density. Each sampling period involved choosing a roadway in either a high or low density area and collecting groundwater from the domestic wells along that roadway (estimated 10 to 20 households per sampling period). Twenty samples were collected between January 18 and March 1 of 2014, and an additional 40 samples were collected between June 10 and August 1 of 2014.

4.1.2. Field measurements

At each household, groundwater was sampled directly from an outside faucet upstream of any filtration system using methods adopted from Jackson et al (2013). A hose was connected to the faucet and run into a 3 gallon bucket. Water was then continuously drained into the bucket at low flow to avoid turbulence and degassing within the bucket. Each well was flushed for 10 minutes until temperature, pH, TDS, dissolved oxygen (DO), and oxidation/reduction potential (ORP) were stable. These parameters were measured using a YSI 556 Multiparameter System. Additionally, dissolved Fe^{2+}, total Fe, nitrate (NO_3^-), (SO_4^{2-}), and sulfide (S^{2-}) concentrations were measured in situ using a Hach DR900 Multiparameter Colorimeter. The concentration of dissolved bicarbonate (HCO_3^-) was measured in situ using a LaMotte field titration kit. Finally, GPS data for each sample site was collected for later spatial analysis.

Samples taken for additional chemical and isotope analyses were bottled in separate containers according to the specifications of each analytical method (see **Chapters 4.1.3** through **4.1.7** for details). All samples were kept on ice during transit, and afterward stored at 4ºC in the laboratory.

4.1.3. Dissolved cations/anions in groundwater

Ions were sampled using methods adopted from Szynkiewicz et al (2012). For cations, 60 mL of water was drawn from the sample bucket into a syringe and ejected through a 0.45 μm nylon filter into a 60 mL plastic bottle. Afterward, each sample was acidified to a pH < 2 using 40 % weight/volume (w/v) HNO_3 to prevent precipitation and adsorption of metals inside the bottle. Anions were separately bottled in the same manner as cations, but were not acidified for storage. Both sets of samples were analyzed within 6 months of collection (see **Chapter 4.2.1**).

4.1.4. Dissolved ^{222}Rn in groundwater

^{222}Rn was sampled for analysis of bulk concentration by liquid scintillation counting (LSC) using methods adopted from Passo and Cook (1994). A syringe was submerged into the collection bucket and 20 mL of water were slowly withdrawn from the bottom of the bucket to avoid degassing inside the syringe. Afterward, the water from the syringe was ejected into a 25 mL glass scintillation vial containing 15 mL of Perkin Elmer High Efficiency Mineral Oil Scintillator. The water was injected underneath the mineral oil (to avoid degassing of ^{222}Rn) until

the vial was full with about 10 mL of groundwater sample under 15 mL of mineral oil. Once full, the vial was capped without headspace using an aluminum-lined plastic screw cap and agitated by shaking to facilitate degassing of ^{222}Rn into the less-dense scintillation fluid. Vials were kept in the dark in the field cooler for 24 hours prior to storage in the laboratory. Concentrations were analyzed within 3 days of collection (see **Chapter 4.2.2**).

4.1.5. Dissolved CH_4 in groundwater

Groundwater samples were collected for analyses of bulk concentration and the C and H isotope composition of CH_4 using methods adopted from Kampbell and Vandergrift (1998) and Yarnes (2013), respectively. For bulk concentration, a 60 mL glass bottle was plugged with a butyl rubber cap, crimp-sealed, and evacuated in the laboratory using a KNF vacuum pump. In the field, a syringe was submerged into the collection bucket and 60 mL of water were slowly withdrawn from the bottom of the bucket to avoid degassing inside the syringe. The sampled groundwater was then inserted into the evacuated bottle through the rubber cap via a needle, drawing water out of the syringe until the bottle reached equilibrium with the atmosphere outside the bottle. At this point, water ceased to exit the syringe and the needle was removed from the bottle. Afterward, the bottle was placed upside down to avoid CH_4 escape through the rubber septum and CH_4 was allowed to degas into the remaining headspace. CH_4 concentrations were analyzed within 14 days of collection (see **Chapter 4.2.3**).

Separate groundwater samples were collected for analysis of C and H isotope composition of CH_4 ($\delta^{13}C$ and $\delta^{2}H$, respectively). An additional 60 mL of CH_4-bearing water was drawn into a submerged syringe. Sampled water was then ejected into a 40 mL glass vial and acidified to a pH < 2 using 20 % w/v HCl to prevent microbial methanotrophic consumption of CH_4. Once full, each glass vial was then capped without headspace. The $\delta^{13}C$ and $\delta^{2}H$ values of CH_4 were measured within six months of collection (see **Chapter 4.2.4**).

4.1.6. Dissolved SO_4^{2-} in groundwater

Groundwater samples were collected for analysis of S and O isotope composition of dissolved SO_4^{2-} ($\delta^{34}S$ and $\delta^{18}O$, respectively) using methods adopted from Szynkiewicz et al (2012). Approximately, 1 L of water was vacuum pumped through a glass microfiber filter into a 1 L plastic bottle and capped with a plastic lid. Immediately upon returning from the field, the filtered sample was transferred to a glass beaker and acidified to a pH < 2 using 20 % w/v HCl. Afterward, 10 mL of 10 % w/v $BaCl_2$ was added to the sample to precipitate $BaSO_4$. This precipitate was then allowed to settle overnight to the bottom of the beaker. After rinsing several times with deionized (DI) water, the precipitate was then dried in an oven at 90ºC for 24 hours and stored in a glass vial prior to isotope analysis. The $\delta^{34}S$ and $\delta^{18}O$ values of $BaSO_4$ were measured within six months of collection (see **Chapter 4.2.5**)

4.1.7. Bedrock sampling

Each of the major geologic units described in chapter 3.1 (the Middle/Lower Breathitt Formations, Lee Formation, Pennington Formation, and Chattanooga Shale) was sampled for S isotope analysis of S-bearing minerals in bedrock (e.g., sulfides, sulfates) using methods adopted from Szynkiewicz et al (2009). Samples were collected from surface outcrops along where Kentucky State Highway 119 passes over PMR at the south side of Letcher County. As previously explained in **Chapter 3.1.7**, all of the geologic units down to the Chattanooga Shale were exposed by the PMTF at the northern base of PMR. Upon encountering an outcrop in the field, the specific geologic unit was determined by correlating it with a geologic map. All rock

types present at that outcrop (e.g., shale, coal, sandstone, etc.) were then collected and placed in plastic bags for transport to the laboratory.

4.2. Laboratory analyses

4.2.1. Cation and anion concentrations

Cation and metal concentrations (Ca^{2+}, Fe^{2+}, K^{+}, Mg^{2+}, Mn^{2+}, Na^{+}, Pb^{2+}, Se^{2-}, Sr^{2+}, S^{2-}) were measured via inductively coupled plasma optical emission spectrometry (ICP-OES) in the Center for Mass Spectrometry of the Department of Chemistry at the University of Tennessee, Knoxville (UTK) using methods adopted from Szynkiewics et al (2012). This instrument uses electromagnetically ignited/ionized plasma to excite atoms/ions to the point that they emit radiation at wavelengths characteristic of a particular element. The intensity of this emission is then correlated to the concentration of a given element compared against a known standard, with a reported error of ± 6 %. Each groundwater sample was measured at 1:1, 1:10, and 1:100 dilution ratios and the concentrations retroactively calibrated. Standards were prepared at 10, 5, 1, 0.5, and 0.1 mg/L dilutions.

Anion concentrations (Cl^{-}, NO_3^{-}, NO_2^{-}, SO_4^{2-}) were measured via ion chromatography (IC) in the Aqueous Geochemistry and Microbiology Laboratory of the Department of Earth and Planetary Sciences (EPS) at UTK using methods adopted from Szynkiewics et al (2012). This process allows for the separation of ions based on their affinity to an oppositely charged ion exchanger, with a detection limit of 0.5 mg/L minimum and 100 mg/L maximum. Samples were measured at either 1:1, 1:2, or 1:10 dilution ratios, depending on their previously measured conductivity values.

4.2.2. ^{222}Rn concentrations

Bulk ^{222}Rn concentration was measured using beta liquid scintillation spectrometry (LSC) in the Hydrochemical Dynamics Group Laboratory of the Environmental Sciences Division at Oak Ridge National Laboratory (ORNL) using methods adopted from Passo and Cook (1994). This method works by immersing decaying ^{222}Rn into an organic scintillation fluid that is able to convert emissions of beta particles from radioactive decay into measurable pulses of light. These emissions are then measured over a set period of time to produce a counts-per-minute (cpm) value that is converted to a finite radionuclide concentration (in pCi/L) upon comparison to a standard with a known ^{222}Rn concentration.

Each sample vial was counted for 60 minutes with a region of interest between 0 and 2000 MeV. Ideally, ^{222}Rn is counted using discrimination between alpha and beta emissions, as opposed to counting beta emissions alone. There are multiple advantages to using alpha/beta LSC, including increased counting efficiency and better distinction of ^{222}Rn from other interfering radionuclides. However, for the purpose of this study, counting efficiency was sufficient using only beta LSC. Additionally, the scintillation fluid used is specifically non-aqueous so as to only allow for adsorption of ^{222}Rn gas, thus, isolating it from other radionuclides physically prior to counting.

4.2.3. CH_4 concentrations

The concentration of dissolved CH_4 was measured using gas chromatography (GC) in the Aqueous Geochemistry and Microbiology Laboratory of the EPS Department at UTK using methods adopted from Kampbell and Vandergrift (1998). Prior to analysis, each sample bottle was weighed at room temperature for calibration purposes. Afterward, 1 mL of gas headspace air

was then withdrawn into a syringe through the bottle's rubber septum cap and injected into the GC. Total gas composition was then analyzed within the GC using a combination of flame ionization (FID), flame photometric (FPD), and thermal conductivity (TCD) detection units. Increasing the temperatures of these detectors produces various spectra with specific gas signatures, which can then be converted to a concentration-in-air (ppm) value upon comparison to a known standard. For this study, a Scotty SGL-4-1-S multicomponent gas standard was used, consisting of ~15 ppm acetylene, butane, ethane, ethylene, methane, propane, propylene, methlacetylene, and a remaining balance of nitrogen. With this information, the concentration of dissolved CH_4 in water could then be calculated retroactively using Henry's Law.

4.2.4. C and H isotope composition of CH_4

The $\delta^{13}C$ and $\delta^{2}H$ values of CH_4 were measured in the Stable Isotope Facility of the Department of Plant Sciences at the University of California, Davis using methods adopted from Yarnes (2013). Headspace was generated from each vial and sampled via a gas bench, interfaced with a Delta V Plus isotope ratio mass spectrometer (IRMS). Headspace was generated in vials from water samples containing dissolved gases (i.e., CH_4). Gas samples were then purged from vials through a double-needle sampler into a helium carrier stream, which was passed through a H_2O/CO_2 scrubber (ascarite, $Mg(ClO_4)_2$) and a cold trap cooled by liquid nitrogen. CH_4 then was separated from residual gases by an Rt-Q-BOND GC column. Upon elution from the column, the remaining CH_4 was either oxidized or pyrolized and transferred to the IRMS. Ionized gas was then deflected through a magnetic field and measured upon impact with a detector. Isotope values were reported in units of per mil (‰) with respect to a Vienna Pee Dee Belemnite (VPBD) standard for $\delta^{13}C$ and a Vienna Standard Mean Ocean Water (VSMOW) standard for $\delta^{2}H$. Only water samples with CH_4 concentrations > 1 mg/L were analyzed for their isotope composition. Reported error was ± 0.2 ‰ for $\delta^{13}C$ and ± 2.0 ‰ for $\delta^{2}H$.

4.2.5. S and O isotope composition of SO_4^{2-}

The $\delta^{34}S$ values of SO_4^{2-} were measured using a Costech elemental analyzer (EA) interfaced with a Delta V isotope ratio mass spectrometer in the Stable Isotope Research Facility of the Department of Geological Sciences at Indiana University, Bloomington using methods adopted from Studley et al (2002). $\delta^{18}O$ values of SO_4^{2-} were measured using a continuous flow system with a Thermo high temperature conversion elemental analyzer (TC/EA) interfaced with a Delta Plus XL isotope ratio mass spectrometer in the Stable Isotope Laboratory of the EPS Department at UTK. For $\delta^{34}S$ analysis, 0.36 to 0.44 mg of $BaSO_4$ was enclosed in tin capsules with 1 to 2 mg of V_2O_5 prior to ionization. For $\delta^{18}O$ analysis, 0.2 to 0.4 mg of $BaSO_4$ was enclosed in silver capsules. Isotope values were reported in ‰ with respect to a Vienna Cañon Diablo Troilite standard (VCDT) for $\delta^{34}S$ and a VSMOW standard for $\delta^{18}O$, with a reported error of ± 0.3 ‰.

4.2.6 H and O isotope composition of H_2O

The $\delta^{2}H$ and $\delta^{18}O$ values of water were measured using a Los Gatos liquid isotope analyzer in the Stable Isotope Laboratory of the EPS Department at UTK using methods adopted from Penna et al (2010). For each sample, 1.5 mL of water was transferred to a glass vial with a septum cap. Afterward, 0.8 μL of water was withdrawn by an autosampler into a syringe, injected through a heated septum, and allowed to evaporate into the measurement cell of the isotope analyzer. A tunable laser was projected through the cell and the time taken for the intensity of light within the cell to decay was measured. This time differs based on the isotope

composition of water vapor within the cell. Isotope values for both δ^2H and $\delta^{18}O$ were reported in ‰ with respect to VSMOW, with a reported error of ± 0.7 ‰ for δ^2H and ± 0.2 ‰ for $\delta^{18}O$.

4.2.7. S isotope composition of bedrock

The following method for sequential extraction of S-bearing minerals in bedrock was adopted from Szynkiewicz et al (2009). Upon arrival to the laboratory, bedrock samples were freeze-dried for 24 hours and then ground into a fine sediment using an agate mortar and pestle. About 5 g of sediment was used for extraction of elemental sulfur with dichloromethane (DCM) in a Soxhlet apparatus. Activated copper (Cu) granules were added to the sample flask to recover elemental sulfur as CuS and then treated with 15 mL of hot deoxygenated 6 M HCl while bubbling the solution with N_2 gas. H_2S was evolved from reduction of elemental sulfur bound to the copper granules and precipitated as Ag_2S.

After DCM extraction, the residual sediment was treated with 30 mL of 6 M HCl in the same way as the previously mentioned copper granules. Evolved H_2S from the decomposition of acid-volatile sulfides (e.g., monosulfides) was precipitated as Ag_2S. Afterward, the acid leachate was separated from the sediment using a centrifuge. Dissolved Fe^{2+} was removed from the acid leachate by precipitation as FeO following the addition of NaOH to adjust the pH of the solution to 9. After treatment with NaOH, the acid-dissolved SO_4^{2-} was precipitated from the remaining solution as $BaSO_4$. Finally, the remaining sediment was treated with a mixture of 20 mL 12 M HCl and 20 mL of 1 M CrCl2·6H2O under N_s gas to dissolve chromium-reducible sulfides (e.g., disulfides). The amounts of acid soluble sulfates, elemental sulfur, monosulfides, and disulfides were then calculated based on the air-dried mass of the initial sediment sample used for extraction.

4.2.8. Spatial statistics and proximity analyses

For spatial analysis, the GPS data collected for each sampling site were uploaded into ArcGIS and related to various geographic features in Letcher County (e.g., the locations of gas wells, coal mines, faults, etc.). This geographic information was acquired via public datasets available through the Kentucky Geological Survey's (KGS) Online Map Information Service (KGS, 2014). From this database, available point data were obtained for practically all natural gas wells permitted within the county since 1900, including: conventional, non-fractured gas wells; conventional, fractured gas wells; unconventional (deviated), fractured gas wells; currently active fractured gas wells (deviated and non-deviated); and delinquent and incomplete gas wells.

However, this study was only concerned with three primary well classifications for use in spatial analyses: 1) all hydraulically fractured natural gas wells permitted after 1980 (referred to from this point simply as ALL (1980 – 2014)), 2) all deviated hydraulically fractured natural gas wells permitted between 2006 and 2012 (referred from this point simply as DEVIATED (2006 – 2012)), and 3) all active hydraulically fractured natural gas wells permitted after 2011 (referred from this point simply as ACTIVE (2011 – 2014); **Figure A.4**) Additionally, polygon data for all surface mines throughout the county – including abandoned, active, delinquent, and incomplete mines – as well as vector data for previously mapped geologic formations, faults, and other tectonic features were obtained for additional spatial analysis.

Using these data, chemical and isotope results from the field were correlated with: 1) the distance from each sampling site to the nearest hydraulically fractured natural gas well of each major gas well category (i.e., ALL (1980 – 2014), DEVIATED (2006 – 2012), and ACTIVE (2011 – 2014)), 2) the distance from each sampling site to the nearest occurrence of the PMTF,

and 3) the percentage of area covered by surface mining (past and present) within a 1 km radius of each sampling site. Spatial metrics were adopted from Jackson et al (2013).

The observed relationships between various measured parameters for each site and their corresponding proximity metrics were tested primarily using linear regression in the statistical program, R. For this test, reported P-values less than 0.05 and reported R^2-values greater than 0.5 were considered significant (Crawley, 2007). All the data that were not normally distributed were transformed to meet the assumption of normality necessary for linear regression. In some cases where such transformations were not possible, the observed relationships were alternatively tested using either logistic regression or Spearman's rank-order correlation. A logistic regression (or generalized linear model) attempts to quantify variation in binary (categorical) response data as a function of some continuous predictor variable. Similar to linear regression, logistic regression measures significance using P-values and goodness of fit as residual deviance (D). Unlike R^2 values, though, D-values are bound between zero and infinity. P-values less than 0.05 and D-values less than 2.0 were considered significant (Crawley, 2007). For Spearman's rank-order correlation, reported ρ (rho) values greater than 0.5 were considered significant (Crawley, 2007).

Additionally, any statistical relationships that involved discrete/categorical predictor variables (i.e., treatment vs. control categories, non-continuous measurements, etc.) were tested using an analysis of variance test (ANOVA) in place of a linear regression, because linear regression requires that both predictor and response variable data be continuous. Specifically, this test was used to compare 1) mean ORP of sampling sites with < 30 % of the area within a 1 km radius covered by surface mining against 2) mean ORP of sampling sites with > 30 % of the area within a 1km radius covered by surface mining. The primary difference in the result of this test compared to a linear regression is that variance is measured using the F-ratio, which quantifies if the variances between predictor categories are equal. Similar to D-values for logistic regression, F-values are bound between zero and infinity. For an ANOVA, reported P-values less than 0.05 and reported F-ratios greater than 4.0 were considered significant (Crawley, 2007).

For any regressions involving spatial metric data (i.e., distance between sampling points or percent area covered within a given radius), a Moran's *I* test was run to account for the effect of any spatial autocorrelation within the data. Moran's *I* is a statistic, bound between -1 and +1, and quantifies the amount of spatial clustering between points for a given parameter (Sokal and Oden, 1978). For example, a sample population with an *I*-value of -1 would demonstrate perfect dispersion of like-values for a given parameter. Conversely, a sample population with *I* value of +1 would demonstrate perfect clustering of like-values for a given parameter.

To generate this value, a spatial weights matrix was first generated for all sampling points using the program, GeoDa. The resulting matrix was then used to quantify the amount of clustering or dispersion for the residuals of each regression. Regressions with positive I-values (I > +0.3) were considered positively spatially autocorrelated (clustered) and regressions with negative *I*-values (I < -0.3) were considered negatively spatially autocorrelated (dispersed) (Sokal and Oden, 1978). Regressions with *I*-values between -0.3 and +0.3 are not spatially autocorrelated (randomly dispersed) (Sokal and Oden, 1978). Furthermore, this test generated corresponding *P*-values. *P*-values associated with this test less than 0.05 were considered significant, meaning that the reported *I*-value could be considered valid enough to reject the null assumption that the specified parameter value for a given population is randomly distributed (Sokal and Oden, 1978).

4.2.9. Characterizing water chemistry

General water chemistry was characterized using both a Piper diagram and principle component analysis (PCA). The Piper diagram was constructed using the USGS program called GW Chart. Water types were classified according to the measured concentrations of Cl^-, SO_4^{2-}, HCO_3^-, CO_3^2, Na^+, K^+, Mg^{2+}, and Ca^{2+}. PCA was implemented to account for certain limitations of the Piper classification and allowed for better delineating water types based on constituents not present in the original Piper scheme, including concentrations of iron (Fe^{2+}), manganese (Mn), selenium (Se), lead (Pb), strontium (Sr), silicon (Si), and CH_4. Additionally, this method was able to take into account bulk water properties such as pH, temperature, ORP, TDS, and DO.

In order to make sense of this additional information, PCA generates component vectors (referred to as eigenvectors) that account for as much of the variability in the data as possible within a multi-dimensional framework that evaluates all variables for each sampling site simultaneously (Crawley, 2007). Afterward, each variable is assigned a value (referred to as an eigenvalue) with respect to each component vector based on its orthogonal deviation (error) from that vector (Crawley, 2007). Those vectors with the lowest residual scores (the least error, thus explaining the greatest variability across the dataset) can be generally interpreted as potential factors controlling the distribution of some or all of those variables (Crawley, 2007). For the purpose of this analysis, these vectors were interpreted as specific water types, which may be otherwise controlled by geographic location, geology, etc.

5. RESULTS

5.1. Water chemistry and groundwater origin across Letcher County

5.1.1. Piper classification

The results of the Piper diagram (**Figure B.1**) showed two distinctive water types across Letcher County. Type 1 was characterized by higher concentrations of Na^+ and Cl^- and lower concentrations of SO_4^{2-}, and can be classified as Na-HCO_3-Cl-rich water. Na^+ concentrations for Type 1 groundwater ranged from 12 mg/L to 268 mg/L (mean: 87 mg/L), and Cl^- concentrations ranged from 3 mg/L to 310 mg/L (mean: 56 mg/L). SO_4^{2-} concentrations for Type 1 groundwater ranged from 1 mg/L to 34 mg/L (mean: 6 mg/L). Ca^{2+} concentrations for Type 1 groundwater ranged from < 0.5 mg/L to 87 mg/L (mean 34 mg/L). Additionally, Type 1 groundwater showed higher concentrations of CH_4, ranging from 1 mg/L to 9 mg/L (mean: 5 mg/L).

Type 2 groundwater was characterized by higher concentrations of SO_4^{2-} and lower concentrations of Na^+ and Cl^-, and can be classified as predominantly Ca-HCO_3-SO_4-rich water. Na^+ concentrations for Type 2 groundwater ranged from 3 mg/L to 123 mg/L (mean: 39 mg/L), and Cl^- concentrations ranged from 1 mg/L to 69 mg/L (mean: 13 mg/L). SO_4^{2-} concentrations for Type 2 groundwater ranged from 1 to 289 mg/L (mean: 54 mg/L). Ca^{2+} concentrations were higher for Type 2 groundwater than for Type 1, ranging from < 0.5 mg/L to 406 mg/L (mean: 62 mg/L). Additionally, Type 2 groundwater showed lower concentrations of CH_4, ranging from 0 mg/L to 1 mg/L (mean: 0.25 mg/L).

Both water types contained similar concentrations of HCO_3^-, though HCO_3^- made up a smaller proportion of the overall ionic content for Type 1 groundwater than it did for Type 2. HCO_3^- concentrations for Type 1 groundwater ranged from 124 mg/L to 368 mg/L (mean: 185 mg/L). HCO_3^- concentrations for Type 2 groundwater ranged from 28 mg/L to 492 mg/L (mean: 167 mg/L). Na^+ and Cl^- concentrations were positively correlated with one another for both water types ($R^2 = 0.7$, $P << 0.0001$, **Figure B.2**).

5.1.2. Principal component analysis

PCA resulted in 4 principle components that explained ~75 % of the variation among twenty variables analyzed by the model. Principle component 1 (PC1) accounted for ~50 % of the total variation, and was therefore interpreted as the most important component. The remaining 25 % of the variation in the data was explained more or less equally by the remaining 3 components. By plotting PC1 against components 2, 3, or 4, it was possible to differentiate between two major water types (**Figure B.3**), similar to those identified using Piper classification.

Oriented along principle component 2 (PC2), Type 1 groundwater was correlated with higher concentrations of Na^+, Cl^-, and CH_4 and was also slightly correlated with higher concentrations of Se^{2-} and Pb^{2+}. Oriented along principle component 1 (PC1), Type 2 groundwater was correlated with higher concentrations of SO_4^{2-}, Mg^{2+}, and Ca^{2+} and slightly correlated with higher concentrations of Fe^{2+} and Mn^{2+}. Conversely, the concentrations of HCO_3^-, K^+, and Sr^{2-} were equally correlated with both PC1 and PC2, indicating that these constituents are common in both water types.

5.1.3. Isotope composition of H_2O

$\delta^{18}O$ values for all groundwater sampled ranged from -8 ‰ to -6 ‰ (mean: -6.7 ‰) and δ^2H values ranged from -49 ‰ to -37 ‰ (mean: -42.3 ‰). The slope and intercept corresponding

to these values were also statistically similar to that of the Kentucky meteoric water line (Kendall and Coplen, 2001) when compared using a T-test (T_{57} = 0.67, P > 0.05, **Table C.1**). Both $\delta^{18}O$ and $\delta^{2}H$ values were normally distributed and characteristic of a single sample population (**Figure B.4**).

5.1.4. Isotope composition of groundwater SO_4^{2-} and bedrock S

$\delta^{34}S$ and $\delta^{18}O$ of SO_4^{2-} were measured for groundwater samples with SO_4^{2-} concentrations > 1 mg/L. In these samples $\delta^{34}S$ values ranged from -1‰ to +59 ‰ (mean: +14.5 ‰) and $\delta^{18}O$ values from +2 ‰ to +19 ‰ (mean: +9.1 ‰). Generally, the $\delta^{34}S$ values of S-bearing bedrock minerals (e.g., sulfates, sulfides) varied within a smaller range, from -3 ‰ to +26 ‰ (mean: +0.95 ‰), compared to those of dissolved SO_4^{2-} in groundwater (**Figure B.5, Table C.2**).

$\delta^{18}O$ values were positively correlated with $\delta^{34}S$ values (R^2 = 0.47, P < 0.0001, **Figure B.6**). $\delta^{34}S$ values were not correlated with concentrations of SO_4^{2-} (R^2 = 0.0035, P > 0.05, **Figure B.7**). For the few groundwater samples in which H_2S was present, increasing H_2S concentrations did not correlate significantly with decreasing SO_4^{2-} concentrations (R^2 = 0.16, P > 0.05).

5.1.5. Oxidation-reduction potential (ORP)

ORP values were normally distributed, ranging from -353.6 mV to +232.8 mV (mean: -121.8 mV). ORP values were randomly distributed across Letcher County (I = 0.075, P = 0.02). Concentrations of CH_4, SO_4^{2-}, Fe^{2+}, Na^{+}, and Cl^{-} were correlated marginally with ORP, though many of these correlations produced low R^2 values due to poor model fit (**Table C.3**). This relationship was most significant for CH_4 and SO_4^{2-}, with measured ORP being the strongest predictor of their occurrence (**Figure B.8**). Generally, CH_4 was more abundant in more reducing groundwater (R^2 = 0.40, P < 0.0001), and SO_4 was more abundant in more oxidizing groundwater (R^2 = 0.21, P < 0.001). Additionally, CH_4 and SO_4^{2-} were inversely correlated to one another (ρ = -0.74, **Figure B.9**), meaning that CH_4 concentrations were highest in samples with very low concentrations of SO_4^{2-} (< 10 mg/L), and SO_4^{2-} concentrations were highest in samples with very low concentrations of CH_4 (< 1 mg/L). There was no spatial autocorrelation effect on CH_4 or SO_4^{2-} concentrations as a function of ORP (I = 0.02, P > 0.05 and I = 0.19, P < 0.0001, respectively).

5.2. Stray gas migration with proximity to hydraulic fracturing

5.2.1. ^{222}Rn and proximity to hydraulically fractured natural gas wells

Only seven households among the 59 sampled contained measurable ^{222}Rn (> 10 cpm) dissolved in groundwater. This sample number was too low to meaningfully test the occurrence of ^{222}Rn with proximity to hydraulic fracturing using standard linear regression. Alternatively, ^{222}Rn concentration data were bimodally distributed between sites with concentrations above detection limit (> 100 pCi/L) and sites with ^{222}Rn concentrations below detection limit (< 100 pCi/L). Consequently, the occurrence of ^{222}Rn as a function of proximity to hydraulically fracturing was modeled using logistic regression to determine if the simple presence or absence of ^{222}Rn varied significantly as a function of proximity to hydraulically fractured natural gas wells (Crawley, 2007). According to this analysis, there was no correlation between measured ^{222}Rn concentrations and proximity hydraulically fractured natural gas wells (**Figures B.10** through **B.12**). This is true for all natural gas well categories for which proximity metrics (i.e., distance from each sample site to the nearest well) were calculated – i.e., ALL (1980 – 2014), ACTIVE (2011 – 2014), and DEVIATED (2006 – 2012) (**Tables C.4** through **C.6**).

5.2.2. CH_4 and proximity to hydraulically fractured natural gas wells

Approximately half of the households sampled showed elevated CH_4 concentrations (> 1 mg/L). CH_4 concentrations measured in groundwater ranged from < 0.05 mg/L to ~10 mg/L (mean: 4.92 mg/L). These data were bimodally distributed between sites with CH_4 concentrations < 1 mg/L and sites with CH_4 concentrations > 1 mg/L.

Similar to ^{222}Rn, the occurrence of CH_4 as a function of proximity to hydraulic fracturing were modeled using logistic regression to determine if the simple presence or absence of CH_4 varied significantly as a function of proximity to hydraulically fractured natural gas wells (Crawley, 2007). Accordingly, there was no correlation between CH_4 concentrations and proximity to the hydraulically fractured natural gas wells (**Figures B.13** through **B.15**). The occurrence of CH_4 across Letcher County was not significantly clustered spatially ($I = 0.17$, $P < 0.0001$, **Table C.7**). This was true for natural gas well categories for which proximity metrics (i.e., distance from each sample site to the nearest well) were calculated – i.e., ALL (1980 – 2014), ACTIVE (2011 – 2014), and DEVIATED (2006 – 2012) (**Tables C.4** through **C.6**).

5.2.3. ^{222}Rn and CH_4

No significant relationship was observed between ^{222}Rn and CH_4 for sampling sites at which ^{222}Rn was present above detection limit when tested using non-parametric correlation ($\rho = 0.05$, **Figure B.16**). In fact, ^{222}Rn was only present in groundwater with low (< 1 mg/L) concentrations of CH_4.

5.2.4. Isotope composition of CH_4

The C and H isotope composition of CH_4 was measured for sampling sites with CH_4 concentrations > 1 mg/L. $\delta^{13}C$ values of CH_4 ranged from -66 ‰ to -16 ‰ (mean: -46 ‰), and δ^2H values ranged from -286 ‰ to -86 ‰ (mean -204 ‰) (**Figure B.17**). $\delta^{13}C$ and δ^2H values were normally distributed and characteristic of a single sample population.

5.2.5. CH_4, Na^+, and Cl^-

Despite the co-occurrence of CH_4, Na^+, and Cl^- in Type 1 groundwater as demonstrated by PCA analysis, CH_4 concentrations appeared to be weakly, positively correlated with Na^+ ($R^2 = 0.34$, $P < 0.0001$) and Cl^- ($R^2 = 0.34$, $P < 0.0001$) concentrations (**Figures B.18** and **B.19**).

5.3. Additional comparisons: Stray gas migration with proximity to other environmental factors

5.3.1. ORP, TDS, ^{222}Rn, CH_4, Na^+, and Cl^- with proximity to the PMTF

Given the lack of randomization in the original sample distribution with respect to the PMTF, sampling site distance from the PMTF was not normally distributed, and could not be transformed to meet the assumption necessary to test this relationship by linear regression. Therefore, all correlations between measured ORP, TDS, ^{222}Rn, CH_4, Na^+, and Cl^- values and sampling site proximity to the PMTF were tested using non-parametric correlation (**Table C.8**).

ORP was weakly positively correlated with proximity to PMTF ($\rho = 0.31$, **Figure B.20**), meaning ORP values generally increased (became more oxidizing) with increasing distance from the PMTF. TDS was also weakly positively correlated with proximity to the PMTF ($\rho = 0.25$, **Figure B.21**). ORP was not spatially autocorrelated as a function of proximity to the PMTF ($I = -0.044$, $P > 0.05$, **Table C.7**). CH_4 concentrations were weakly negatively correlated with

proximity to the PMTF and generally increased as distance to the PMTF decreased (ρ = -0.20, **Figure B.22**). ^{222}Rn concentrations were too weakly negatively correlated with proximity to the PMTF to be considered significant (ρ = -0.17), though this test was restricted due to low (7) sample size. Na^+ and Cl^- concentrations were not correlated with proximity to PMTF (ρ = -0.062 and ρ = -0.020, respectively).

5.3.2. ORP, TDS, ^{222}Rn, SO_4^{2-}, and CH_4 with proximity to surface mining

Unlike values for sampling site proximity to the PMTF (i.e., nearest distance to the PMTF from each sampling site), values for proximity to surface mining (i.e., the percentage of area within a 1 km radius of each sampling site covered by surface mining) were normally distributed and able to be tested by linear regression. Although a number of sampling sites with high (> 30 %) percentages of surface mining within a 1 km radius demonstrated elevated ORP and TDS values (**Figures B.23** and **B.24**), none of the tracers tested – ORP, TDS, CH_4, ^{222}Rn, SO_4^{2-}, Na^+, Cl^- – were correlated with proximity to surface mining for all sampling sites (**Table C.9**). However, mean ORP values for sampling sites with < 30 % area within a 1 km radius covered by surface mining were still significantly lower than mean ORP values for sampling sites with > 30 % area within a 1 km radius covered by surface mining when compared alternatively by ANOVA (**Figure B.25**, **Table C.9**). Neither ORP nor TDS were spatially autocorrelated as a function of proximity to surface mining (I = -0.072, P > 0.05 and I = 0.096, P > 0.05, respectively, **Table C.9**).

6. DISCUSSION

6.1. Groundwater chemistry and origins in Letcher County

The isotope composition of water is a valuable tracer for evaluating water sources and mixing processes in aquifers. Usually, the δ^2H and $\delta^{18}O$ values of shallow groundwater represent the average isotope composition of local precipitation that has fallen relatively recently within a given aquifer's recharge area (Sharp, 2007). The δ^2H and $\delta^{18}O$ values of groundwater sampled in Letcher County were normally distributed and varied in relatively narrow range (-37 ‰ to -47 ‰ and -6 ‰ to -8 ‰, respectively). These values were consistent with previously reported H and O isotope compositions for Kentucky meteoric precipitation (Kendall and Coplen, 2001). This indicates that groundwater sampled for this study was primarily sourced from the recent recharge of local meteoric precipitation (e.g., rain and snowmelt).

Aside from anthropogenic factors, many natural processes control the chemical composition of groundwater, such as dissolution of bedrock minerals, consumption and alteration of nutrients and trace metals by microbes, overall residence time of water within an aquifer, etc. Using Piper classification and PCA analysis, two major water types were distinguished among groundwaters sampled within Letcher County: Type 1, characterized by higher concentrations of Na^+, Cl^-, and CH_4, and Type 2, characterized by higher concentrations of Ca^{2+}, Mg^{2+}, Fe^{2+}, and SO_4^{2-} (**Figures B.1** and **B.3**). Both water types contained relatively similar concentrations of HCO_3^-.

In Appalachia, groundwater chemistry is generally dominated by high concentrations of HCO_3^- originating from dissolution of calcite ($CaCO_3$) and dolomite ($CaMg(CO_3)_2$) present in Paleozoic carbonate formations (Sheets and Kozar, 2000). This is consistent with the observed elevated concentrations of HCO_3^- in both water types found in Letcher County. Generally, the δ^2H and $\delta^{18}O$ values of Type 1 and 2 groundwater were very similar, suggesting that they both originated from local precipitation (**Figure B.4**). However, considerable differences observed between the chemical compositions of Type 1 (Na-HCO_3-Cl-rich) and Type 2 (Ca-HCO_3-SO_4-rich) groundwater suggest that some additional process (or processes) is responsible for further changing groundwater chemistry along the flow path.

In carbonate-rich aquifers, dedolomitization is often proposed as a major factor responsible for increasing Na^+ and Cl^- concentrations in groundwater with depth. This process is driven by dissolution of evaporites (e.g., gypsum, $CaSO_4 \cdot H_2O$, and anhydrite, $CaSO_4$), which leads to dissolution of dolomite and its subsequent replacement by calcite (Szynkiewicz et al, 2012; Plummer et al, 1990; Sacks et al, 1995). Consequently, dedolomitization causes groundwater depletion in Ca^{2+} and HCO_3^- followed by enrichment in Na^+, Cl^- and SO_4^{2-} ions. However, in Letcher County this process does not explain the elevated concentrations of HCO_3^- and low concentrations of SO_4^{2-} observed in the Type 1 groundwater with higher Na^+ and Cl^- concentrations. Most likely, dedolomitization may be less important in groundwater sampled for this project because the shallow bedrock of the Breathitt Formation is largely absent of evaporite minerals (Noger, 1988). This observation was further confirmed by the relatively low concentrations of acid-soluble sulfate minerals (0.001 to 0.049 wt. %) extracted from bedrock sediments for this study using sulfur sequential extraction (**Chapter 4.2.7**).

Previous studies suggested that Na-Cl-rich groundwater with higher abundances of CH_4 (i.e., Type 1 water) might also occur as a result of diffuse mixing with basinal brine water residing at greater depths (Warner et al, 2012; Osborn and McIntosh, 2010). Given the slightly elevated Na^+ and Cl^- content of Type 1 groundwater, this process could provide an alternative explanation for the presence of CH_4 in Letcher County groundwater. Usually, deep basinal brines

have distinctively higher δ^2H and $\delta^{18}O$ isotope values compared to meteoric precipitation because they either 1) originated from paleoseawater trapped in sedimentary formations (Davisson et al, 1994), or 2) have undergone prolonged isotope exchange with the surrounding bedrock (Clayton et al, 1966). Mean δ^2H and $\delta^{18}O$ values of basinal brines are approximately -41 ‰ and -5 ‰, respectively (Osborn et al 2011). Additionally, basinal brines are extremely saline, with TDS values > 50 g/L, Cl^- concentrations > 60,000 mg/L, and Na^+ concentrations > 20,000 mg/L (Gat, 1996; Osborn et al, 2011). Warner et al (2012) suggested that shallow groundwater having undergone limited mixing with basinal brines (< 20 % brine water in solution) should exhibit increases in Na^+ and Cl^- concentrations (> 100 mg/L), but would still remain indistinguishable from meteoric water in terms of its H and O isotope composition. Alternatively, Gat (1996) suggested that shallow, meteoric groundwater interacting with deeper basinal brines should exhibit increases in $\delta^{18}O$ values as a function of TDS.

While Na^+ and Cl^- concentrations for Type 1 groundwater in Letcher County may be somewhat elevated relative to Type 2 groundwater, the $\delta^{18}O$ values of Type 1 groundwater did not show any significant increases relative to Na^+ or Cl^- ($R^2 = 0.045$, $P > 0.05$ and $R^2 = 0.12$, $P < 0.01$, respectively; **Table C.1**). Instead, the studied groundwater plotted within a range typical of only mild $\delta^{18}O$ enrichment as a result of O isotope exchange following prolonged interaction of meteoric water with bedrock (**Figures B.26** and **B.27**). This suggests that brine mixing is negligible in shallow groundwater in Letcher County, and that most of the Na^+ and Cl^- present in Type 1 groundwater likely originated from shallower halite (NaCl) dissolution. Halite is a common mineral that occurs in trace amounts in sedimentary rocks of marine origin (Chi and Savard, 1997; Kesler et al, 1996). Because of high solubility of halite in water, Na^+ and Cl^- concentrations generally increase over time as groundwater interacts more extensively with bedrock.

Type 2 groundwater showed significantly higher SO_4^{2-} and Fe^{2+} concentrations (mean concentrations = 54 mg/L and 7 mg/L, respectively) compared to Type 1 groundwater (mean concentrations = 6 mg/L and 2 mg/L, respectively). Generally, $\delta^{34}S$ and $\delta^{18}O$ are useful isotope tracers to determine sources of dissolved SO_4^{2-} since different rock types can exhibit wide isotope variations in nature. For example, SO_4^{2-} formed due to the dissolution of evaporites is characterized by higher $\delta^{34}S$ and $\delta^{18}O$ values (+10 to +35 ‰ and +10 to +18 ‰, respectively) compared to SO_4^{2-} formed due to the oxidation of sulfide minerals (-35 to +5 ‰ and -6 to +10 ‰, respectively) (Krouse and Grinenco, 1991; Clark and Fritz, 1997). In groundwater sampled in Letcher County, $\delta^{34}S$ and $\delta^{18}O$ values varied from -1 to +59 ‰ and +2 to +19 ‰, respectively, and were positively correlated with each other (**Figure B.6**), suggesting plausible mixing between two SO_4^{2-} endmembers from evaporite dissolution and sulfide oxidation (Knöller et al., 2005). However, bedrock samples analyzed from this area showed rather low values of $\delta^{34}S$ in sulfides (-2.5 to +4.7 ‰) and acid-soluble sulfates (-1.9 to +4.6 ‰), which did not match observed variations of $\delta^{34}S$ values in groundwater. Moreover, evaporite formations are not present in Letcher County, thus, the majority of groundwater SO_4^{2-} must be sourced from the oxidation of sulfide minerals, primarily pyrite (FeS_2), which is a common mineral in coal (Blodau, 2006). The formation of SO_4^{2-} by sulfide oxidation does not involve significant sulfur isotope fractionation (Krouse and Grinenco, 1991; Clark and Fritz, 1997). Accordingly, the extracted sulfate phases from bedrock samples had very similar $\delta^{34}S$ values to bedrock sulfide phases, implying that sulfide-derived SO_4^{2-} is a major source of SO_4^{2-} in the studied area.

Microbial sulfate reduction is a common anaerobic process responsible for the removal of SO_4^{2-} from groundwater (Head et al, 2003), as well as the subsequent enrichment of $\delta^{34}S$ and $\delta^{18}O$ values in remaining SO_4^{2-} (Canfield, 2001) due to kinetic isotope fractionation (Detmers et

al, 2001; Bottcher et al, 2001). This occurs because microbes preferentially metabolize isotopically lighter ^{32}S and ^{16}O isotopes (Detmers et al, 2001; Bottcher et al, 2001). Given that bedrock sulfur sources sampled in Letcher County showed relatively low $\delta^{34}S$ values compared to groundwater (**Figure B.5**), this process is likely responsible for the observed enrichment of $\delta^{34}S$ and $\delta^{18}O$ values in groundwater SO_4^{2-} (**Figure B.6**). A great number of wells with Type 1 groundwater contained very low SO_4^{2-} concentrations (< 5 mg/L), and in some cases SO_4^{2-} was below detection limit (< 0.05 mg/L). This suggests that microbial processes can lead to the near complete removal of SO_4^{2-} in Type 1 groundwater.

Hydrogen sulfide (H_2S) is a gaseous product of microbial sulfate reduction. Its concentrations, however, were relatively low (<1 mg/L) in most groundwater sampled for this study, even in samples with SO_4^{2-} concentrations < 1 mg/L. This suggests that H_2S may be either degassing from domestic groundwater wells or undergoing further alteration in situ due to formation of secondary pyrite, as the latter is a common process in sediments actively undergoing microbial sulfate reduction (Szynkiewicz et al, 2009).

In addition to the formation of SO_4^{2-}, pyrite oxidation releases Fe^{2+}, which generally becomes mobile in water with lower pH (< 5). While there was no significant correlation between SO_4^{2-} and Fe^{2+} concentrations (**Table C.3**), Type 2 groundwater with higher Fe^{2+} concentrations might be also affected by the dissolution of other iron-rich minerals, such as siderite ($FeCO_3$), present in adjacent sandstone deposits of the Middle and Lower Breathitt Formations. In contrast, Type 1 groundwater was depleted in SO_4^{2-} and Fe^{2+} (**Figure. B.3**). This may be a result of secondary pyrite formation due to microbial sulfate reduction at lower depths. Nevertheless, mineral saturation indexes (SI) calculated for a subset of Type 2 groundwater samples with notably high ratios of SO_4^{2-} to Fe^{2+} concentrations (> 100) suggest that they were under-saturated with respect to pyrite and siderite (SI range: -103 to -80 and -5 to -1, respectively), but over-saturated with respect to hematite Fe_2O_3 (SI range: +13 to +20). This suggests that dissolved Fe^{2+} may be re-precipitating to more oxidative Fe^{2+} phases as groundwater interacts more with bedrock.

Overall, ORP appeared to be a useful geochemical predictor of groundwater types in Letcher County. Type 2 groundwater was more oxidizing (ORP > -120 mV), exhibited limited interaction with bedrock (e.g., less dissolved solids), and was characterized by higher proportions of SO_4^{2-}, HCO_3^-, Ca^{2+}, and Fe^{2+} due to pyrite oxidation and carbonate dissolution. In contrast, Type 1 groundwater was more reducing (ORP < -120 mV) and exhibited more extensive alteration along the flow path related to microbial sulfate reduction (removal of SO_4^{2-}) and halite dissolution (enrichment in Na^+ and Cl^-). Because of its more pronounced chemical and isotope changes, Type 1 groundwater is likely representative of groundwater with longer residence time in a more reducing environment, compared to Type 2 groundwater, which is more representative of more recent recharge in a more oxidizing environment.

6.2. Stray gas migration with proximity to hydraulic fracturing

Previous studies showed that $\delta^{13}C$ and δ^2H values of CH_4 are useful isotope tracers to distinguish between thermogenic and microbial CH_4 (Vengosh et al, 2014; Jackson et al, 2012; Osborn et al, 2011). In groundwater sampled throughout Letcher County, the $\delta^{13}C$ and δ^2H values of CH_4 were characteristic of a less mature thermogenic and/or mixed thermogenic/biogenic origin (**Figure B.17**). However, the isotope composition of CH_4 alone was not useful in further distinguishing between shallow formations in situ (e.g., by microbes or in coal) versus migration from deeper Devonian shale as a result of hydraulic fracturing. One problem obstructing this distinction is that CH_4 from shallower coal deposits can also

demonstrate thermogenic or mixed thermogenic/biogenic isotope signatures, depending on its depositional history (Cheung et al, 2010; Stapoc et al, 2007; Clayton, 1998; Schoell, 1979). For example, coalbed CH_4 from Pennsylvanian coalfields in western Kentucky has been shown to have a more mature, thermogenic isotope signature (mean $\delta^{13}C$ = -49 ‰, mean $\delta^{2}H$ = -217 ‰; Strapoc et al, 2007) similar to that measured in Letcher County groundwater (mean $\delta^{13}C$ = -42 ‰, mean $\delta^{2}H$ = -203 ‰). This suggests that, in addition to (or instead of) CH_4 migrating from Devonian shale, some portion of the CH_4 measured in Letcher County groundwater might have originated from shallow Pennsylvanian coal deposits of the Middle and Lower Breathitt Formations.

In groundwater sampled for this study, CH_4 concentrations appeared to be largely controlled by ORP. Generally, higher CH_4 concentrations were observed in Type 1 groundwater with lower ORP (< -120 mV) compared to lower CH_4 concentrations in Type 2 groundwater with higher ORP (> -120 mV) (**Figures B.1**, **B.3**, and **B.8**). Because of the more oxidative condition of shallower Type 2 groundwater, CH_4 is likely more prone to oxidation in more aerobic subsurface environments.

Additionally, higher CH_4 concentrations were accompanied by higher Na^+ and Cl^- concentrations in Type 1 groundwater (**Figures B.1** and **B.3**). As previously discussed in **Chapter 6.1**, Na^+ and Cl^- enrichment in Type 1 groundwater likely originated from progressing water-rock interaction (i.e., carbonate/halite dissolution) along the flow path, rather than from mixing with deeper basinal brines. Given that the salinity in Type 1 groundwater does not appear to originate from basinal brines (**Chapter 6.1**), it is likely that CH_4 measured in this groundwater also does not occur as a result of diffusion from brine.

However, the occurrence of CH_4 in Na-Cl-rich groundwater in Letcher County also suggests that this CH_4 likely did not occur as a result of stray gas migration from Devonian shale. Previous studies have found that CH_4 concentrations in groundwater affected by stray gas migration do not correlate with Na^+ or Cl^- concentrations, even in cases where CH_4 exhibits a more thermogenic isotope composition (Jackson, 2014). Stray gas migration occurs as a result of the buoyant, rapid displacement of water by continuous-phase gas bodies (Gurevich et al, 1993). Therefore, dissolved solids in groundwater (i.e., Na^+ and Cl^-) cannot make use of the same mechanisms to migrate upwards, and so they remain trapped in deeper groundwater longer while dissolved gases are able to escape from the formation. Therefore, CH_4 in waters with higher Na^+ and Cl^- concentrations in Letcher County is likely formed in situ and simply characteristic of a shallower (relative to depths of formation brine), CH_4-rich water type.

As mentioned previously (**Chapter 6.1**), SO_4^{2-} cycling in Letcher County groundwater appears to be considerably controlled by microbial processes. Previous literature suggested that various microbial processes may also oxidize CH_4 by using it as an electron donor, causing its enrichment in heavier ^{13}C and ^{2}H isotopes (Van Stempvoort et al, 2005). This, in turn, can alter biogenic CH_4 to create a falsely thermogenic signature with higher $\delta^{13}C$ and $\delta^{2}H$ values. In Letcher County, only one groundwater sample had CH_4 with an isotopic signature indicative of microbial oxidation ($\delta^{13}C$ = –16 ‰ and $\delta^{2}H$ = -195 ‰). In other samples, the $\delta^{13}C$ and $\delta^{2}H$ values were indicative of mixing between immature thermogenic and biogenic CH_4 (**Figure B.17**). Generally, microbial CH_4 oxidation leads to increases of HCO_3^- in groundwater, resulting in a negative correlation between CH_4 and HCO_3^- (Van Stempvoort et al, 2005). However, this was not the case in the groundwater of Letcher County (**Figure B.28**). While this result cannot rule out the possibility of some microbial CH_4 oxidation, the influence of such processes on HCO_3^- concentrations is difficult to further delineate due to the high abundance of carbonate minerals in the local bedrock. In this context, groundwater HCO_3^- is more likely to be controlled

by the widespread dissolution of carbonate bedrock, rather than oxidation of much smaller, localized amounts of CH_4 found during the course of this study.

According to the results from this study, it is unlikely that CH_4 measured in Letcher County groundwater occurred as a result of stray gas migration from Devonian shale. Furthermore, there is also strong evidence to suggest that hydraulic fracturing has had little to no impact on processes of stray gas migration in Letcher County groundwater. For example, CH_4 concentrations > 1 mg/L were not correlated with proximity to hydraulically fractured natural gas wells of any production category – ALL (1980 – 2014), ACTIVE (2011 – 2014), or DEVIATED (2006 – 2012) (**Figures B.13** through **B.15, Tables C.4** through **C.6**). Additionally, CH_4 concentrations of groundwater sampled were considerably lower (< 10 mg/L) than those observed in previous studies (between 20 to 60 mg/L) where groundwater was shown to be directly impacted by stray gas migration due to hydraulic fracturing (Vengosh et al, 2014; Jackson et al, 2013; Osborn et al, 2014).

It is also pertinent to note that no CH_4 concentrations observed in Letcher County were above the range recommended by the US Dept. of the Interior for remediation (10 mg/L to 28 mg/L) (Eltschlarger et al, 2001). In waters impacted by stray gas migration from previous studies, CH_4 concentrations regularly exceeded these thresholds, reaching as high as almost 70 mg/L in some cases (Jackson et al, 2013; Osborn et al, 2011). However, some residents of Letcher County were able provide anecdotal accounts of domestic wells combusting as a result of excessive methane accumulation or after being compromised by delinquent gas drilling or surface mining practices. If CH_4 concentrations are in any way being altered/mitigated in situ, then excessive accumulations of fugitive gases as a result of these processes may be hard to characterize over more prolonged time scales.

Similar to CH_4, ^{222}Rn has been documented to originate from multiple bedrock sources throughout Appalachia, including coal (Mahur et al, 2008). In Letcher County, most of the groundwater sampled had negligible concentrations of ^{222}Rn. Of the 59 households sampled, only seven contained ^{222}Rn concentrations above detection limit, ranging from 100 to 300 pCi/L (**Figures B.10** through **B.12**). Although elevated ^{222}Rn concentrations were observed in three sampling sites within 1km of a hydraulically fractured natural gas well (permitted between 2006 and 2012, **Figure B.12**), there was no significant relationship between ^{222}Rn occurrence and sampling site proximity to hydraulically fractured natural gas wells (**Tables C.4** through **C.6**). Therefore, these results suggest that hydraulic fracturing activity has had no measurable effect on the occurrence of groundwater ^{222}Rn in Letcher County groundwater.

Nevertheless, there are contextual limitations preventing this study from better characterizing the occurrence of stray gas migration with proximity to older (before 2006) hydraulic fracturing activity in Letcher County. For instance, the sheer density of past natural gas development in Letcher County made it difficult to find households far enough away (more than 1 km) from any previous (1980 – 2006) hydraulic fracturing activity (**Figure A.4**). Therefore, most of the groundwater samples collected for this study were taken from areas that had been actively fractured at least once in the past three decades. This means that for the broadest gas well category – ALL (1980 – 2014) – it was impossible to establish any kind of reliable subset of control data against which to compare potentially impacted sites. Given the ubiquitous distribution of gas wells in this category, it may not be possible to explicitly isolate and test the relationship between older instances of hydraulic fracturing and the occurrences of CH_4 and ^{222}Rn. Conversely, previous research in the Marcellus shale region of northwest Pennsylvania has greatly benefited from a current moratorium of hydraulic fracturing in neighboring New York. This differentiation has allowed researchers the chance to directly compare groundwater

between active and inactive regions, but is unfortunately not easily applicable to contexts outside of the Marcellus shale.

In contrast, the other two categories of hydraulically fractured natural wells (i.e., ACTIVE (2011 – 2014), and DEVIATED (2006 – 2012)) were much more sparsely distributed across the study area (**Figure A.4**). Consequently, the results of proximity analyses for the occurrence of CH_4 and ^{222}Rn in relation to these newer forms of hydraulic fracturing (**Tables C.5** and **C.6**) are considerably more reliable, suggesting that proximity to ACTIVE (2011 – 2014) and DEVIATED (2006 – 2012) hydraulically fractured natural gas wells had no measurable effect on groundwater CH_4 and ^{222}Rn concentrations in Letcher County.

Furthermore, according to the previous studies (Etiope & Martinelli, 2002; Etiope & Lombardi, 1995; Gurevich et al, 1993), any CH_4 occurring as a result of stray gas migration from Devonian shale should coincide with the occurrence of ^{222}Rn, regardless of whether or not it can be spatially correlated to hydraulic fracturing. In Letcher County, however, concentrations of CH_4 and ^{222}Rn were not correlated (**Figure B.16**, **Table C.3**), suggesting that CH_4 is likely not directly involved in the transport of ^{222}Rn to the shallow subsurface.

6.3. Stray gas migration with proximity to the PMTF

It is possible that stress fractures propagating northwest from the PMTF could alter the occurrence of some chemical tracers at sampling sites closer to the fault, particularly dissolved gases such as CO_2, CH_4, and ^{222}Rn that have already been demonstrated to occur with greater likelihood near fault zones (Etiope & Lombardi, 1995). These fractures have not been previously mapped or characterized; however, the density of stress fractures may increase with some degree of increasing proximity to the fault. As a result, there may be conduit structures near the PMTF through which fluids – particularly dissolved gases – may propagate. In addition, these fractures may allow for greater mixing of shallow groundwater with deeper, meteoric groundwater from recharge areas further northwest of the fault (Lopez & Smith, 1995).

Generally, faults have been shown to convey meteoric water from deeper aquifers with more extensive bedrock interaction (Bouchaou et al, 2008; Chen et al, 2006). This deeper groundwater is generally less oxygenated as a consequence of mineral oxidation along the flow path (Clayton et al, 1966). For sampling sites in Letcher County, however, ORP values, TDS values, and CH_4 concentrations were only weakly correlated with proximity to the PMTF (**Figures B.20** through **B.22, Table C.8**) when analyzed using Spearman's rank-order correlation. This suggests that proximity to the PMTF does not appear to have any major effect on groundwater chemistry in Letcher County.

^{222}Rn occurrence was not correlated with proximity to the PMTF for the 7 sites exhibiting measurable ^{222}Rn concentrations in groundwater (**Table C.8**). This result does not match predictions by previous investigations that attributed fault features with the highest (albeit, not ubiquitous) probability for ^{222}Rn occurrence (Etiope & Lombardi, 1995). One problem, though, was that a limited number of groundwater samples was taken within 0.5 km to the PMTF – the representative threshold within which fault-derived ^{222}Rn has been previously detected by other literature (Etiope & Lombardi, 1995). As a result, a large portion of samples taken for this study might not have been close enough to detect ^{222}Rn (or its carrier gases, such as CH_4 and CO_2) emanating from the fault.

Furthermore, the measured values for all of these tracers (ORP, TDS, CH_4, and ^{222}Rn) exhibited a wide range of variability among sampling sites at all distances from the PMTF. Although model fit cannot be quantified using Spearman's rank-order correlation, it would be unreasonable to accept such low ρ values for any of these correlations without the data appearing

more coherently clustered, especially for sampling sites in near proximity (< 5 km) from the PMTF.

6.4. Oxidation of groundwater with proximity to surface mining

Surface mining has been previously demonstrated to expose minerals present in bedrock (e.g., pyrite, FeS_2) to chemical weathering by meteoric precipitation, subsequently oxidizing shallow groundwater (Evangelou et al, 1998; Eychaner, 1998; Clark 1995). In Letcher County, however, proximity to surface mining proved to be a poor predictor of groundwater ORP values or concentrations of any other chemical tracers (TDS, CH_4, ^{222}Rn, SO_4^{2-}, Na^+, and Cl^-) when tested by linear regression, primarily due to poor model fit (**Table C.9**). However, proximity to surface mining did have a significant effect on groundwater ORP values when alternatively modeled using an analysis of variance test (ANOVA) (**Table C.9**). The main reason for the observed differences between these two analyses (linear regression and ANOVA) is that elevated ORP values were not universal among sampling sites with higher percentages of mining (> 30 %) within a 1 km radius. Instead, only a limited number of groundwater sampling sites with particularly high percentages of mining (> 30 %) within a 1 km radius showed considerably elevated ORP values compared to other sampling sites (**Figures B.24** and **B.25**). While these instances of substantial groundwater oxidation in close proximity to surface mining were not frequent enough to generate a distinctly linear trend in the entire sample population, they were more likely to occur above a given threshold of proximity (i.e., at sampling sites with at least > 30 % area within a 1 km radius mined).

Generally, groundwater sampled appeared to have a higher likelihood of oxidation for sampling sites located closer to surface mining (i.e., sites with > 30% area within a 1 km radius mined; mean ORP = -75 mV) when compared to sites further away from surface mining (i.e., sites with < 30% area within a 1 km radius mined; mean ORP = - 175 mV) (**Figure B.25**). This higher potential for groundwater oxidation closer to mining sites is likely a result of increased infiltration and oxygenation rates in neighboring bedrock. The latter is greatly enhanced by methods of explosive excavation (i.e., dynamite blasting) implemented during surface mining, which increases the secondary permeability of newly exposed strata (Guebert and Gardner, 2001). Additionally, surface mining increases the total surface area of bedrock exposed to infiltration of meteoric precipitation within macropore structures in mountain slopes that have been reconsolidated after excavation (Guebert and Gardner, 2001). Over time, these factors can enhance recharge of shallow oxygenated water.

There are regulatory procedures in place to limit the effects of groundwater oxidation on neighboring aquifers and streams (e.g., capturing and treating discharges from mining sites). Ideally, groundwater oxidation should not occur outside the boundaries of surface mines. The fact that instances of groundwater oxidation were not universally observed throughout the study area suggests the environmental impacts due to surface mining in Letcher County are still somewhat incidental. The likelihood of groundwater oxidation by surface mining occurring (outside the boundaries of a given mine) most likely depends on some additional factor, such as the direction of groundwater flow in relation to mining sites and/or the effective management of surface and groundwater discharges from individual mining sites. However, this conclusion is still largely speculative, because it goes beyond the original methodological scope of this study.

7. CONCLUSIONS

Generally, the chemical and isotope results of this study suggest that hydraulic fracturing for natural gas has had no direct impact on groundwater quality in Letcher County, and that the occurrence of CH_4 and other chemical tracers in sampled groundwater was more affected by shallow processes, such as bedrock dissolution, surface mining, etc. (see **Figure A.6**). The H and O isotope compositions of groundwater sampled within this area suggest and origin derived from shallow recharge of local meteoric precipitation. Two major groundwater types were recognized based on their chemical composition – Type 1 groundwater dominated by high abundances of Na^+, Cl^-, HCO_3^-, and CH_4, and Type 2 groundwater dominated by high abundances of Ca^{2+}, HCO_3^-, Fe^{2+}, and SO_4^{2-}. Based on its measured ORP values, Type 1 groundwater was more reducing compared to Type 2 groundwater, which was more oxidizing. Both water types were similarly influenced by carbonate mineral dissolution as they likely interacted more with bedrock. This differentiation of water types is also similar to previous characterizations of groundwater quality in neighboring counties in Southeast Kentucky (Wunsch, 1992; Minns, 1993).

CH_4 was more common in Type 1 groundwater than in Type 2 groundwater, and the C and H isotope compositions of Type 1 samples showed primarily mixed thermogenic/biogenic signatures. The chemical and isotope compositions of waters with higher concentrations of CH_4 did not appear to have been impacted by stray gas migration or significant mixing with Appalachian Basin brines. This suggests that CH_4 measured in Letcher County was not directly sourced from Devonian shale. Generally, the C and H isotope composition of CH_4 found in this area was found to be similar to that of CH_4 sampled from other Pennsylvanian coal deposits occurring in Kentucky. Given that CH_4 was usually absent in more oxygenated Type 2 groundwater, some amount of CH_4 was likely oxidized by natural processes in shallower environments with higher ORP values (i.e., Type 2 groundwater).

The S isotope compositions of bedrock and groundwater samples showed that groundwater SO_4^{2-} is likely sourced from pyrite oxidation in coal and subsequently undergoes microbial SO_4^{2-} reduction in more reducing environments. Consequently, the measured $\delta^{34}S$ and $\delta^{18}O$ values of groundwater SO_4^{2-} were considerably higher in comparison to the $\delta^{34}S$ values of bedrock sampled from the major geologic formations of Letcher County.

^{222}Rn occurred very infrequently and in relatively low concentrations in sampled groundwater. Therefore, its source was more difficult to conclusively ascertain. Given that groundwater CH_4 was not a result of stray gas migration and that the occurrence of ^{222}Rn and CH_4 were not correlated, it is likely that these two gases were derived from different sources in Letcher County bedrock. Consequently, groundwater CH_4 did not have any influence on any subsequent migration of dissolved ^{222}Rn observed in Letcher County.

Overall, hydraulic fracturing did not appear to significantly increase the likelihood of stray gas migration or the occurrence of either ^{222}Rn or CH_4 in Letcher County groundwater. However, attempts to comprehensively evaluate the environmental impacts of hydraulic fracturing development in Letcher County were also limited by a number of factors. Firstly, it was difficult to find representative sampling sites that were adequately spatially isolated from past hydraulic fracturing activities. Secondly, the diversity of groundwater environments sampled across Letcher County produced large amounts of heterogeneity in the resulting chemical and isotopic data that proved difficult to compare to one another. Thirdly, this study was only able to investigate broad correlative relationships and neglected to analyze specific spatial correlations between factors like groundwater flow direction, domestic well depth, and specific aquifers intersected/sampled.

Furthermore, neighboring processes of fossil fuel extraction (i.e., surface mining of coal) were shown to a higher likelihood of impacting groundwater quality (i.e., by increasing oxygenation of Type 2 groundwater). This subsequently served to increase bedrock dissolution and the likelihood of CH_4 oxidation in shallow environments, which obstructed any attempts to characterize CH_4 at sampling sites in near proximity to surface mining.

Although more difficult to adequately characterize, it is unlikely that stress fractures emanating from the PMTF had any significant effect on groundwater chemistry or processes of stray gas migration across most of Letcher County. Further research documenting the orientation and extent of these fractures would be useful prior to any additional investigation of gas migration processes in near proximity to the PMTF. Additionally, the lack of information about groundwater flow direction, aquifers interrogated, and the depths domestic wells sampled also inhibits specific understanding of spatial correlations with respect to the PMTF.

Given the large variety of environmental and anthropogenic factors that could potentially alter the composition of groundwater throughout Letcher County, future research in this area would likely benefit from a reduction in scale (i.e., more intensive sampling within a smaller area and in relation to fewer of geographic features). This would allow for better isolation and characterization of the hydrogeological flow regimes within which relationships between other tracers are to be delineated. Indeed, a major shortcoming of the sampling methodology of this study was its failure to better characterize and account for heterogeneity in the hydrogeological conditions influencing domestic wells across Letcher County. Future sampling sites should also be more rigorously screened to include consistent, prior water quality and well construction records filed with the state. Knowledge of the depths of wells and aquifers tapped, in concert with information on regional and local groundwater flow directions, would facilitate better separation of sampling locations with respect to different aquifers, and allow differentiation of up-gradient versus down-gradient sources of groundwater contamination. Finally, it would benefit future investigators to survey surrounding counties for suitable control sites absent of any prior gas drilling or coal mining activity. These measures would likely provide more comparable information about various processes controlling water chemistry that, in the end, would better serve any citizens and communities potentially impacted by pollution due to hydraulic fracturing, surface mining, etc.

Beyond the context of Letcher County, further research on hydraulic fracturing should perhaps redirect its focus towards other processes besides stray gas migration (e.g., wastewater disposal) that are now known to be more impactful to water quality. Any future work that does attempt to characterize stray gas migration – especially any efforts relying on the isotope composition of CH_4 as a primary tracer of shale gas – should always take into account the potential for impacts by other anthropogenic and geologic processes. In particular, researchers should be aware of and able to characterize other bedrock sources of CH_4 (e.g., coal) and oxygenation by either microbes or various surface activities (e.g., surface mining). For other research contexts, proximity to surface mining and high abundances of SO_4^{2-} in sampled groundwater might serve as a preliminary indicator that groundwater CH_4 is no longer a reliable environmental tracer, especially for any type of spatial analysis. Therefore, additional alternative tracers (see: Jackson et al, 2012; Warner et al, 2014) should be implemented whenever possible to account for any potential alternation or removal of groundwater CH_4 as a result of either microbial or inorganic oxidation. Furthermore, the concentrations of dissolved noble gases, higher chain hydrocarbons, and the isotope composition of dissolved inorganic carbon (DIC) and SO_4^{2-} can help to delineate major sources of CH_4 in cases where CH_4 may have already undergone alteration in situ (Jackson et al, 2012; Van Stempvoort et al, 2005).

REFERENCES

Annunziatellis, A., Beaubien, S., Bigi, S., Ciotoli, G., Coltella, M., & Lombardi, S. (2008). Gas migration along fault systems and through the vadose zone in the Latera caldera (central Italy): Implications for CO2 geological storage. *International Journal of Greenhouse Gas Control*, *2*(3), 353–372.

Barker, J. F., & Fritz, P. (1981). Carbon isotope fractionation during microbial methane oxidation. *Nature*, *293*(5830), 289–291.

Beauchamp, R. O., Bus, J. S., Popp, J. A., Boreiko, C. J., Andjelkovich, D. A., & Leber, P. (1984). A Critical Review of the Literature on Hydrogen Sulfide Toxicity. *Critical Reviews in Toxicology*, *13*(1), 25–97.

Blodau, C. (2006). A review of acidity generation and consumption in acidic coal mine lakes and their watersheds. *Science of The Total Environment*, *369*(1-3), 307–332.

Böttcher, M. E., Thamdrup, B., & Vennemann, T. W. (2001). Oxygen and sulfur isotope fractionation during anaerobic bacterial disproportionation of elemental sulfur. *Geochimica et Cosmochimica Acta*, *65*(10), 1601–1609.

Bouchaou, L., Michelot, J. L., Vengosh, A., Hsissou, Y., Qurtobi, M., Gaye, C. B., & Zuppi, G. M. (2008). Application of multiple isotopic and geochemical tracers for investigation of recharge, salinization, and residence time of water in the Souss–Massa aquifer, southwest of Morocco. *Journal of Hydrology*, *352*(3-4), 267–287.

Canfield, D. E. (2001). Biogeochemistry of sulfur isotopes. *Stable Isotope Geochemistry, 43, 607-636.*

Carey, D., Dinger, J., Davidson, O. B., Sergeant, R., Taraba, J., Ilvento, T., … Knoth, L. (1993). Quality of Private Ground-water Supplies in Kentucky. Kentucky Geological Survey.

Carey, D. I., & Davidson, O. B., & Hiett, J. K. (2009). Kentucky Coal Production 1790-2001. Kentucky Geological Survey.

Chen, Z., Nie, Z., Zhang, G., Wan, L., & Shen, J. (2006). Environmental isotopic study on the recharge and residence time of groundwater in the Heihe River Basin, northwestern China. *Hydrogeology Journal*, *14*(8), 1635–1651.

Chestnut, D. R., Eble, C. F., Greb, S. F., & Dever, G. R. (1998). Geology of the Pound Gap Roadcut, Letcher County, Kentucky. Kentucky Society of Professional Geologists.

Cheung, K., Klassen, P., Mayer, B., Goodarzi, F., & Aravena, R. (2010). Major ion and isotope geochemistry of fluids and gases from coalbed methane and shallow groundwater wells in Alberta, Canada. *Applied Geochemistry, 25, 1307–1329.*

Chi, G., & Savard, M. M. (1997). Sources of basinal and Mississippi Valley-type mineralizing brines: mixing of evaporated seawater and halite-dissolution brine. *Chemical Geology, 143, 121-125.*

Christian, K., Lautz, L. K., Hoke, G. D., Lu, Z., Siegel, D. I., & Kessler, J. (2014, October 22). Spatial parameters controlling salinity and dissolved methane concentrations in private wells prior to hydraulic fracturing. Oral presented at the Geological Society of America 2014 Annual Meeting, Vancouver, BC, Canada.

Clark, K. I., & Fritz P. (1997). Environmental Isotopes in Hydrogeology. Lewis Publishers, New York.

Clarke, L. B. (1995). Coal Mining and Water Quality. IEA Coal Research, London.

Clayton, J. L. (1998). Geochemistry of coalbed gas – A review. *International Journal of Coal Geology, 35, 159–173.*

Clayton, R. N., Friedman, I., Graf, D. L., Mayeda, T. K., Meents, W. F., & Shimp, N. F. (1966). The origin of saline formation waters: 1. Isotopic composition. *Journal of Geophysical Research*, *71*(16), 3869–3882.

Conant, L. C., & Swanson, V. E. (1961) Chattanooga shale and related rocks of central Tennessee and nearby areas. United States Geological Survey.

Crawley, M. J. (2007). *The R book*. Chichester, England; Hoboken, N.J: Wiley.

Davisson, M. L., Presser, T. S., & Criss, R. E. (1994). Geochemistry of tectonically expelled fluids from the northern Coast ranges, Rumsey Hills, California, USA. *Geochimica et Cosmochimica Acta*, *58*(7), 1687–1699.

De Pater, C. J., & Baisch, S. (2011, November 2). Geomechanical Study of Bowland Shale Seismicity. Cuadrilla Recources Ltd.

Detmers, J., Bruchert, V., Habicht, K. S., & Kuever, J. (2001). Diversity of Sulfur Isotope Fractionations by Sulfate-Reducing Prokaryotes. *Applied and Environmental Microbiology*, *67*(2), 888–894.

Dresel, P. E. & Rose, A. W. (2010). Chemistry and origin of oil and gas well brines in Western Pennsylvania. Pennsylvania Geological Survey.

Eltschlager, K. K., Hawkins, J. W., Ehler, W. C., & Baldassare, F. (2001). Technical measures for the investigations and mitigation of fugitive methane hazards in areas of coal mining: Pittsburg, PA. US Department of the Interior, Office of Surface Mining Reclamation and Enforcement, Appalachian Regional Coordinating Center.

Etiope, G., & Lombardi, S. (1995). Evidence for radon transport by carrier gas through faulted clays in Italy. *Journal of Radioanalytical and Nuclear Chemistry Articles*, *193*(2), 291–300.

Etiope, G., & Martinelli, G. (2002). Migration of carrier and trace gases in the geosphere: an overview. *Physics of the Earth and Planetary Interiors*, *129*(3-4), 185–204.

Evangelou, V. P. (1995). Pyrite Oxidation and its Control. CRC Press, New York.

Evangelou, V. P., Geller, A., Klapper, H., & Salomons, W. (1998). Pyrite chemistry: the key for abatement of acid mine drainage. *Acidic Mining Lakes: Acid Mine Drainage, Limnology and Reclamation*, 197–222.

Eychaner, J. H. (1998). Progress of environmental studies in coal mining areas of western Pennsylvania and central West Virginia. United States Geological Survey.

Fisher, K., & Warpinski, N. (2012). Hydraulic-Fracture-Height Growth: Real Data. *SPE Production & Operations*.

Fletcher, J. B., & Sykes, L. R. (1977). Earthquakes related to hydraulic mining and natural seismic activity in western New York State. *Journal of Geophysical Research*, *82*(26), 3767–3780.

Flohr, K., & Appelman, E. H. (1968). The resistance of radon to oxidation in aqueous solution. *Journal of the American Chemical Society*, *90*(13), 3584–3584.

Friberg, P. A., Besana-Ostman, G. M., & Dricker, I. (2014). Characterization of an Earthquake Sequence Triggered by Hydraulic Fracturing in Harrison County, Ohio. *Seismological Research Letters*, *85*(6), 1295–1307.

Gall, I. K., Ritzi, R. W., Baldwin, A. D., Pushkar, P. D., Carney, & C. K., Talnagi, J. F. (1995) The correlation between bedrock uranium and dissolved radon in ground water of a fractured carbonate aquifer in Southwestern Ohio. *Ground Water, 33(2), 197–206.*

Gat, J. R. (1996). Oxygen and hydrogen isotopes in the hydrological cycle. *Annual Review: Earth and Planetary Science, 24, 225–262.*

Guebert, M. D., & Gardner,T. W. (2001). Macropore flow on a reclaimed surface mine: infiltration and hillslope hydrology. *Geomorphology, 39(3-4), 151–169.*

Gurevich, A. E., Endres, B. L., Robertson, J. O., & Chilingar, G. V. (1993). Gas migration from oil and gas fields and associated hazards. *Journal of Petroleum Science and Engineering*, *9*(3), 223–238.

Head, I. M., Jones, D. M., & Larter, S. R. (2003). Biological activity in the deep subsurface and the origin of heavy oil. *Nature*, *426*(6964), 344–352.

Holland, A. (2011, August). Examination of Possibly Induced Seismicity from Hydraulic Fracturing in the Eola Field, Garvin County, Oklahoma. Oklahoma Geological Survey.

Hunt, A. G., Darrah, T. H., & Poreda, R. J. (2012). Determining the source and genetic fingerprint of natural gases using noble gas geochemistry: A northern Appalachian Basin case study. *AAPG Bulletin*, *96*(10), 1785–1811.

Jackson, R. (2014, October 21). The water intensity and water quality footprint of shale gas extraction. Oral presented at the Geological Society of America 2014 Annual Meeting, Vancouver, BC, Canada.

Jackson, R. B., Vengosh, A., Darrah, T. H., Warner, N. R., Down, A., Poreda, R. J., & Karr, J. D. (2013). Increased stray gas abundance in a subset of drinking water wells near Marcellus shale gas extraction. *Proceedings of the National Academy of Sciences*, *110*(28), 11250–11255.

Johnson, D. B. (2003). Chemical and microbiological characteristics of mineral spoils and drainage waters at abandoned coal and metal mines. *Water Air Soil Pollution: Focus*, *3*, 47–66.

Johnson, D. B., & Hallberg, K. B. (2003). The microbiology of acidic mine waters. *Research in Microbiology*, *154*(7), 466–473.

Kaiser, E. P., King, R. U., Wilmarth, V. R., Stugard, F., Wyant, D. G., Gott, G. R., & others. (1983). Selected papers on uranium deposits in the United States. United States Geological Survey.

Kampbell, D. H., & Vandegrift, S. A. (1998). Analysis of Dissolved Methane, Ethane, and Ethylene in Ground Water by a Standard Gas Chromatographic Technique. *Journal of Chromatographic Science*, *36*(5), 253–256.

Kendall, C., & Coplen, T. B. (2001). Distribution of oxygen-18 and deuterium in river waters across the United States. *Hydrological Processes*, *15*(7), 1363–1393.

Kentucky Geological Survey (KGS). (2014). *Map Information Service*. Kentucky Geological Survey, ESRI.

Kentucky Mesonet. (2014). 2014 Yearly Precipitation Totals Table. Kentucky Mesonet.

Kesler, S. E., Martini, A. M., Appold, M.S., Walter, L. M., Huston, T. J., & Furman, F. C. (1996). Systematics of fluid inclusions from Mississippi Valley-type deposits, Appalachian Basin: Constraints on solute origin and migration paths. *Geochimica et Cosmochimica Acta, 60(2), 225-233.*

Knöller, K., Trettin, R., & Strauch, G. (2005). Sulfur cycling in the drinking water catchment area of Torgau-Mockritz (Germany): insights from hydrochemical and stable isotope investigations. *Hydrologic. Proc., 19, 3445-3465.*

Kolker, A., & Finkelman, R. B. (1998). Potentially Hazardous Elements in Coal: Modes of Occurrence and Summary of Concentration Data for Coal Components. *Coal Preparation*, *19*(3-4), 133–157.

Krouse, H. R., & Grinenko, V. A. (1991). Stable Isotopes: Natural and Anthropogenic Sulphur in the Environment. John Wiley & Sons, Hoboken, New Jersey.

Lautz, L. K., Hoke, G. D., Lu, Z., Siegel, D. I., Christian, K., & Kessler, J. (2014, October 22). Fingerprinting sources of salinity to aquifers overlying shale plays using publically available background water quality data and multivariate stastistical methods. Oral presented at the Geological Society of America 2014 Annual meeting, Vancouver, BC, Canada.

Lewis, M. (2013). Letcher County Water $ Sewer District Water Quality Report for year 2013. Letcher County Water & Sewer District.

López, D. L., & Smith, L. (1995). Fluid Flow in Fault Zones: Analysis of the Interplay of Convective Circulation and Topographically Driven Groundwater Flow. *Water Resources Research*, *31*(6), 1489–1503.

Mahur, A. K., Kumar, R., Mishra, M., Sengupta, D., & Prasad, R. (2008). An investigation of radon exhalation rate and estimation of radiation doses in coal and fly ash samples. *Applied Radiation and Isotopes*, *66*(3), 401–406.

McGrain, P. (1983). The Geologic Story of Kentucky. Kentucy Geological Survey.

Miller, R. L. (1973). Where and why of Pine Mountain and other major fault planes, Virginia, Kentucky, and Tennessee. *American Journal of Science*, *273A*, 353–371.

Minns, S. (1993). Conceptual model of local and regional groundwater flow in the eastern Kentucky coal field. Kentucky Geological Survey, University of Kentucky, Lexington.

Mitra, S. (1988). Three dimensional geometry and kinematic evolution of the Pine Mountain thrust system, southern Appalachians. *Geological Society of America Bulletin*, *100*, 72–95.

Molofsky, L. J., Connor, J. A., Wylie, A. S., Wagner, T., & Farhat, S. K. (2013). Evaluation of Methane Sources in Groundwater in Northeastern Pennsylvania. *Groundwater*, *51*(3), 333–349.

National Water Information System (NWIS). (2014). USGS Gauge Record 03277300 North Fork Kentucky River at Whitesburg, KY. United States Geological Survey.

Noger, M. C. (1988). Geologic map of Kentucky: sesquicentennial edition of the Kentucky Geological Survey. United States Geological Survey and Kentucky Geological Survey.

Nuttall, B. C. (2013). Oil and Gas History of Kentucky. Kentucky Geological Survey.

Ormsbee, L., & Zechman, E. (2001, February). Letcher County Water Quality Assessment. The University of Kentucky Water Research Institute.

Osborn, S. G., & McIntosh, J.C. (2010). Chemical and isotopic tracers of the contribution of microbial gas in Devonian organic-rich shales and reservoir sandstones, northern Appalachian Basin. *Applied Geochemistry 25: 456-471.*

Osborn, S. G., Vengosh, A., Warner, N. R., & Jackson, R. B. (2011). Methane contamination of drinking water accompanying gas-well drilling and hydraulic fracturing. *Proceedings of the National Academy of Sciences*, *108*(20), 8172–8176.

Panno, S. V., Hackley, K. C., Hwang, H. H., Greenberg, S. E., Krapac, I. G., Landsberger, S., & O'Kelly, D. J. (2006). Characterization and Identification of Na-Cl Sources in Ground Water. *Ground Water*, *44*(2), 176–187.

Passo, C. J., & Cook, G. T. (1994). Handbook of environmental liquid scinitillation spectrometry: A compilation of theory and methods. Packard Instrument Company, Meriden, Connecticut.

Penna, D., Stenni, B., Šanda, M., Wrede, S., Bogaard, T. A., Gobbi, A., & Chárová, Z. (2010). On the reproducibility and repeatability of laser absorption spectroscopy measurements for δ²H and δ¹⁸O isotopic analysis. *Hydrology and Earth System Sciences*, *14*(8), 1551–1566.

Plummer, L. N., Busby, J. F., Lee, R. W., & Hanshaw, B. B. (1990). Geochemical Modeling of the Madison Aquifer in Parts of Montana, Wyoming, and South Dakota. *Water Resources Research*, *26*(9), 1981–2014.

Quispe, D., Perez-Lopez, R., Silva, L. F. O., & Nieto, J. M. (2011) Changes in mobility of hazardous elements during coal combustion in Santa Catarina power plant (Brazil). *Fuel, 94, 495–503.*

Sacks, L. A., Herman, J. S., & Kauffman, S. J. (1995). Controls on High Sulfate Concentrations in the Upper Floridan Aquifer in Southwest Florida. *Water Resources Research*, *31*(10), 2541–2551.

Schoell, M. (1980). The hydrogen and carbon isotopic composition of methane from natural gases of various origins. *Geochimica et Cosmochimica Acta*, *44*(5), 649–661.

Scott, A. G. (1994). Radon Sources, Radon Ingress, and Models. *Radon Protection Dosimetry*, *56*(1-4), 145–149.

Sharp, Z. D. (2007). Principles of Stable Isotope Geochemistry. Pearson Prentice Hall, Upper Saddle River, New Jersey.

Sheets, C. J., & Kozar, M. D. (n.d.). Ground-water quality in the Appalachian Plateaus, Kanawha River Basin, West Virginia. United States Geological Survey.

Siegel, D. I., Smith, B., Perry, A. E., & Bothun, R. (2014, October 22). The controls over the natural occurrence of methane in potable groundwater in the Appalachian Basin. Oral presented at the Geological Society of America 2014 Annual Meeting, Vancouver, BC, Canada.

Sokal, R. R., & Oden, N. L. (1978). Spatial autocorrelation in biology: 1. Methodology. *Biological Journal of the Linnean Society*, *10*(2), 199–228.

Strapoc, D., Mastalerz, M., Eble, C., & Schimmelmann, A. (2007). Characterization of the origin of coalbed gases in southeastern Illinois Basin by compound-specific carbon and hydrogen stable isotope ratios. *Organic Geochemistry, 38, 267–287.*

Studley, S. A., Ripley, E. M., Elswick, E. R., Dorais, M. J., Fong, J., Finkelstain, D., & Pratt, L. M. (2002). Analysis of sulfides in whole rock matrices by elemental analyzer-continuous flow isotope ratio mass spectrometry. *Chemical Geology,* 192, 141-148.

Szynkiewicz, A., Moore, C. H., Glamoclija, M., & Pratt, L. M. (2009). Sulfur isotope signatures in gypsiferous sediments of the Estancia and Tularosa Basins as indicators of sulfate sources, hydrological processes, and microbial activity. *Geochimica et Cosmochimica Acta*, *73*(20), 6162–6186.

Szynkiewicz, A., Talon Newton, B., Timmons, S. S., & Borrok, D. M. (2012). The sources and budget for dissolved sulfate in a fractured carbonate aquifer, southern Sacramento Mountains, New Mexico, USA. *Applied Geochemistry*, *27*(8), 1451–1462.

Tilley, B., McLellan, S., Hiebert, S., Quartero, B., Veilleux, B., & Muehlenbachs, K. (2011). Gas isotope reversals in fractured gas reservoirs of the western Canadian Foothills: Mature shale gases in disguise. *AAPG Bulletin*, *95*(8), 1399–1422.

Valentine, D. L. (2002). Biogeochemistry and microbial ecology of methane oxidation in anoxic environments: a review. *Antonie van Leeuwenhoek*, *81*(1-4), 271–282.

Van Stempvoort, D., Maathuis, H., Jaworski, E., Mayer, B., & Rich, K. (2005). Oxidation of fugitive methane in ground water linked to bacterial sulfate reduction. *Ground Water*, *43*(2), 187–199.

Vengosh, A., Jackson, R. B., Warner, N., Darrah, T. H., & Kondash, A. (2014). A Critical Review of the Risks to Water Resources from Unconventional Shale Gas Development and Hydraulic Fracturing in the United States. *Environmental Science & Technology*, *48*(15), 8334–8348.

Warner, N. R., Christie, C. A., Jackson, R. B., & Vengosh, A. (2013). Impacts of Shale Gas Wastewater Disposal on Water Quality in Western Pennsylvania. *Environmental Science & Technology*, *47*(20), 11849–11857.

Warner, N. R., Darrah, T. H., Jackson, R. B., Millot, R., Kloppmann, W., & Vengosh, A. (2014). New tracers identify hydraulic fracturing fluids and accidental releases from oil and gas operations. *Environmental Science & Technology 48(21), 12552–12560.*

Warner, N. R., Jackson, R. B., Darrah, T. H., Osborn, S. G., Down, A., Zhao, K., & Vengosh, A. (2012). Geochemical evidence for possible natural migration of Marcellus Formation brine to shallow aquifers in Pennsylvania. *Proceedings of the National Academy of Sciences*, *109*(30), 11961–11966.

Westrich, J. T., & Berner, R. A. (1984). The role of sedimentary organic matter in bacterial sulfate reduction: The G model tested. *American Society of Limnology and Oceanography*, *29*(2), 236–249.

William Carey, J., Svec, R., Grigg, R., Zhang, J., & Crow, W. (2010). Experimental investigation of wellbore integrity and CO2–brine flow along the casing–cement microannulus. *International Journal of Greenhouse Gas Control*, *4*(2), 272–282.

Winfrey, M. R., & Zeikus, J. G. (1977). Effect of sulfate on carbon and electron flow during microbial methanogenesis in freshwater sediments. *Applied Environmental Microbiology*, *33*(2), 275–281.

Wood, W. W., Kraemer, T. F., & Shapiro, A. (2004). Radon (222Rn) in Ground Water of Fractured Rocks: A Diffusion/Ion Exchange Model. *Ground Water*, *42*(4), 552–567.

Wunsch, D. R. (1992). Ground water geochemistry and its relationship to the flow system at an unmined site in the Eastern Kentucky Coal Field. Kentuchy Geological Survey, University of Kentucky, Lexington.

Yarnes, C. (2013). δ^{13}C and δ^{2}H measurement of methane from ecological and geological sources by gas chromatography/combustion/pyrolysis isotope-ratio mass spectrometry: δ^{13}C and δ^{2}H measurement of methane. *Rapid Communications in Mass Spectrometry*, *27*(9), 1036–1044.

APPENDICES

APPENDIX A: MAPS AND CONCEPTUAL MODELS

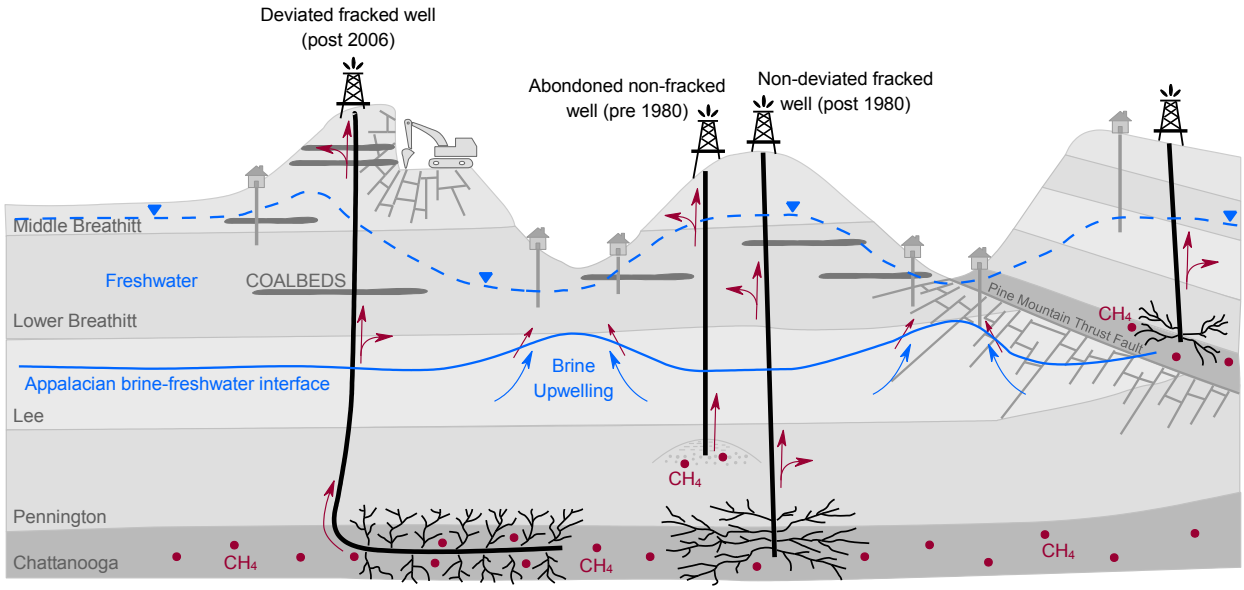

Figure A.1. Conceptual model of Letcher County, Kentucky depicting: 1) major rock and groundwater facies, 2) domestic wells withdrawing groundwater primarily from the Middle and Lower Breathitt Formations, 3) various fractured natural gas wells (i.e., deviated (horizontally drilled) and non-deviated (vertically drilled)) and non-fractured natural gas wells withdrawing CH_4 primarily from the Chattanooga Shale and the Pennington Formation, 4) surface coal mines excavating either the Middle or Lower Breathitt Formations, 5) hypothesized sources of CH_4 (the Chattanooga Shale, Appalachian Basin Brine, and coal beds in the Middle and Lower Breathitt), 6) possible routes of stray gas migration (illustrated in red), and 7) possible stress fractures emanating from the Pine Mountain Thrust Fault (PMTF).

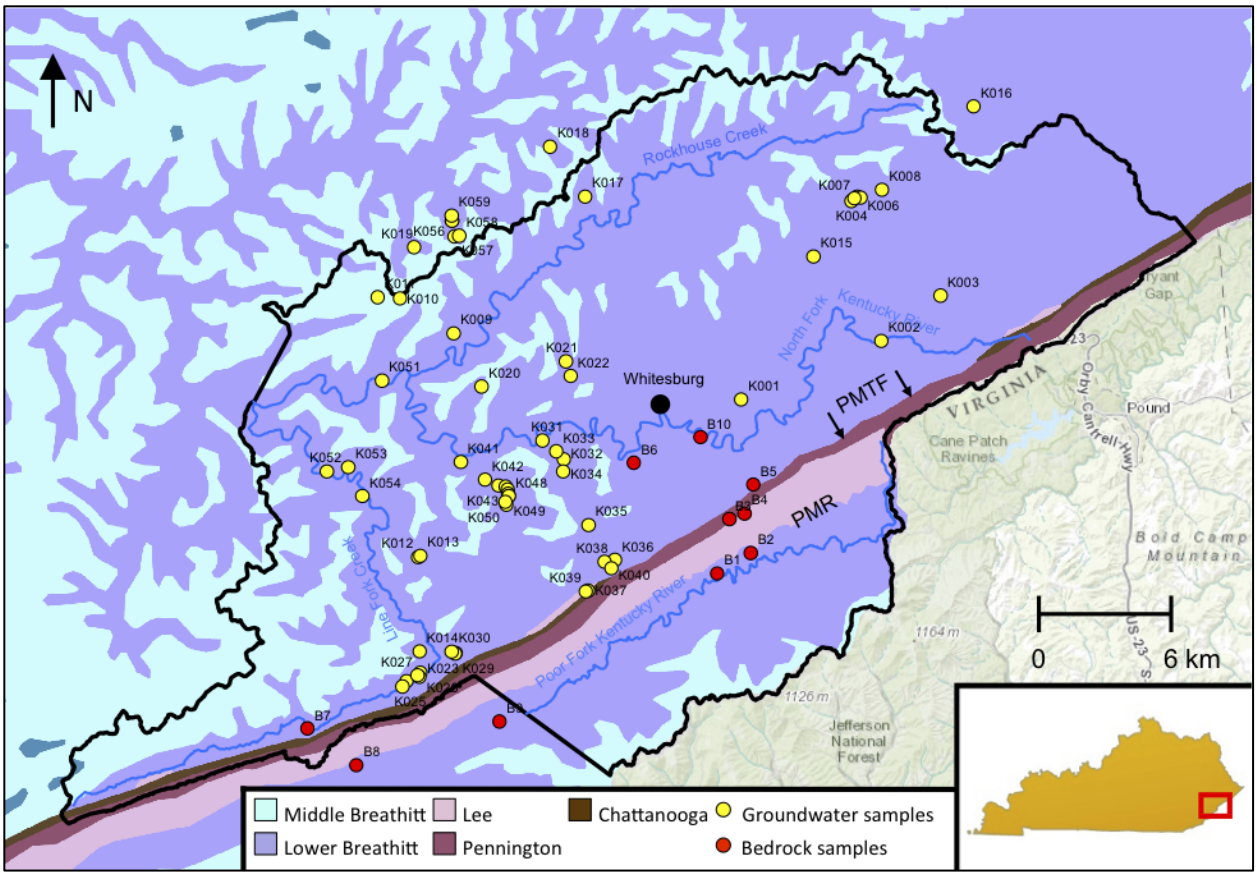

Figure A.2. Geologic map of Letcher County, Kentucky. Geographic features shown include: third order streams (blue lines), groundwater sampling sites (yellow dots), bedrock sampling sites (red dots), the Pine Mountain Thrust Fault (PMTF), and Pine Mountain Ridge (PMR). Major rock formations shown include: Middle Breathitt (light blue), Lower Breathitt (purple), Lee (pink), Pennington (maroon), and Chattanoogia Shale (brown). Original images for this map were provided by the Kentucky Geological Survey (KGS, 2014).

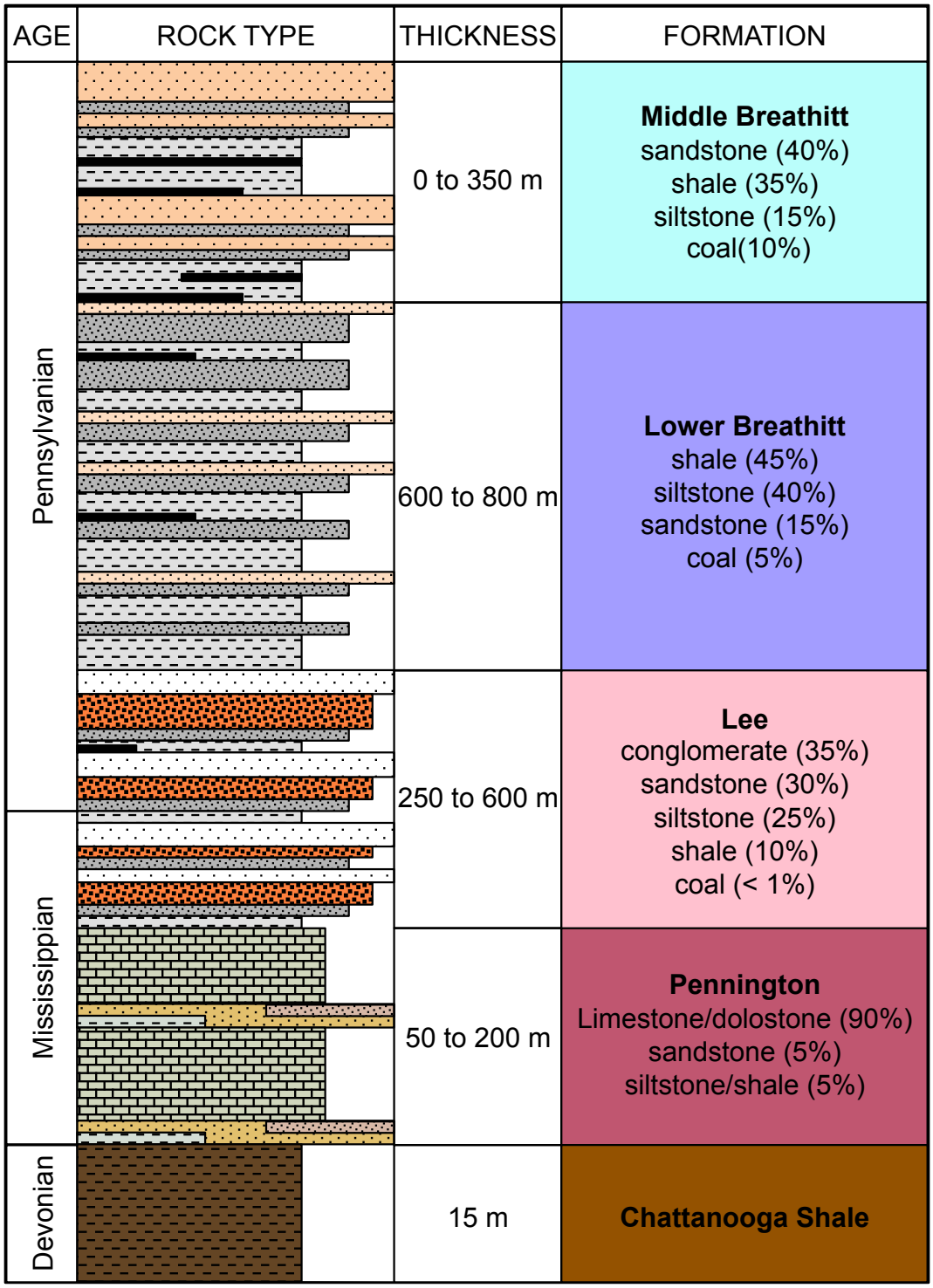

Figure A.3. Stratigraphic column of Letcher County bedrock. Major rock formations shown include: Middle Breathitt (light blue), Lower Breathitt (purple), Lee (pink), Pennington (maroon), and Chattanoogia Shale (brown).

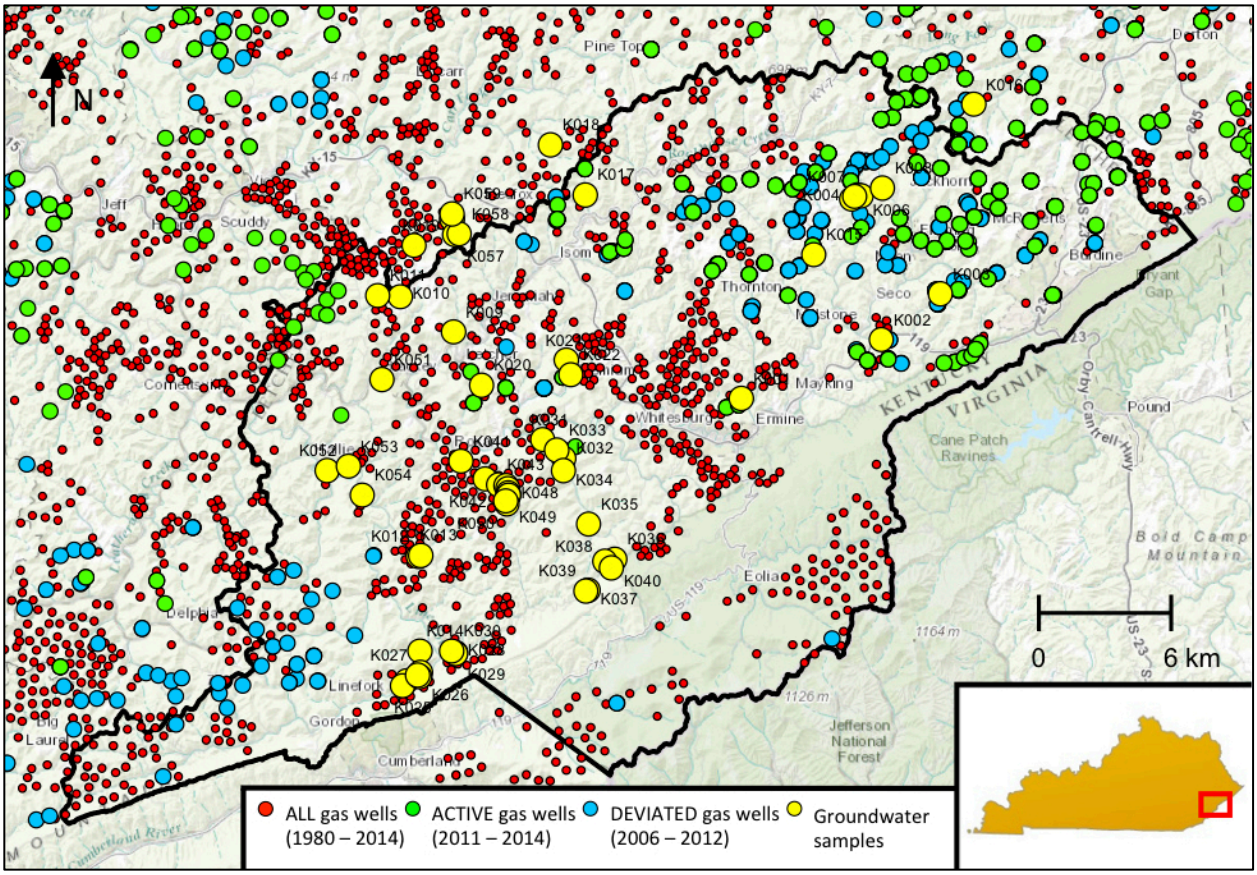

Figure A.4. Map of all hydraulically fractured natural gas wells in Letcher County, Kentucky. Major gas well categories shown include: 1) all natural hydraulically fractured natural gas wells permitted after 1980 (ALL, red dots), 2) all deviated hydraulically fractured natural gas wells permitted between 2006 and 2012 (DEVIATED, blue dots), and 3) all currently actively hydraulically fractured natural gas wells permitted since 2011 (ACTIVE, green dots). This map also shows the location of all groundwater sampling sites (yellow dots). Original images and gas well location data for this map were provided by the Kentucky Geological Survey (KGS, 2014).

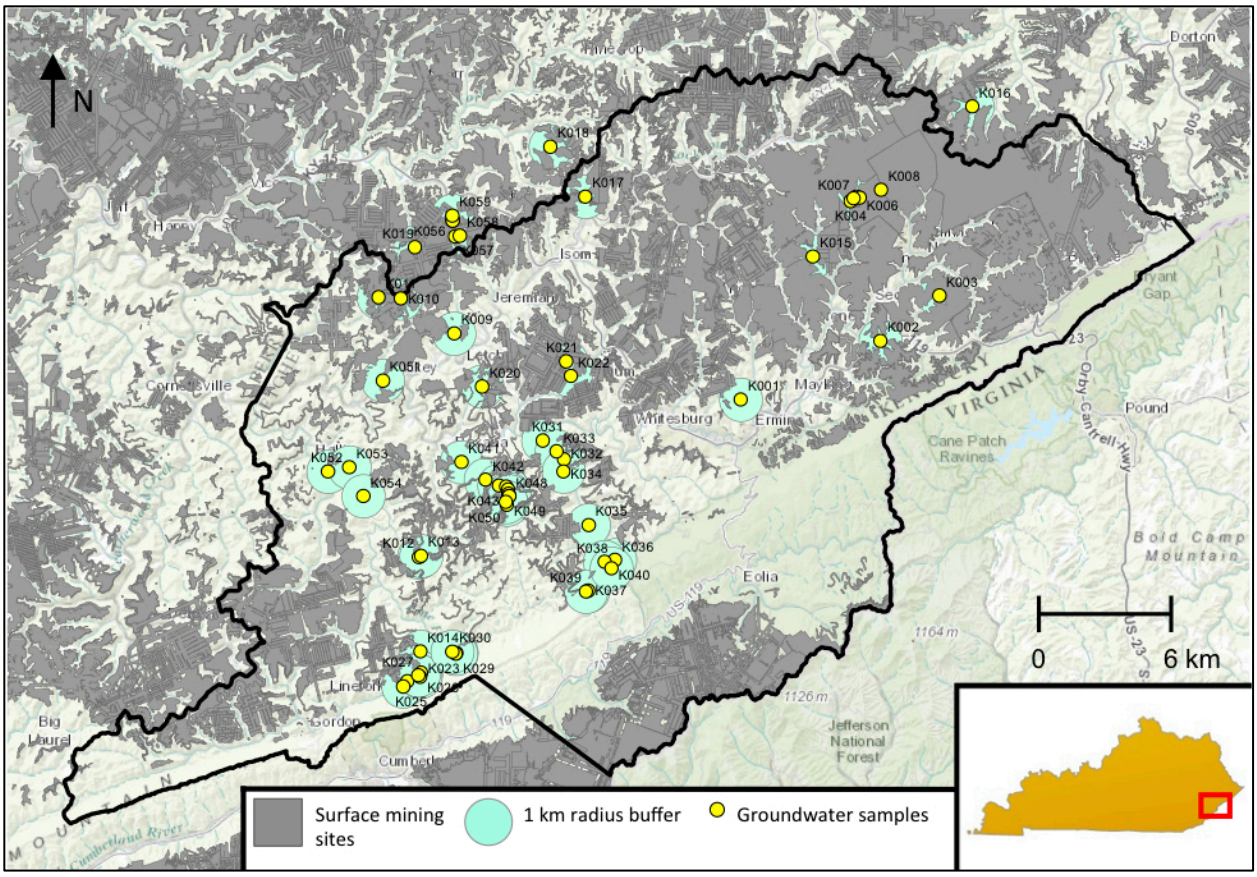

Figure A.5. Map showing the locations of surface coal mining (grey polygons) in Letcher County, Kentucky. This map also shows the location of all groundwater sampling sites (yellow dots), as well the 1 km radius (teal circles) within which the total percent of surface mining surrounding each groundwater sampling site was measured for proximity analysis (**Table C.9**).

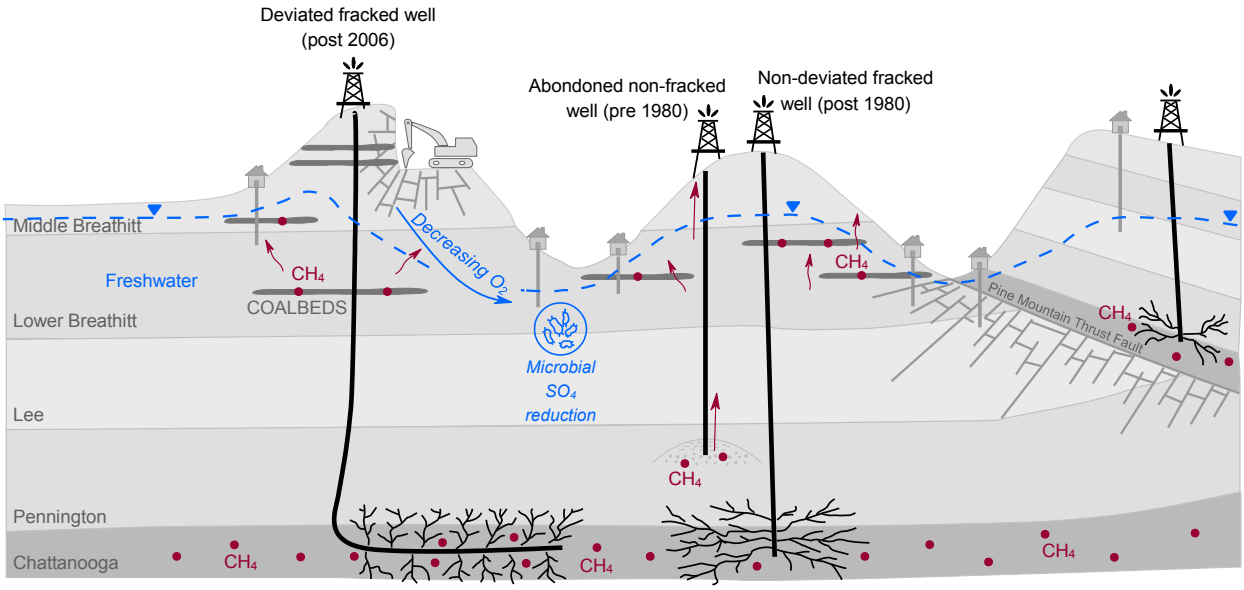

Figure A.6. Final conceptual model of processes controlling chemical composition of groundwater in Letcher County, Kentucky. CH_4 is likely sourced from shallow Pennsylvanian coal beds, and is not directly related to stray gas migration from deeper Devonian shale. CH_4 may be further altered in situ as a result of either microbial oxidation in anaerobic environments or inorganic oxidation in groundwater oxygenated as a result of surface mining. Type 1 groundwater containing CH_4 at concentrations > 1 mg/L appeared not to have mixed significantly with Appalachian Basin Brine. Furthermore, hydraulic fracturing was not shown to have any significant impact on groundwater CH_4 concentrations.

APPENDIX B: FIGURES.

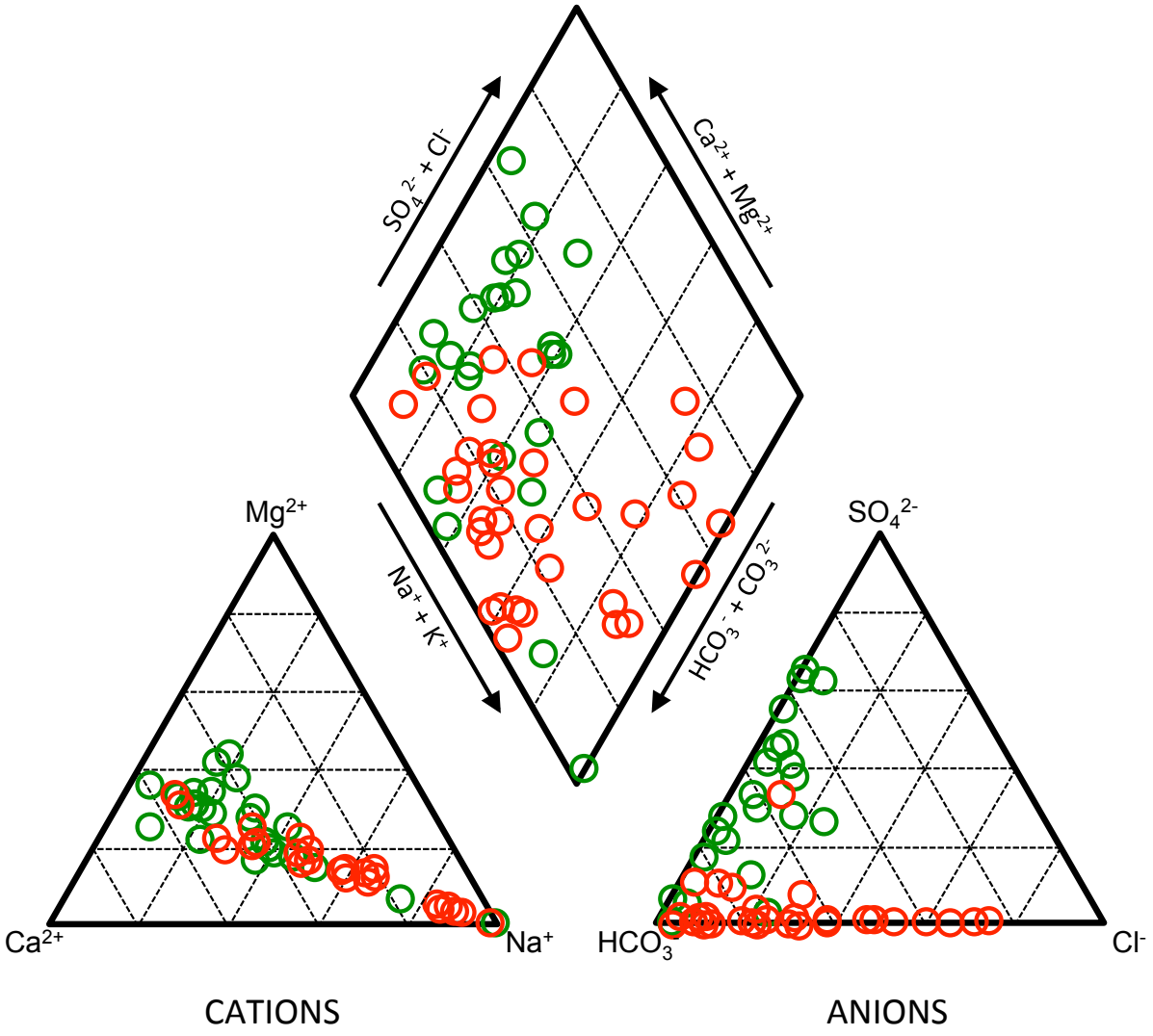

Figure B.1. Piper Diagram. Red points represent sampling sites where CH_4 was present at concentrations > 1 mg/L (Type 1 groundwater). Green points represent sampling sites where CH_4 concentrations were < 1 mg/L (Type 2 groundwater).

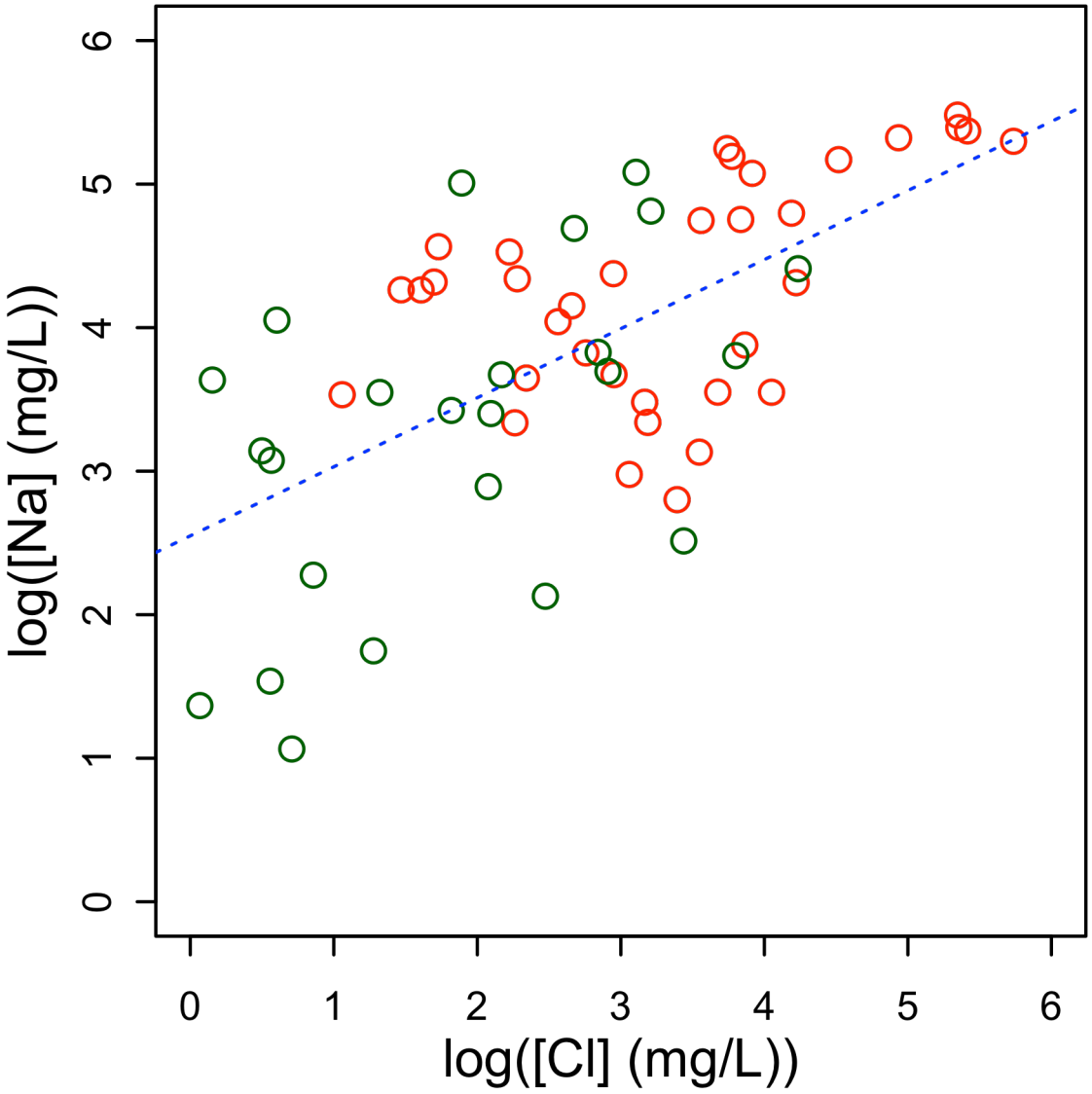

Figure B.2. Na concentrations as a function of Cl concentrations. Analyzed using linear regression (R2 = 0.70, P << 0.0001, regression line in blue). Na and Cl concentrations were logarithmically transformed to meet the assumption of normality required by linear regression. Type 1 groundwater samples are in red, and Type 2 groundwater samples are in green.

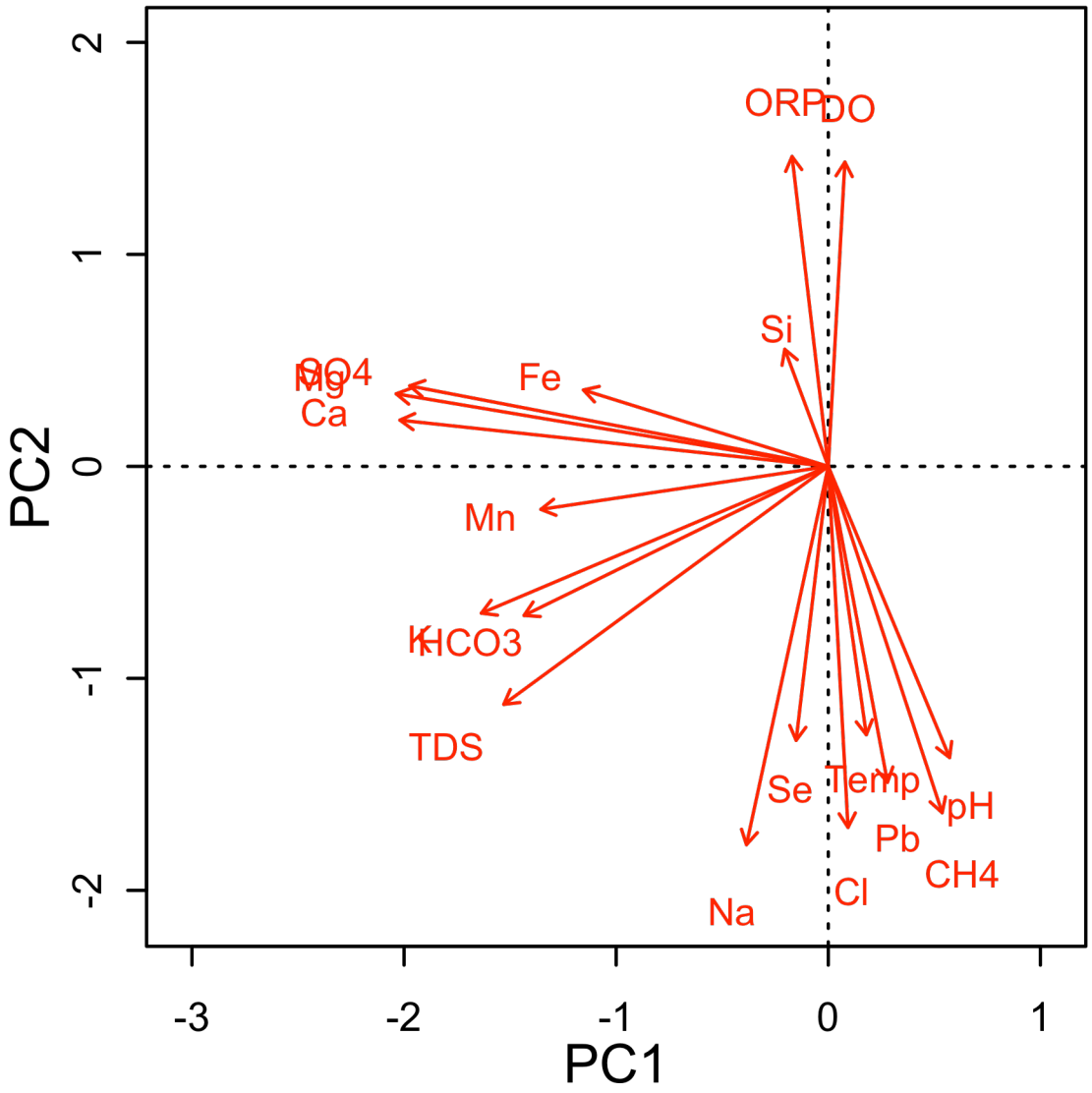

Figure B.3. Principle component analysis of chemical data for groundwater sampled. Type 1 groundwater ($Na/Cl/CH_4$ dominant) is oriented along PC2. Type 2 groundwater ($Ca/Mg/SO_4$ dominant) is oriented along PC1. HCO_3 and K are oriented between both axes and common in both water types.

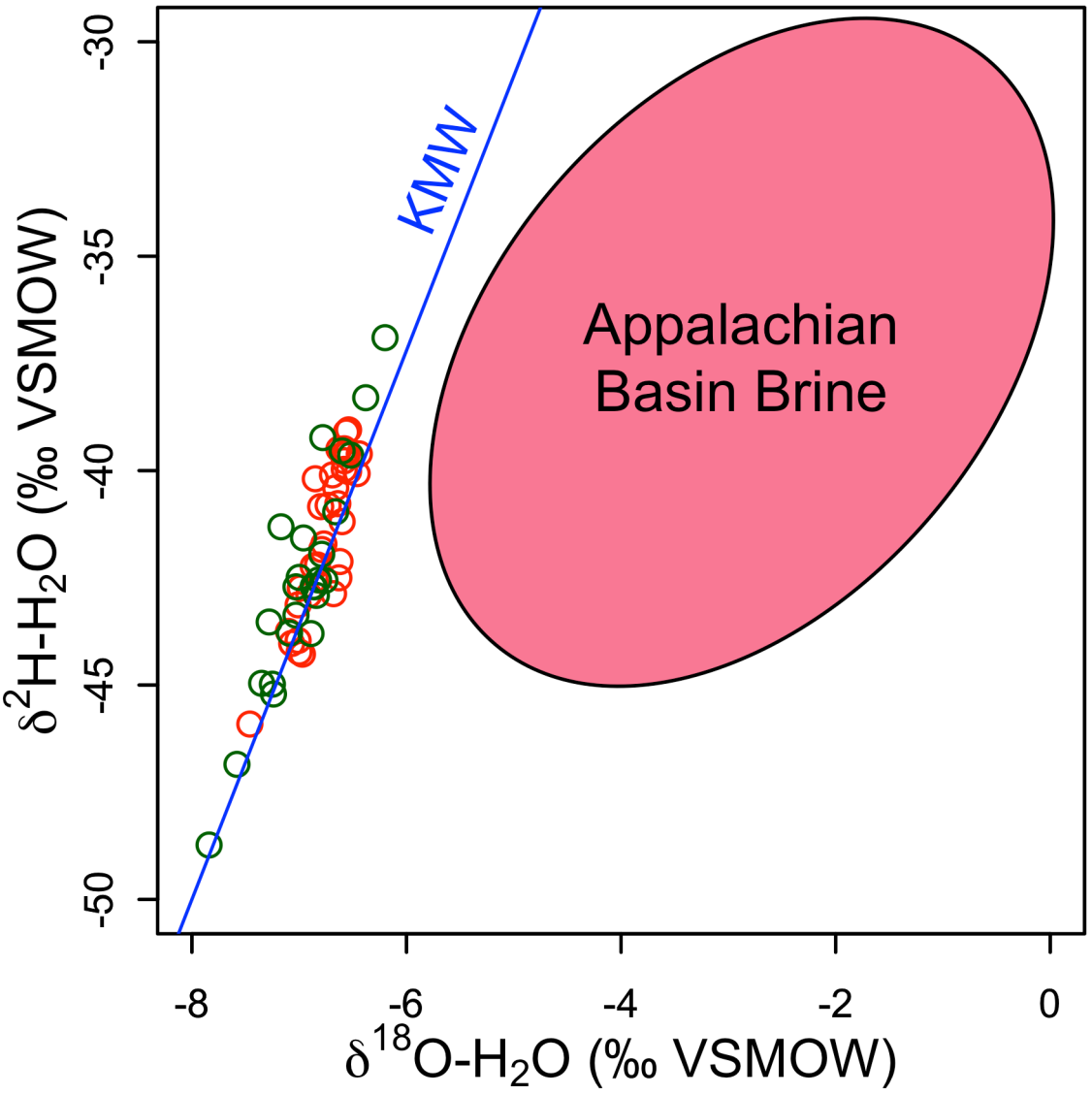

Figure B.4. δ^2H-H_2O as a function of δ^{18}O-H_2O for groundwater sampled in Letcher County. For comparison, sampled values have been plotted alongside mean isotope values for Kentucky meteoric water (KMW, in blue), and the range of values reported for Appalachian Basin brine (in pink). Type 1 groundwater samples are in red, and Type 2 groundwater samples are in green.

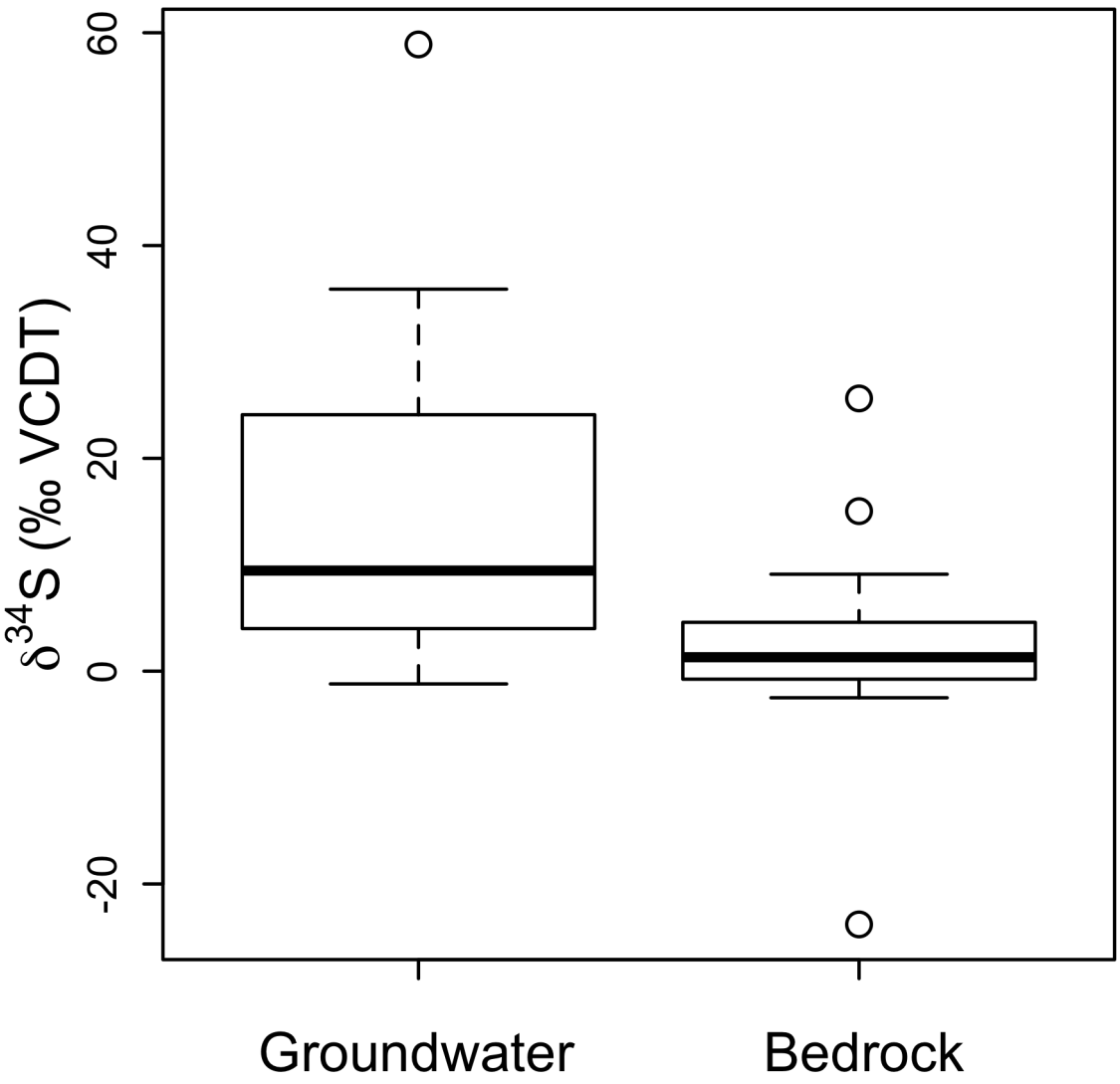

Figure B.5. δ^{34}S-SO_4 of groundwater SO_4 compared to δ^{34}S of bedrock. Mean values of each sample population were compared using an ANOVA ($F_{1,54} = 17.96$, $P < 0.0001$).

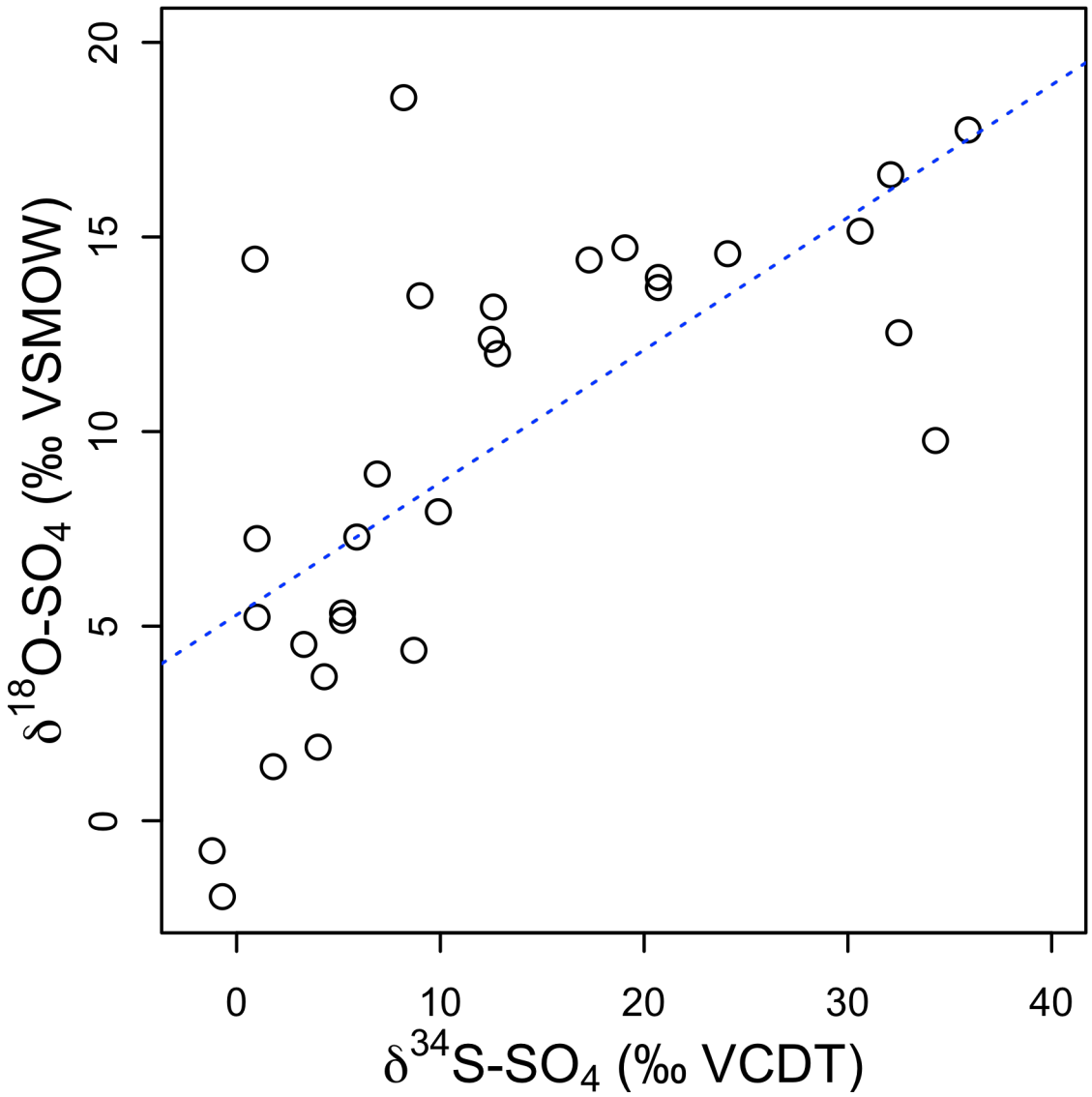

Figure B.6. δ^{18}O-SO_4 as a function of δ^{34}S-SO_4. Analyzed using linear regression ($R^2 = 0.47$, $P < 0.0001$, regression line in blue).

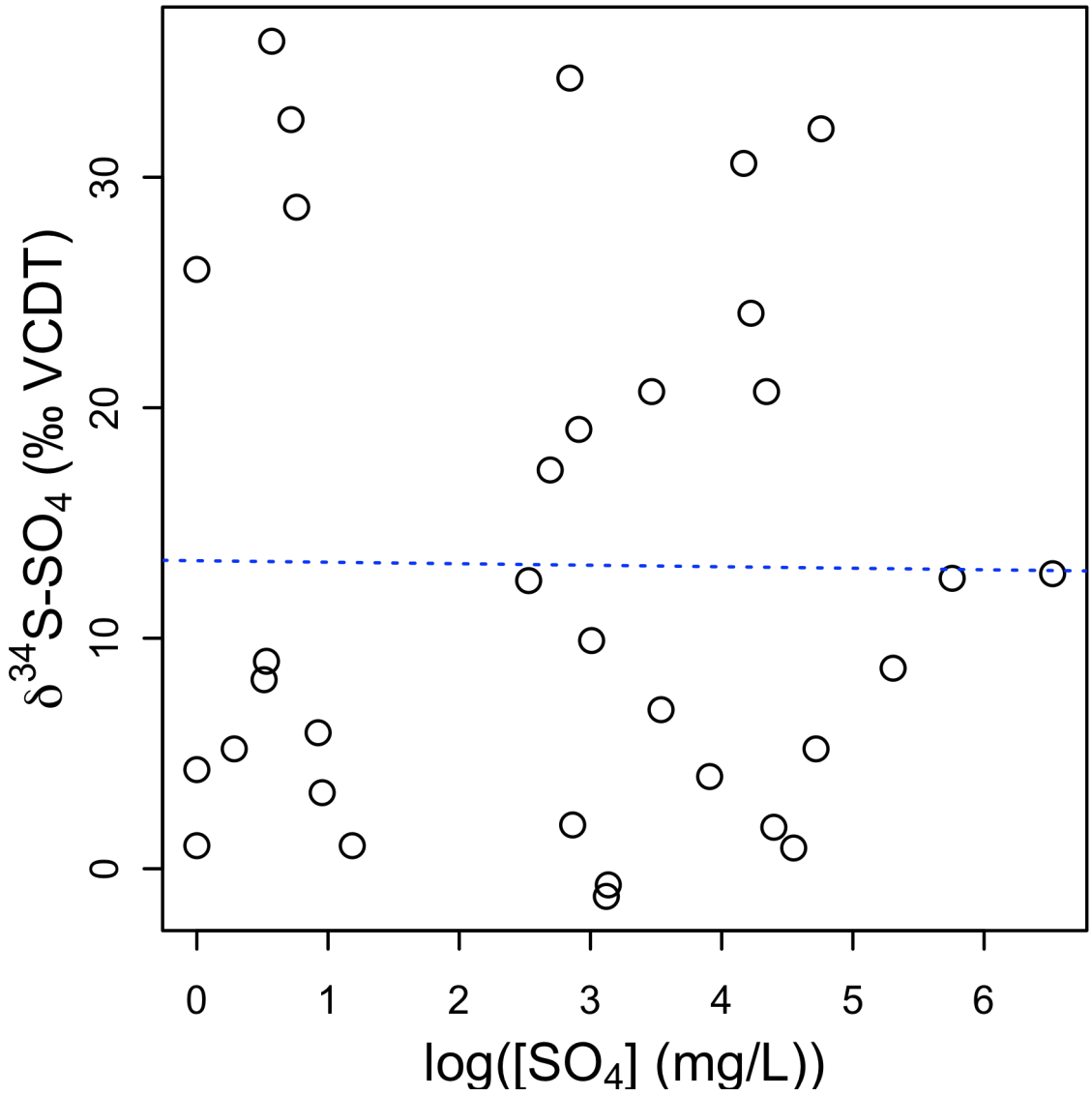

Figure B.7. δ^{34}S-SO_4 as a function of SO_4 concentrations. Analyzed using linear regression (R^2 = 0.19, P = 0.011, regression line in red). SO_4 concentrations were logarithmically transformed to meet the assumption of normality required by linear regression.

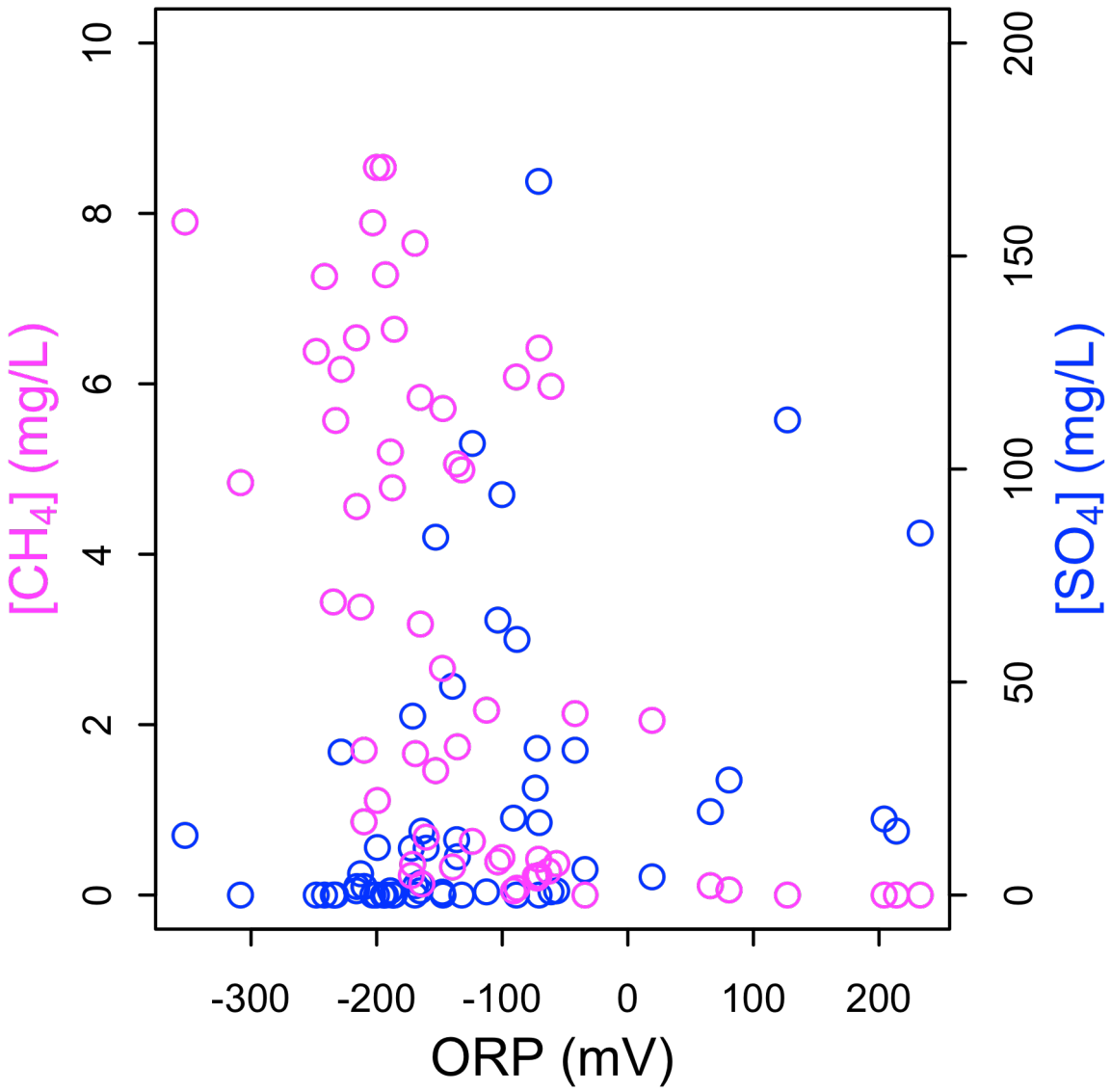

Figure B.8. CH_4 (in pink) and SO_4 (in blue) concentrations as a function of ORP. Both analyzed using linear regression (for CH_4 ~ ORP: $R^2 = 0.40$, $P < 0.0001$; for SO_4 ~ ORP: $R2 = 0.21$, $P < 0.001$).

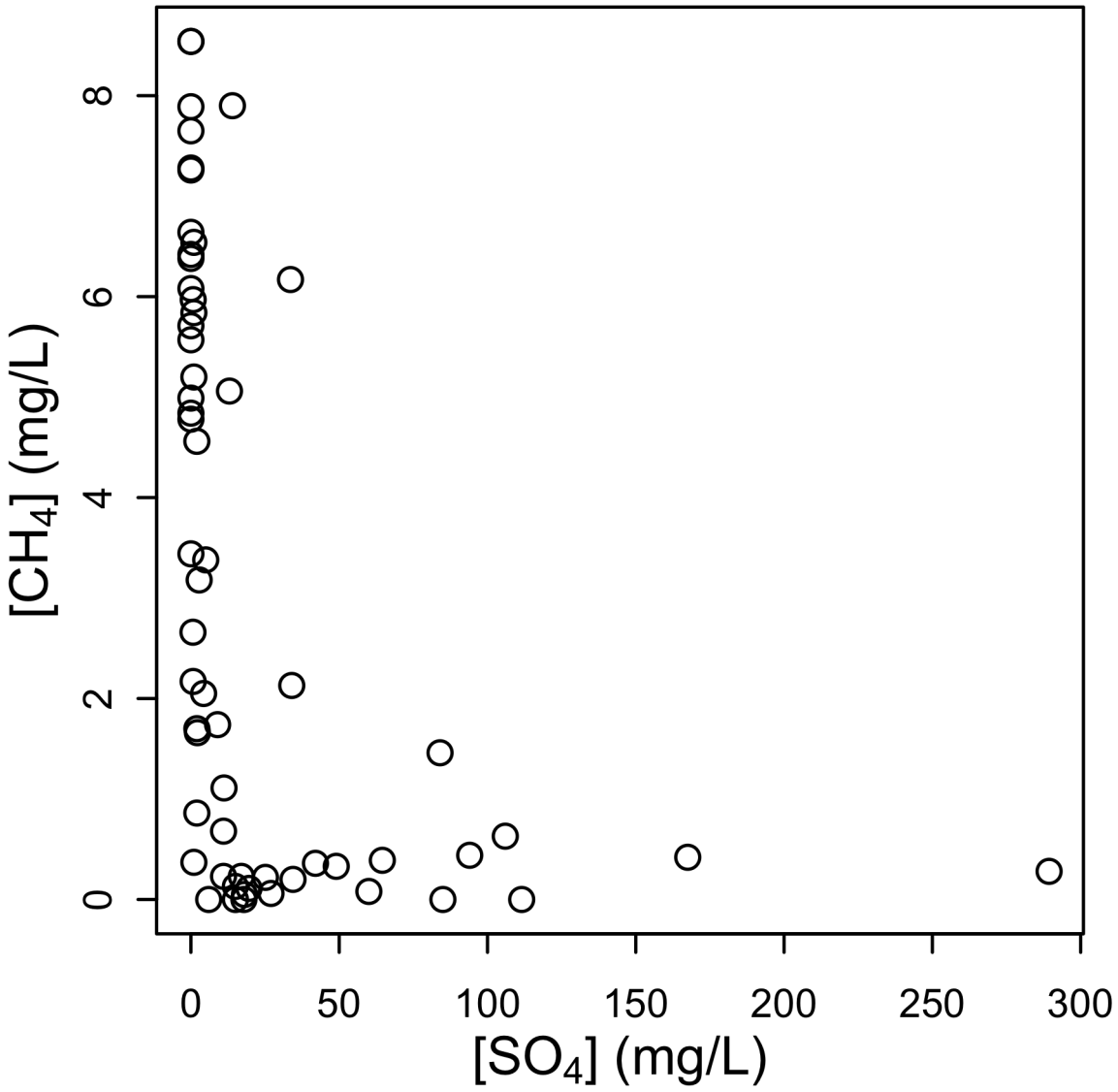

Figure B.9. CH_4 concentrations as a function of SO_4 concentrations. Because CH_4 concentrations could not be transformed to meet the assumption of normality required by linear regression, this relationship was tested using Spearman's rank-order correlation ($\rho = -0.75$).

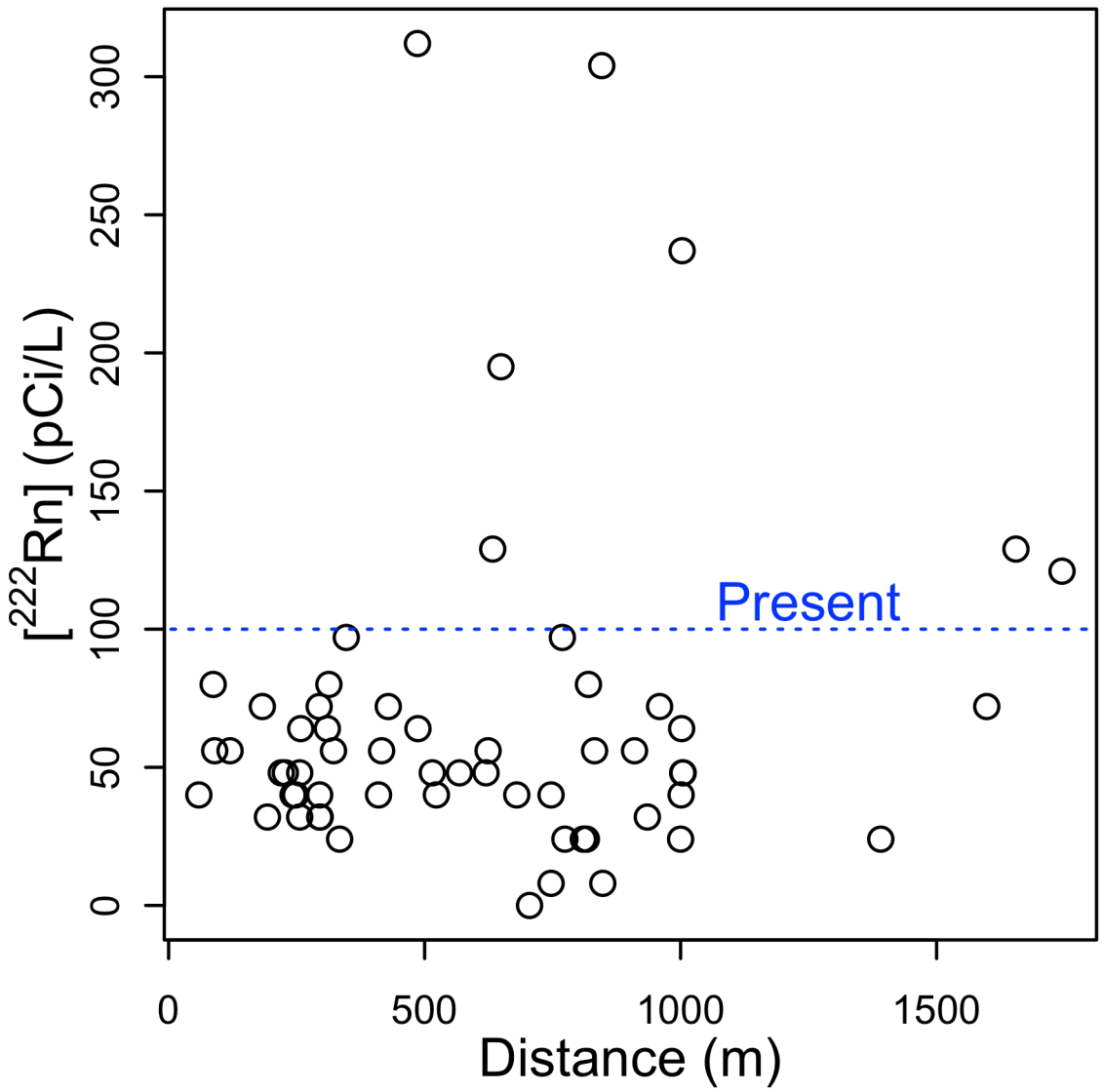

Figure B.10. ^{222}Rn occurrence as a function of proximity to ALL hydraulically fractured natural gas wells (permitted after 1980). Analyzed using logistic regression (D = 41.95, P > 0.05). ^{222}Rn concentrations were binomially distributed between sampling sites above (present) or below (absent) a detection limit of 100 pCi/L (in blue).

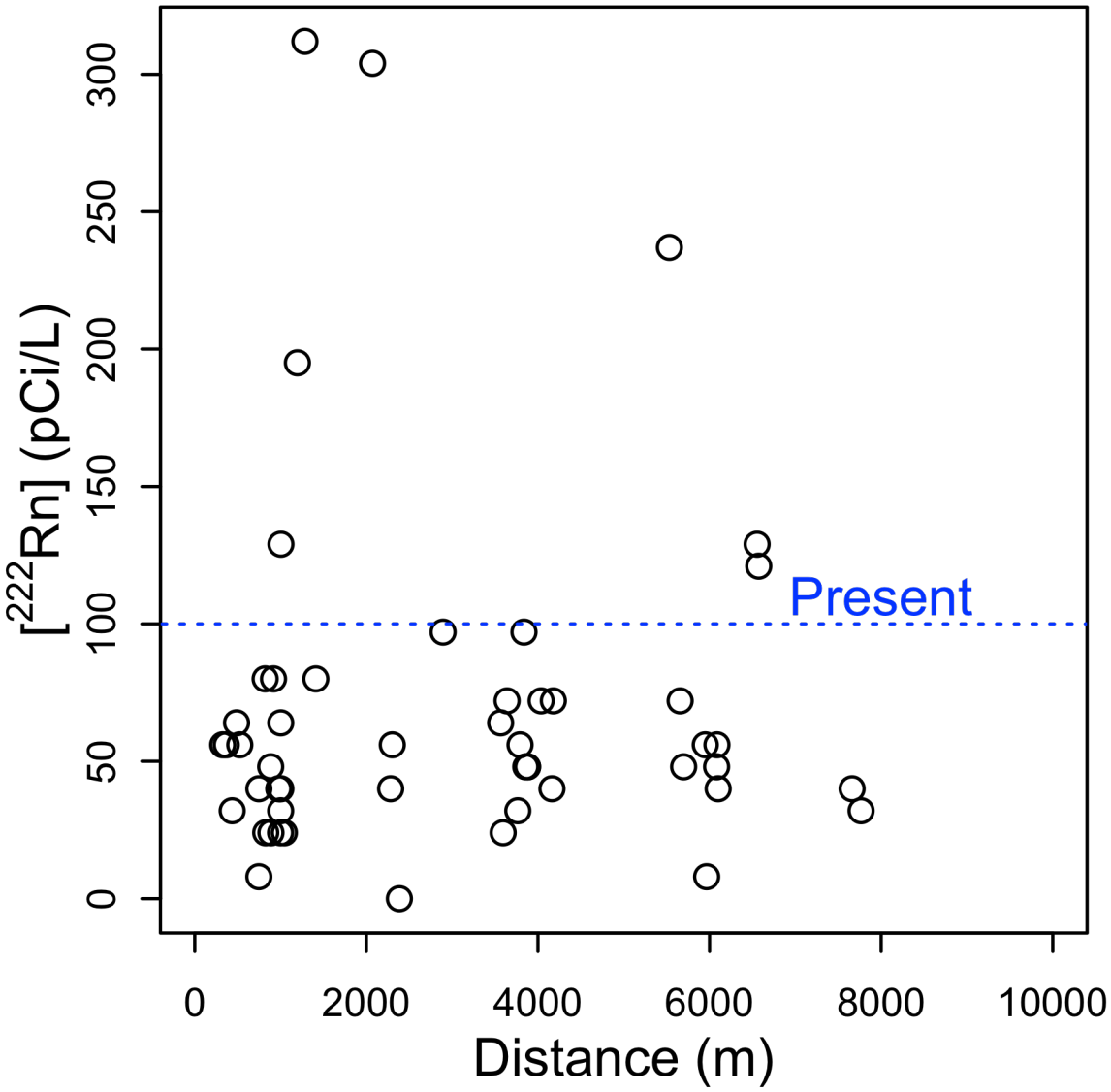

Figure B.11. ^{222}Rn occurrence as a function of proximity to ACTIVE hydraulically fractured natural gas wells (permitted between 2011 and 2014). Analyzed using logistic regression (D = 49.87, $P > 0.05$). ^{222}Rn concentrations were binomially distributed between sampling sites above (present) or below (absent) a detection limit of 100 pCi/L (in blue).

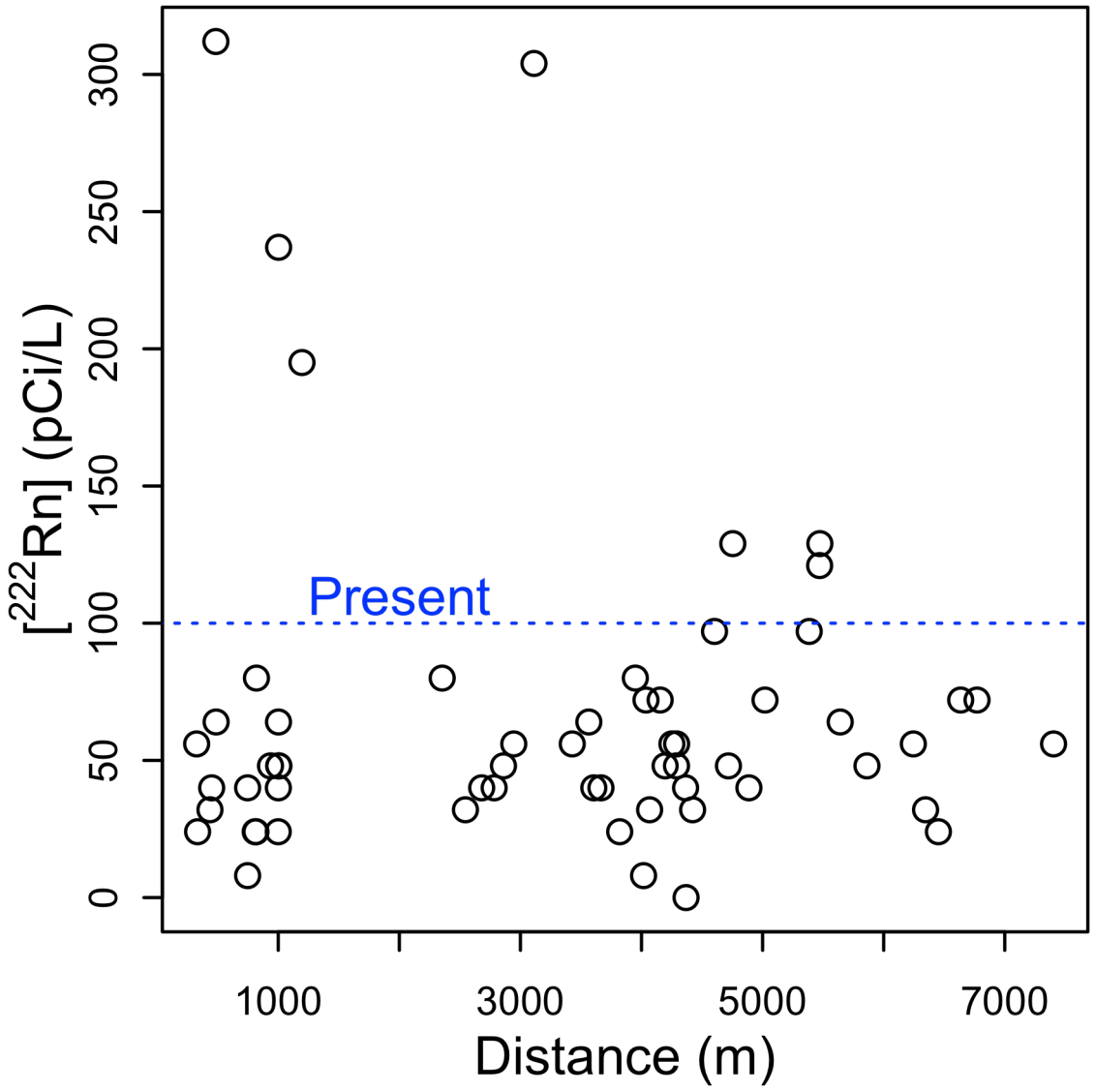

Figure B.12. ^{222}Rn occurrence as a function of proximity to DEVIATED hydraulically fractured natural gas wells (permitted between 2006 and 2012). Analyzed using logistic regression (D = 50.28, P > 0.05). ^{222}Rn concentrations were binomially distributed between sampling sites above (present) or below (absent) a detection limit of 100 pCi/L (in blue).

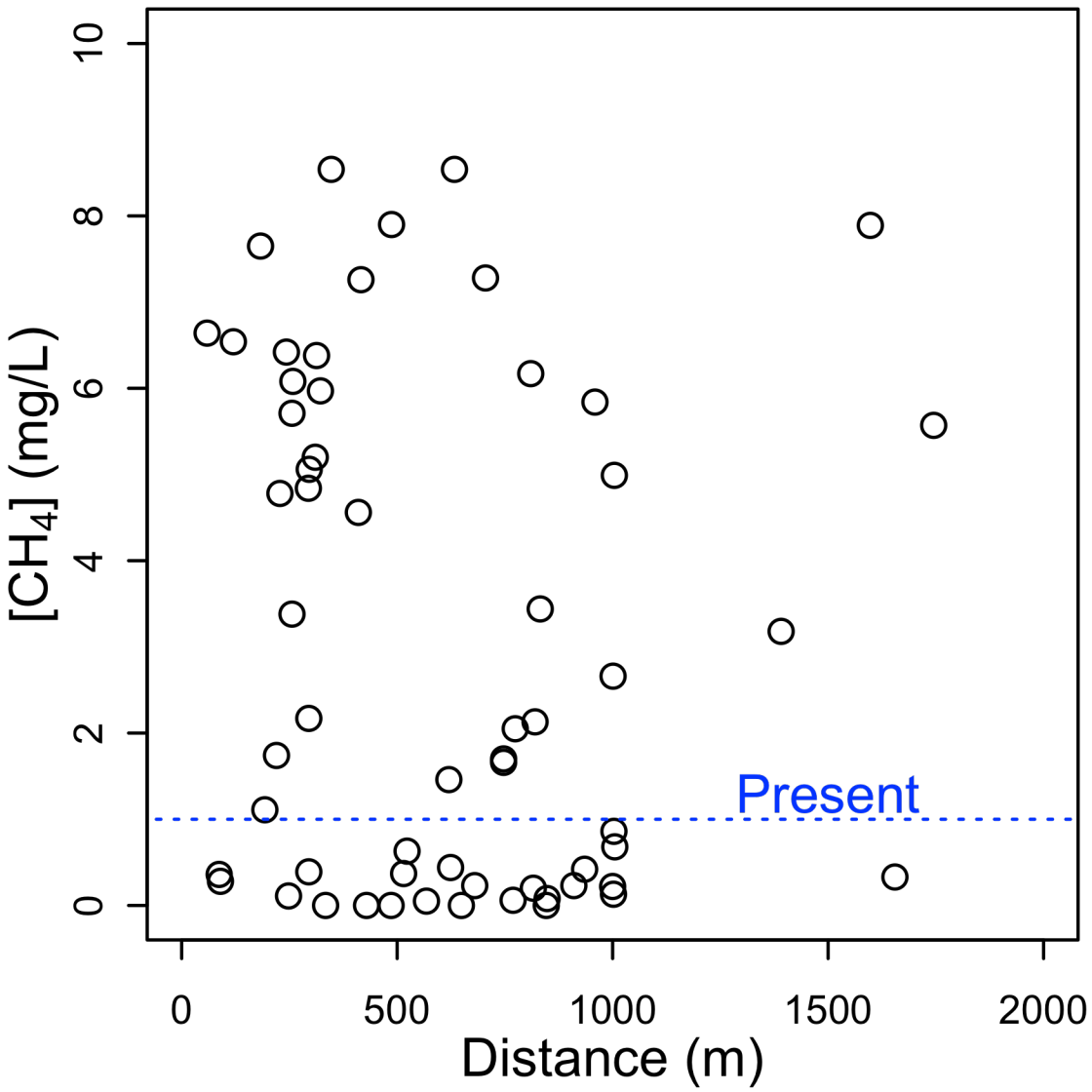

Figure B.13. CH_4 concentrations as a function of proximity to ALL hydraulically fractured natural gas wells (permitted after 1980). Analyzed using logistic regression (D = 78.88, P > 0.05). CH_4 concentrations were binomially distributed between sampling sites above (present) or below (absent) a threshold of 1 mg/L (in blue).

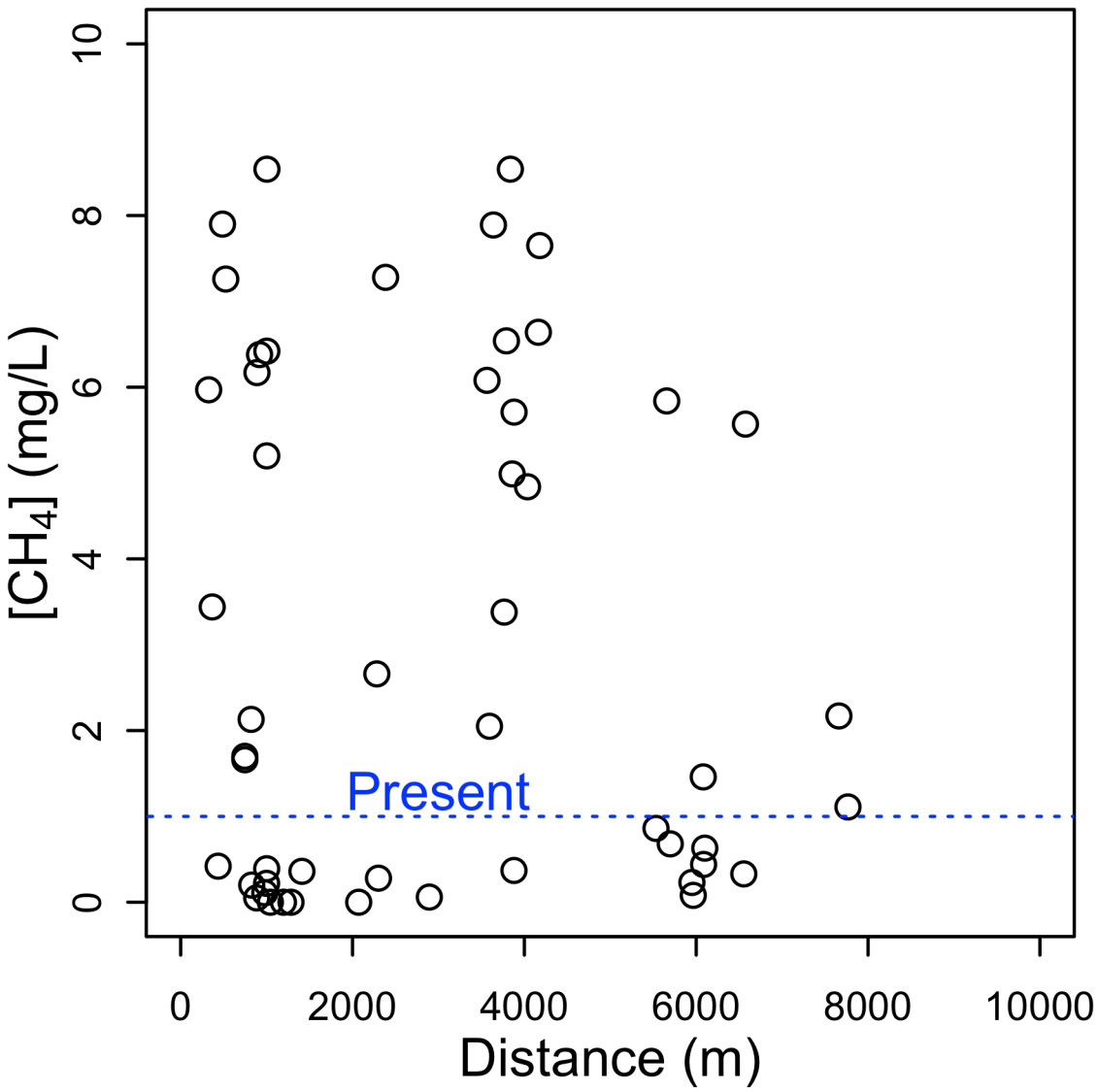

Figure B.14. CH_4 concentrations as a function of proximity to ACTIVE hydraulically fractured natural gas wells (permitted between 2011 and 2014). Analyzed using logistic regression (D = 79.71, P > 0.05). CH_4 concentrations were binomially distributed between sampling sites above (present) or below (absent) a threshold of 1 mg/L (in blue).

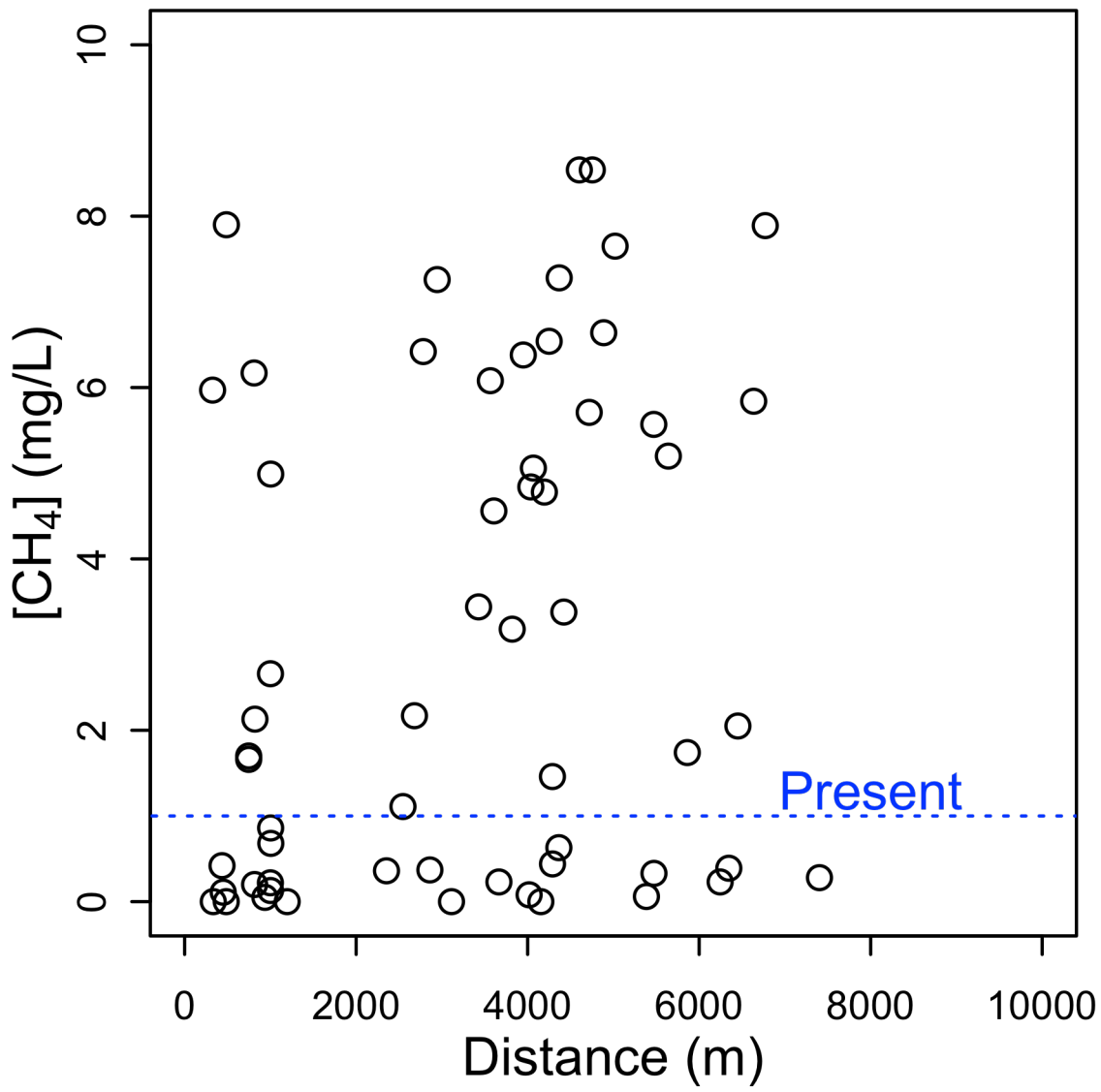

Figure B.15. CH_4 concentrations as a function of proximity to DEVIATED hydraulically fractured natural gas wells (permitted between 2006 and 2012). Analyzed using logistic regression (D = 77.78, $P > 0.05$). CH_4 concentrations were binomially distributed between sampling sites above (present) or below (absent) a threshold of 1 mg/L (in blue).

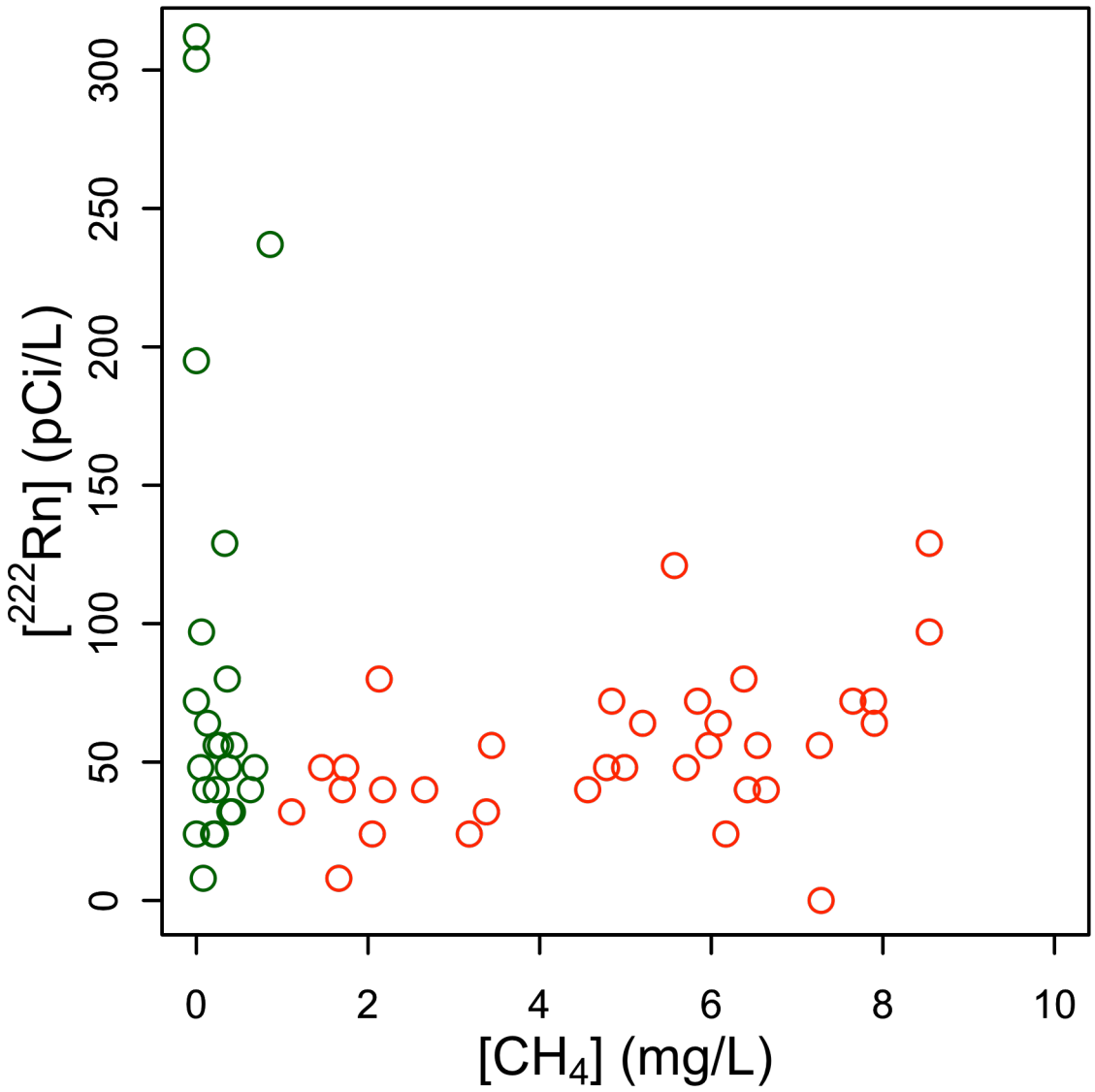

Figure B.16. ^{222}Rn concentrations as a function of CH_4 concentrations. Because data for neither ^{222}Rn nor CH_4 could be transformed to meet the assumption of normality, this relationship was analyzed using Spearman's rank-order correlation ($\rho = 0.05$), excluding BDL values for ^{222}Rn. Type 1 groundwater samples are in red, and Type 2 groundwater samples are in green.

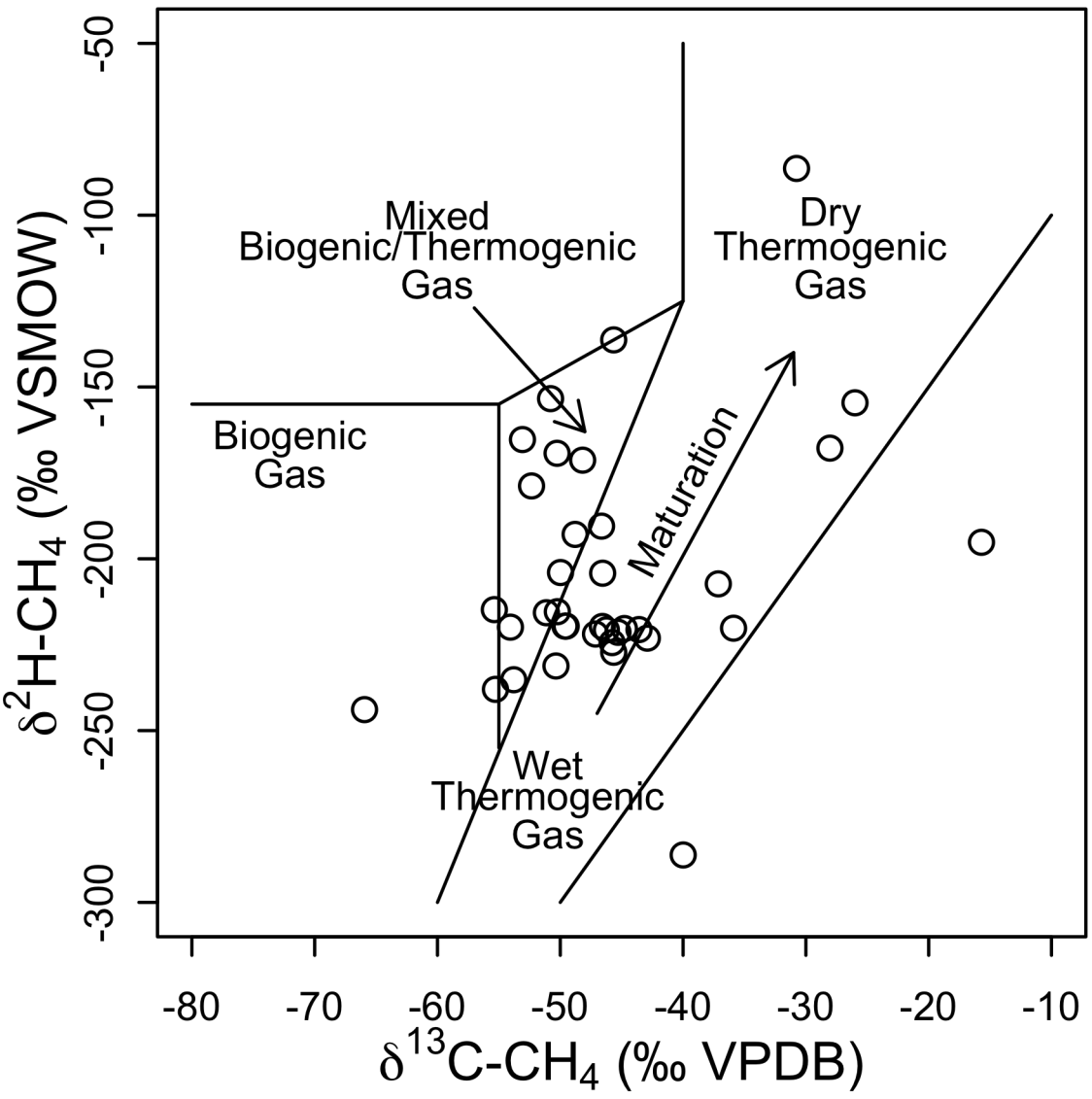

Figure B.17. δ^2H-CH_4 as a function of δ^{13}C-CH_4. CH_4 classifications adopted from Jackson et al (2012).

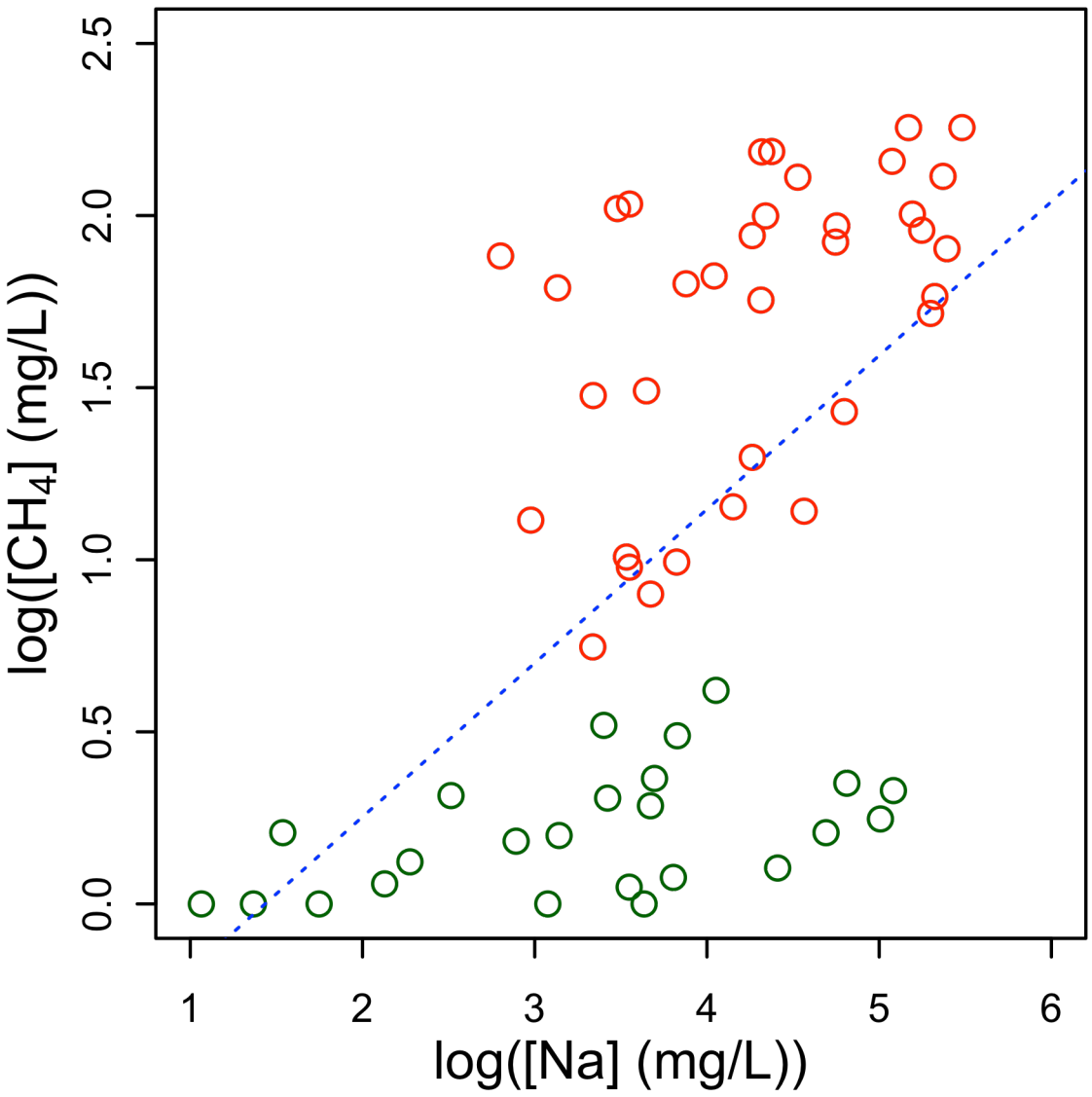

Figure B.18. CH_4 concentrations as a function of Na concentrations. Analyzed using linear regression ($R^2 = 0.34$, $P < 0.0001$, regression line in blue). Both CH_4 and Na concentrations were logarithmically transformed to meet the assumption of normality required by linear regression. Type 1 groundwater samples are in red, and Type 2 groundwater samples are in

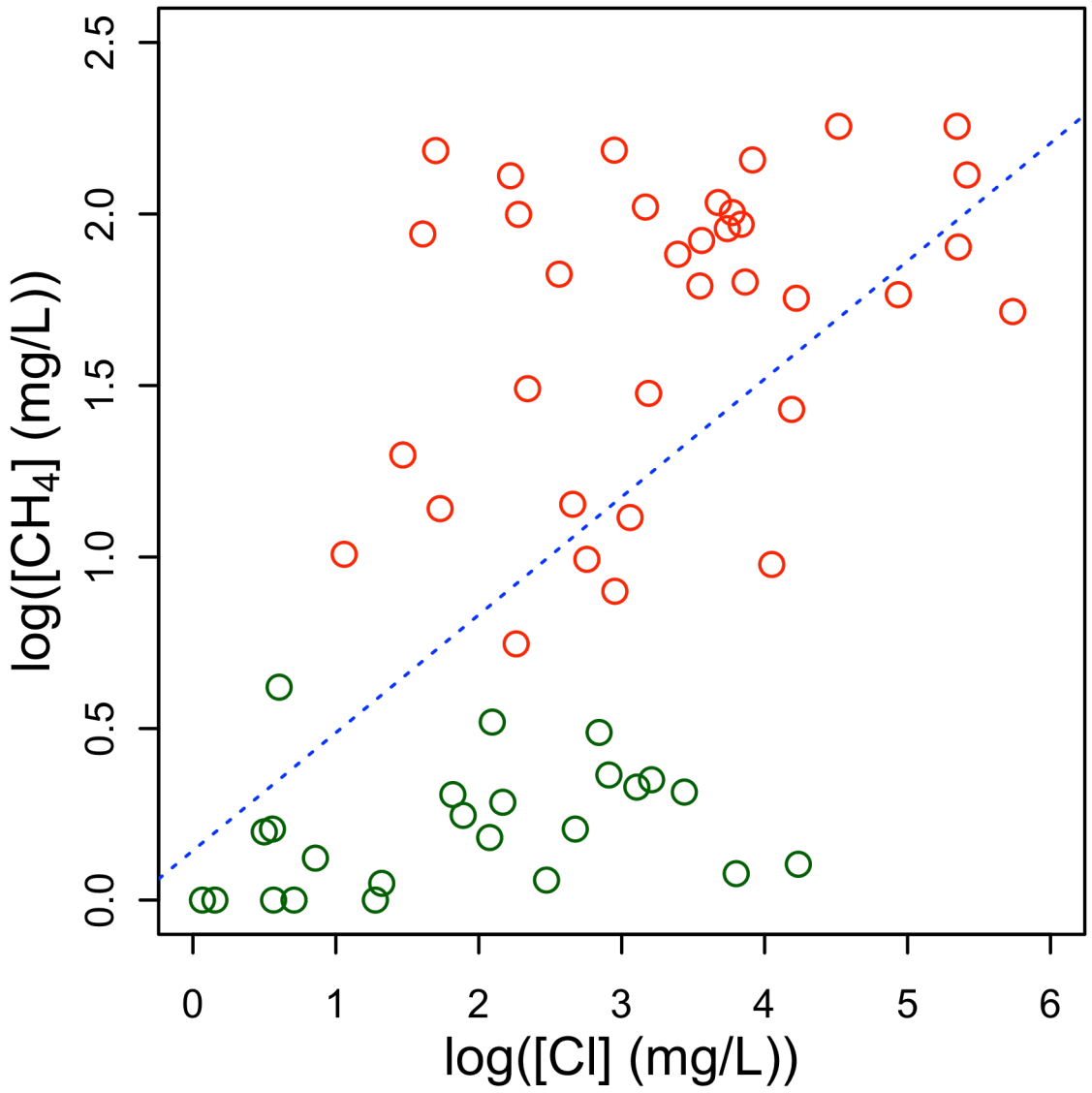

Figure B.19. CH_4 concentrations as a function of Cl concentrations. Analyzed using linear regression (R^2 = 0.34, P < 0.0001, regression line in red). Both CH_4 and Cl concentrations were logarithmically transformed to meet the assumption of normality required by linear regression. Type 1 groundwater samples are in red, and Type 2 groundwater samples are in green.

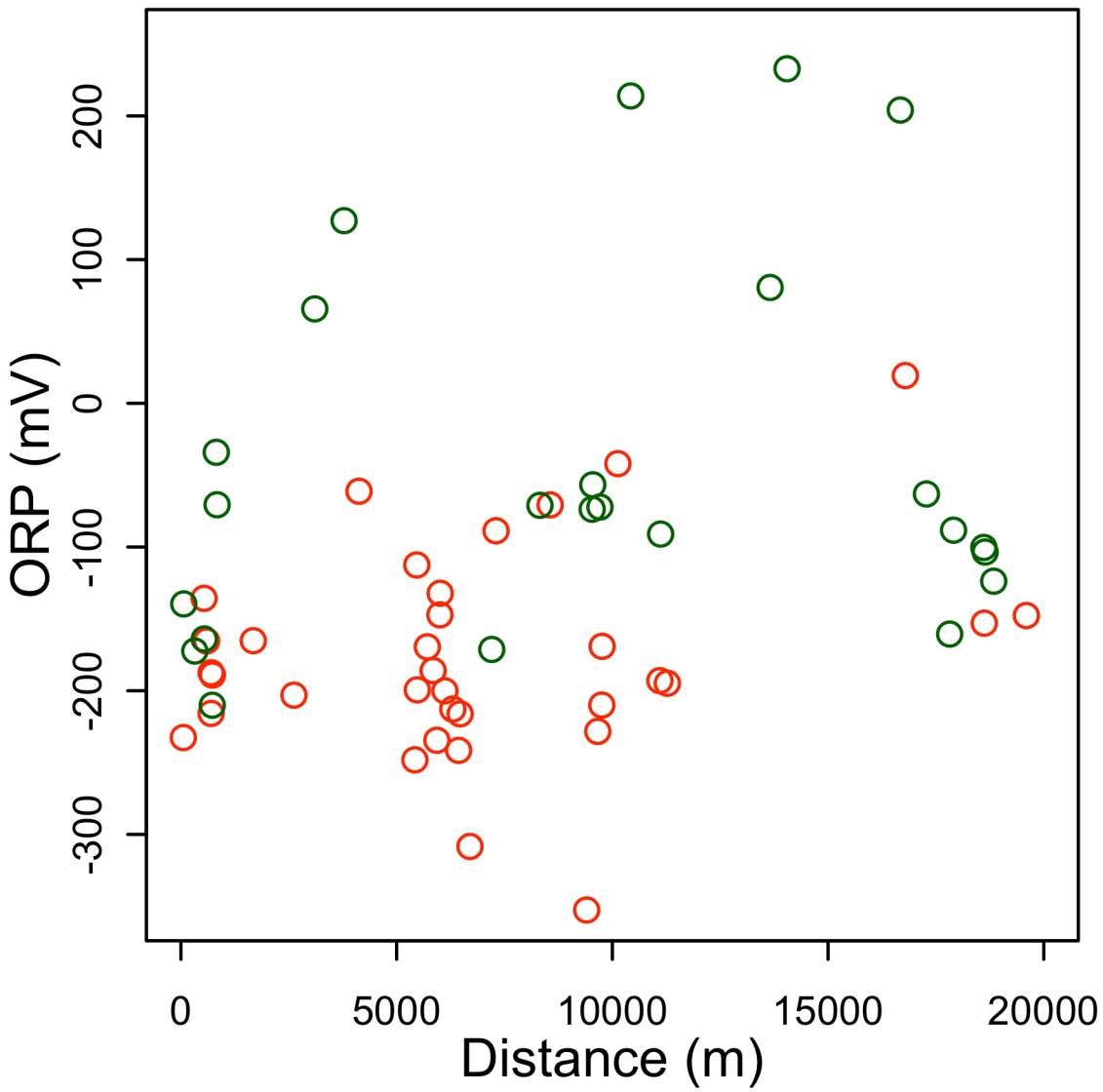

Figure B.20. ORP as a function of proximity to the PMTF. Because data for distance to the PMTF could not be transformed to meet the assumption of normality required by linear regression, this relationship was analyzed using Spearman's rank-order correlation (ρ = 0.31). Type 1 groundwater samples are in red, and Type 2 groundwater samples are in green.

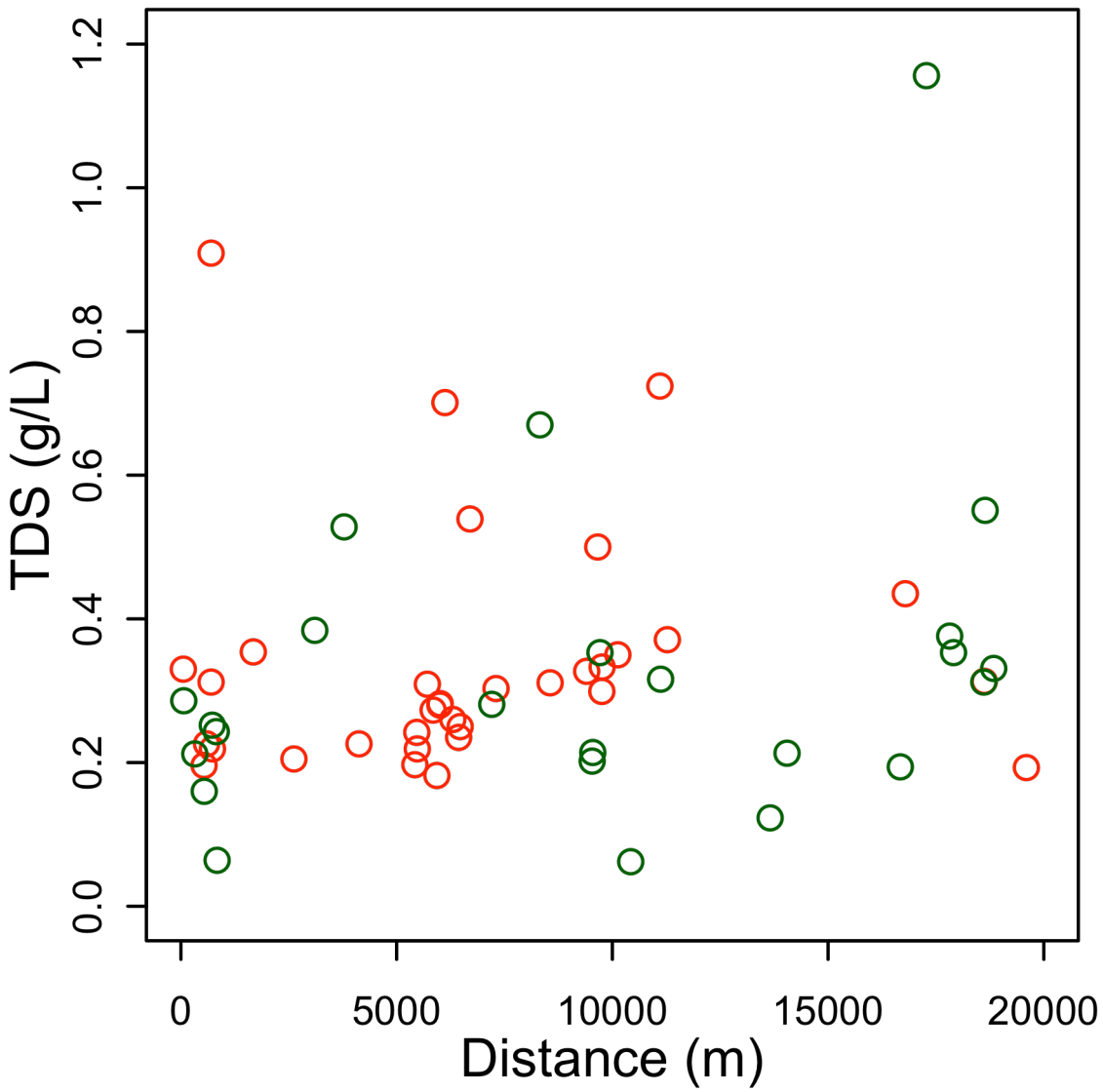

Figure B.21. TDS as a function of proximity to the PMTF. Because data for distance to the PMTF could not be transformed to meet the assumption of normality required by linear regression, this relationship was analyzed using Spearman's rank-order correlation ($\rho = 0.25$). Type 1 groundwater samples are in red, and Type 2 groundwater samples are in green.

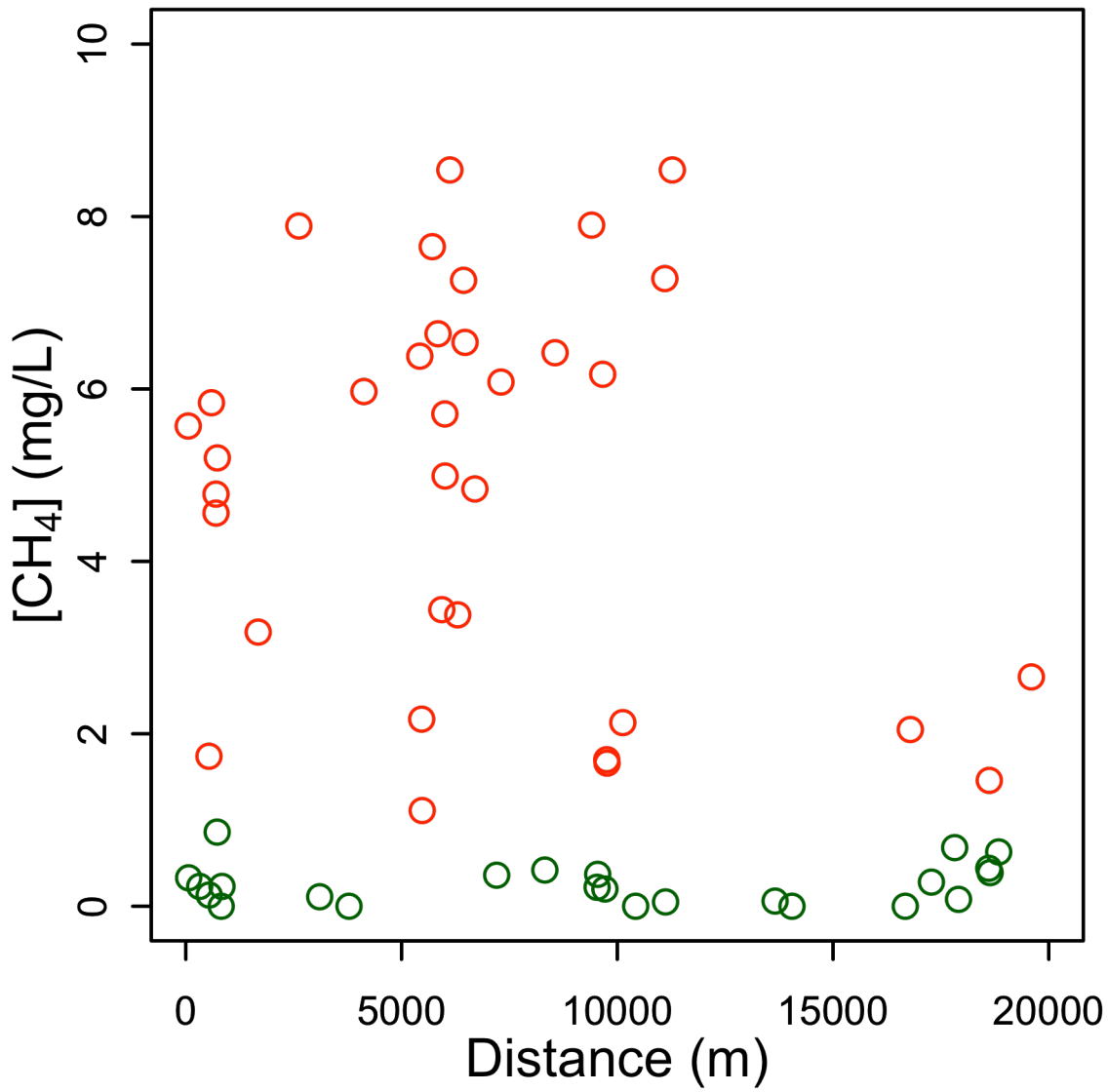

Figure B.22. CH_4 concentrations as a function of proximity to the PMTF. Because data for distance to the PMTF could not be transformed to meet the assumption of normality required by linear regression, this relationship was analyzed using Spearman's rank-order correlation (ρ = -0.20). Type 1 groundwater samples are in red, and Type 2 groundwater samples are in green.

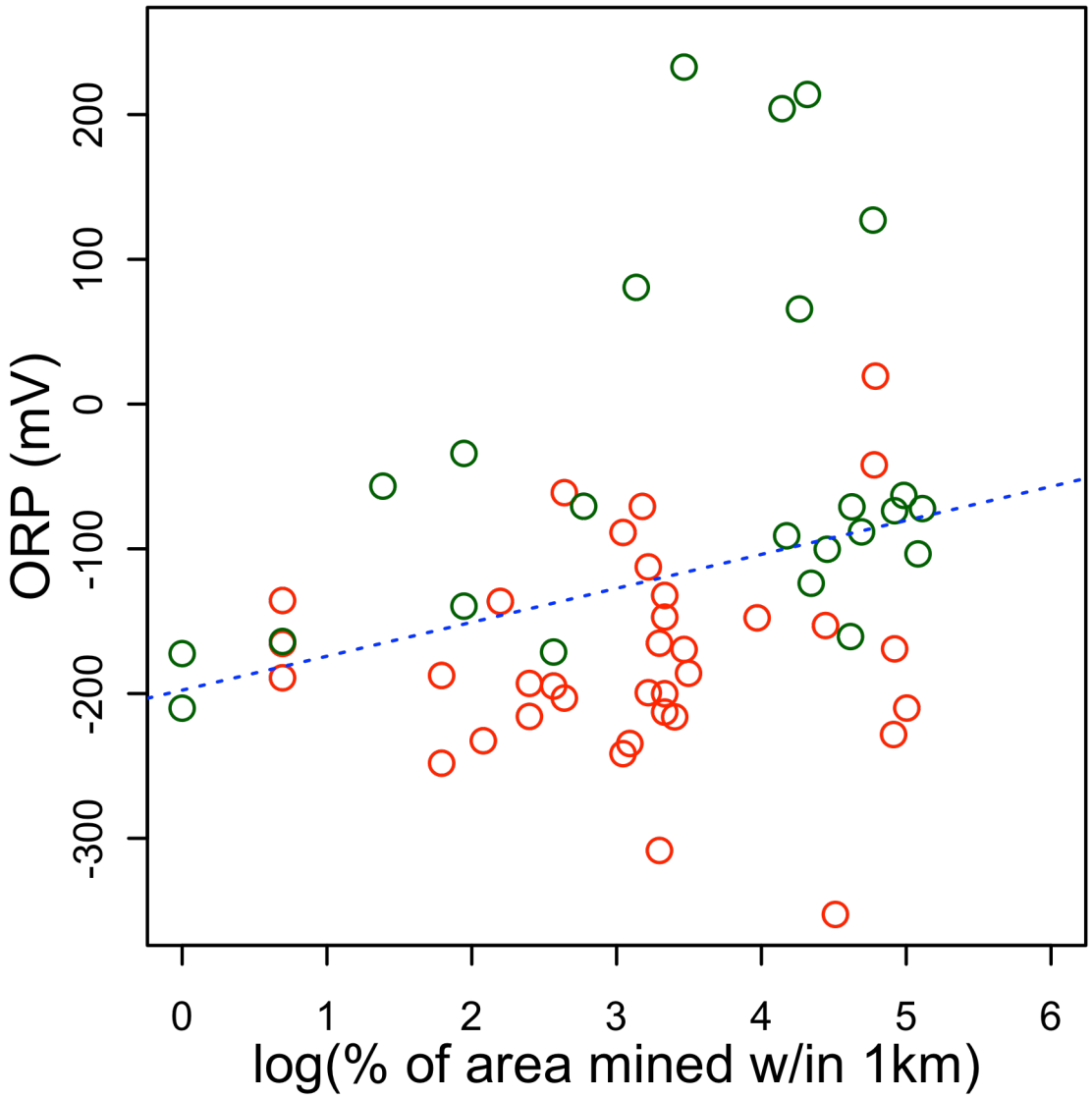

Figure B.23. ORP as a function of proximity to surface mining. Analyzed using linear regression (R^2 = 0.074, P = 0.037, regression line in blue). Data for % of area within a 1km radius were logarithmically transformed to meet the assumption of normality required by linear regression. Type 1 groundwater samples are in red, and Type 2 groundwater samples are in green.

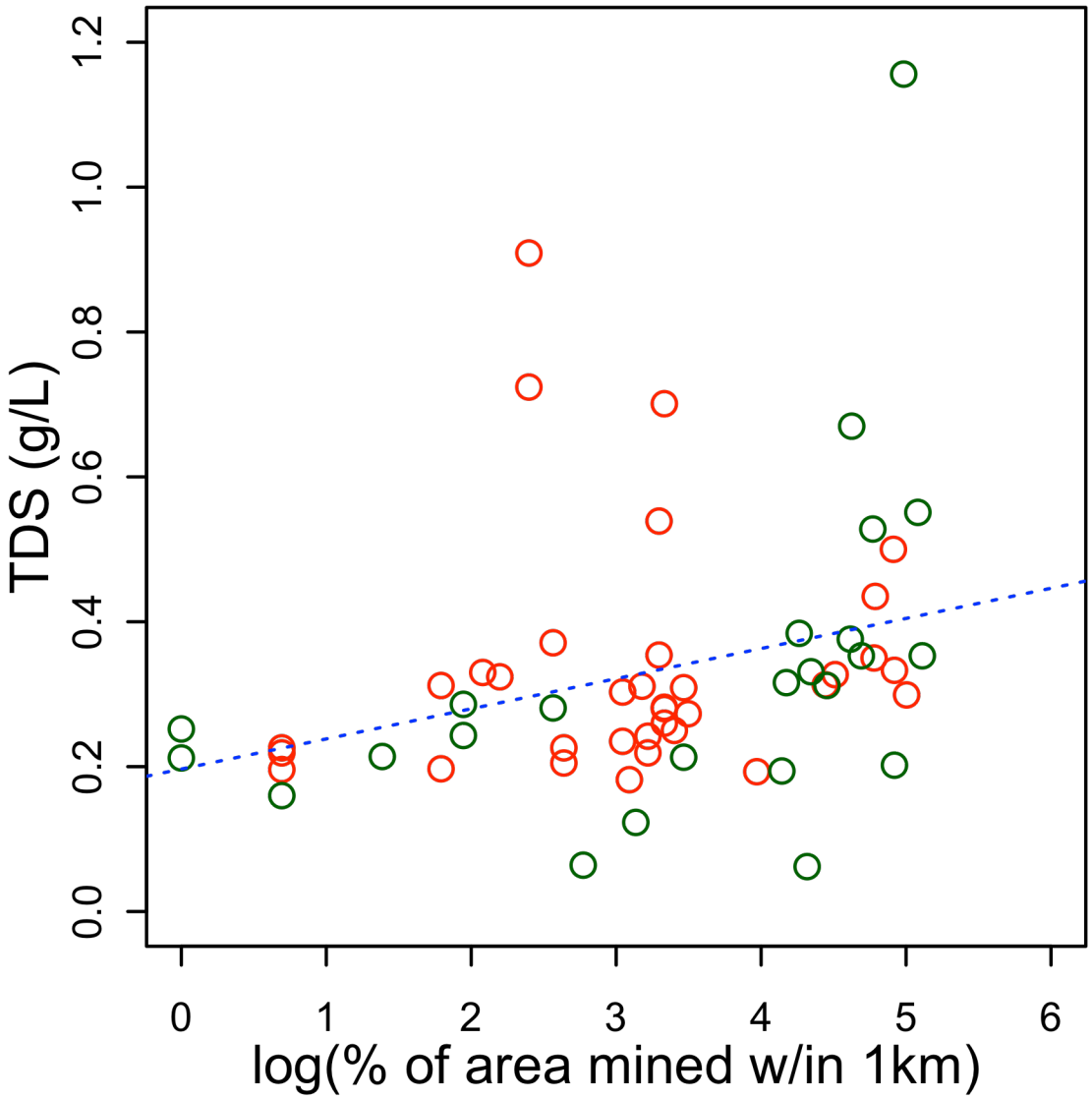

Figure B.24. TDS as a function of proximity to surface mining. Analyzed using linear regression (R^2 = 0.090, P = 0.021, regression line in blue). For this analysis, proximity is defined as the percentage of the area within a 1km radius of each sampling site covered by surface mining. Proximity data were logarithmically transformed to meet the assumption of normality required by linear regression. Type 1 groundwater samples are in red, and Type 2 groundwater samples are in green.

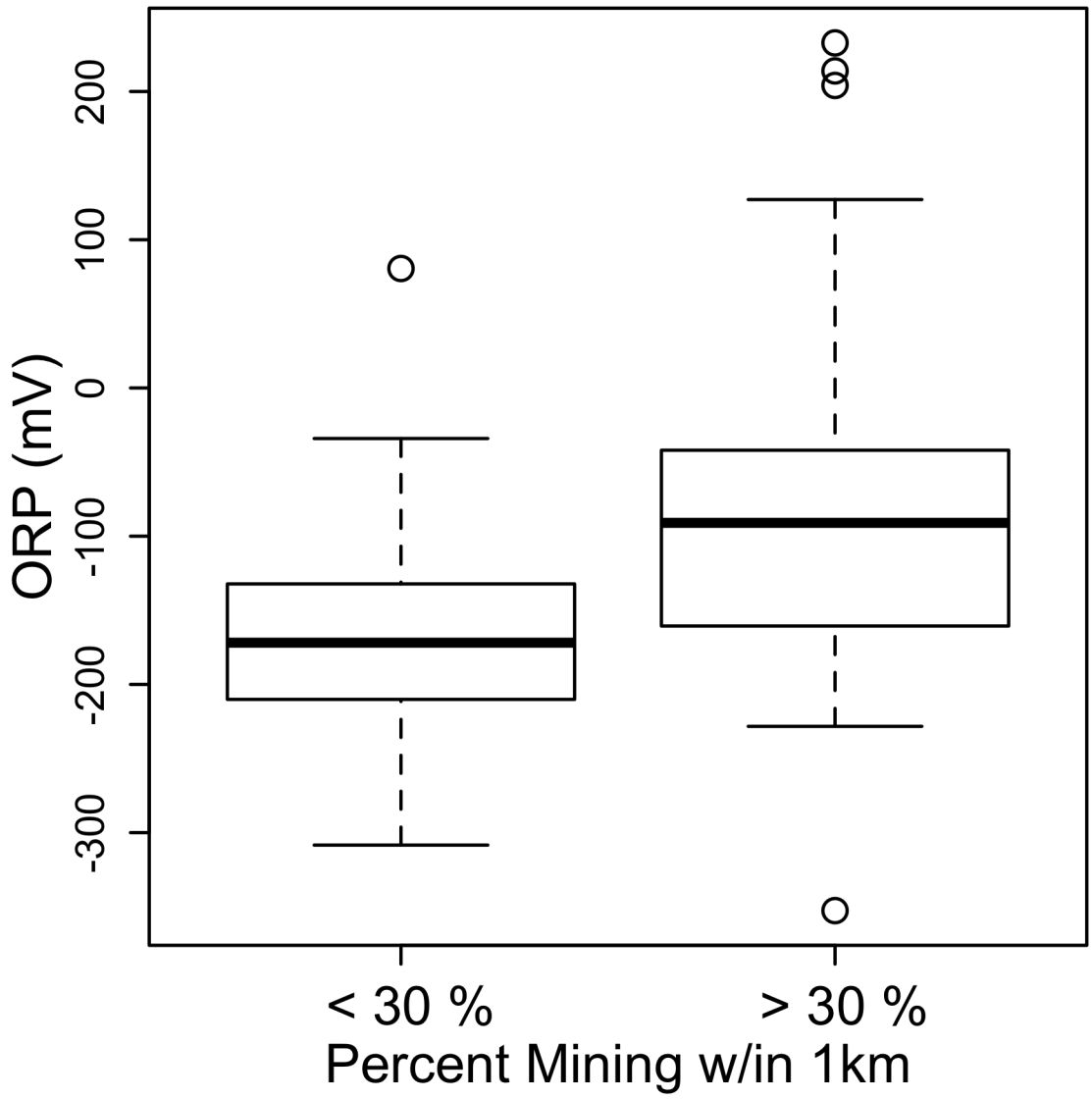

Figure B.25. ORP as a function of proximity to surface mining. Analyzed using ANOVA ($F_{1,57}$ = 9.69, P = 0.0029), comparing ORP values between sampling sites with < 30 % area within a 1 km radius covered by surface mining versus sampling sites with > 30 % area within a 1 km radius covered by surface mining.

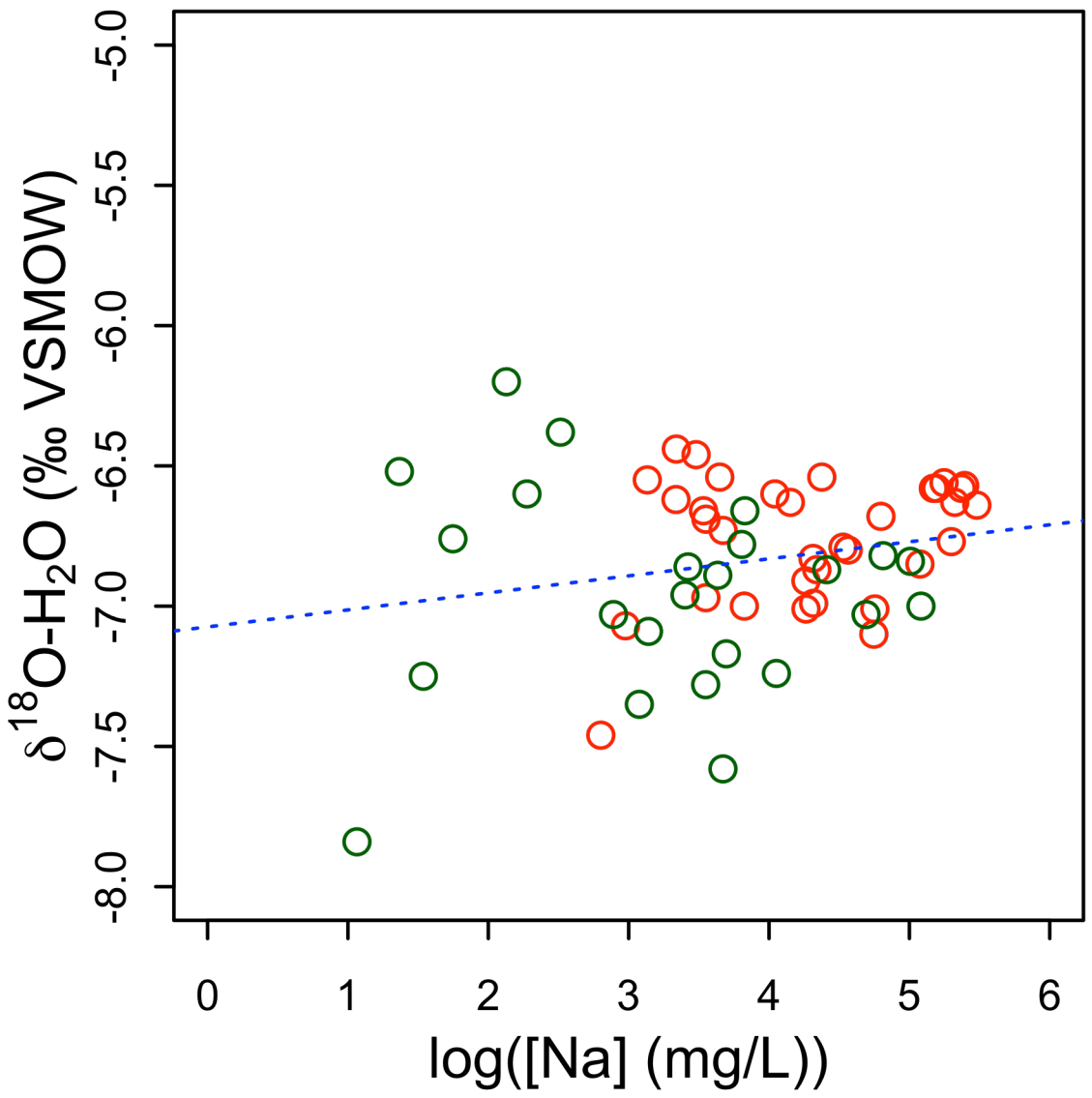

Figure B.26. $\delta^{18}O\text{-}H_2O$ of groundwater as a function of Na concentrations. Analyzed using linear regression ($R^2 = 0.045$, $P = 0.107$, regression line in blue). Type 1 groundwater samples are in red, and Type 2 groundwater samples are in green.

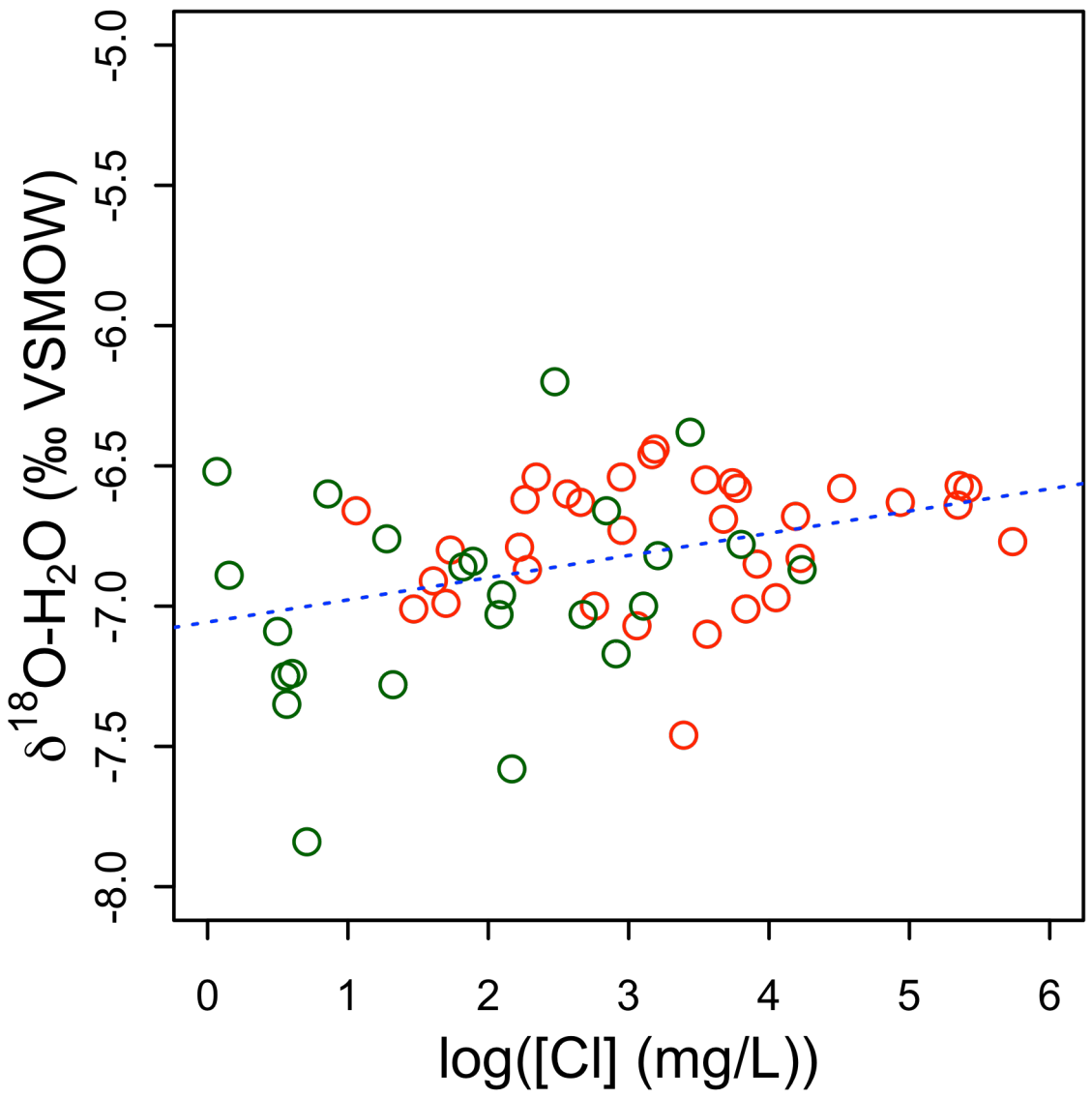

Figure B.27. $\delta^{18}O\text{-}H_2O$ of groundwater as a function of Cl concentrations. Analyzed using linear regression ($R^2 = 0.12$, $P = 0.0045$, regression line in blue). Type 1 groundwater samples are in red, and Type 2 groundwater samples are in green.

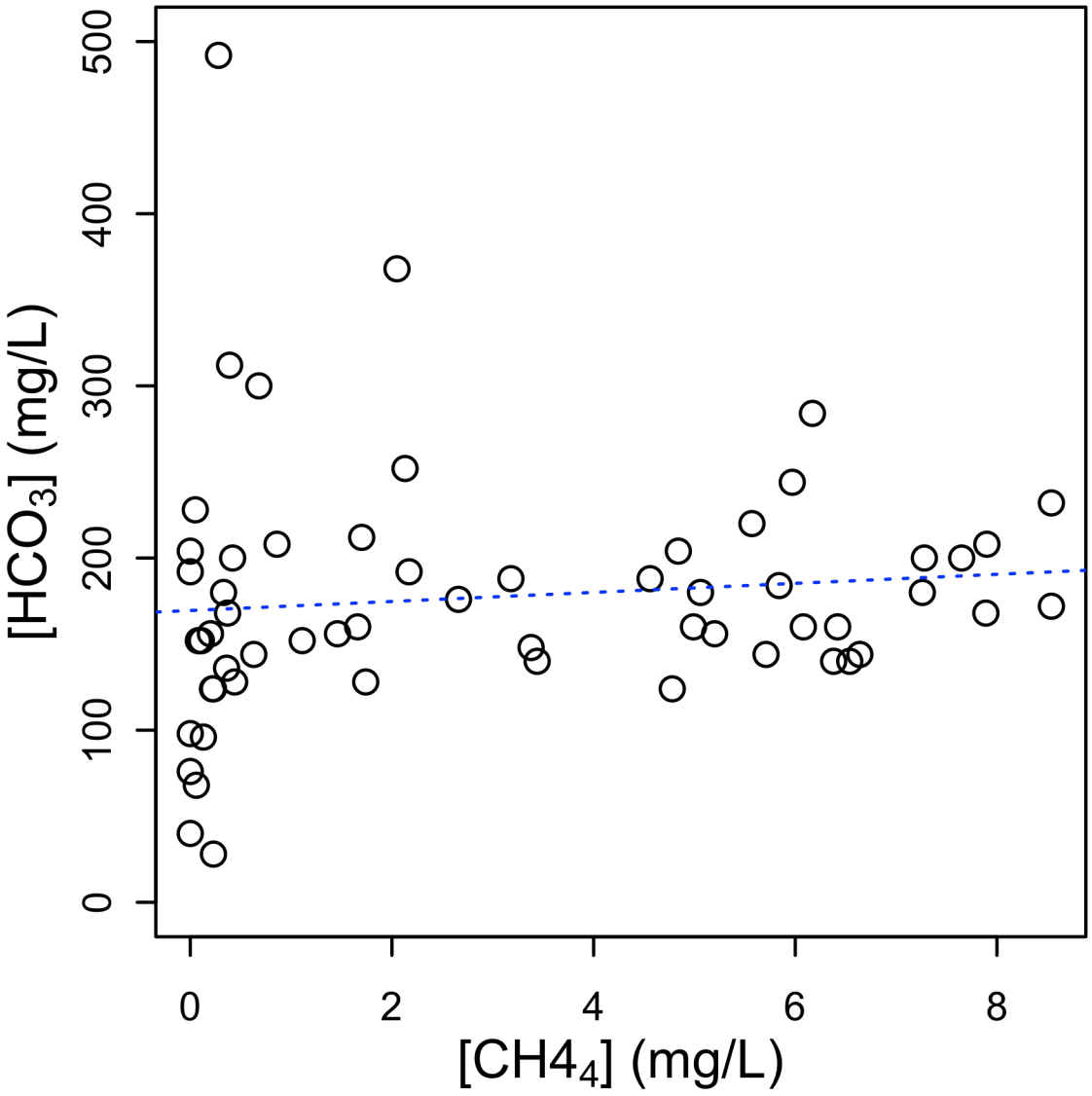

Figure B.28. HCO_3 concentration as a function of CH_4 concentration. Analyzed using linear regression ($R^2 = 0.011$, $P = 0.43$, regression line in blue).

APPENDIX C: STASTICS TABLES

Table C.1. Various statistical relationships between different isotopic tracers, modeled by both linear regression and compared means (T-test).

Function	DF	F	R^2	P	T
H_2O LCGW vs. H_2O KMW	57	n.a.	n.a.	0.88	0.67
$\delta^{18}O\text{-}SO_4 \sim \delta^{34}S\text{-}SO_4$	1,28	24.87	0.47	2.88E-05	n.a.
$\delta^{34}S\text{-}SO_4 \sim [SO4]$	1,31	0.0035	1.11E-04	0.95	n.a.
$\delta^{18}O\text{-}H_2O \sim Na$	1,57	2.688	0.045	0.0107	n.a.
$\delta^{18}O\text{-}H_2O \sim Cl$	1,57	8.764	0.12	0.0045	n.a.

Table C.2. ANOVA comparing $\delta^{34}S$ values of bedrock against $\delta^{34}S\text{-}SO_4$ values of groundwater.

Bedrock Isotopes	DF	F	P
$\delta^{34}S\text{-}SO_4$ of bedrock vs. $\delta^{34}S\text{-}SO_4$ of groundwater	1,54	17.96	8.88E-05

Table C.3. Various statistical relationships between different environmental tracers, modeled by both linear regression (P) and non-parametric correlation (ρ).

Function	DF	F	R^2	P	ρ
$[^{222}Rn] \sim [CH_4]$	1,4	0.87	0.015	0.35	0.05
$[CH_4] \sim [SO_4]$	1,57	12.93	0.18	5.75E-04	-0.74
$[CH_4] \sim [Na]$	1,57	28.88	0.34	1.48E-06	0.59
$[CH_4] \sim [Cl]$	1,57	29.12	0.35	1.37E-06	0.56
$[CH_4] \sim ORP$	1,57	37.27	0.4	9.67E-08	-0.66
$[SO_4] \sim ORP$	1,57	15.27	0.21	2.50E-04	0.52
$[Fe^{2+}] \sim ORP$	1,37	5.62	0.11	2.30E-02	0.36
$[Na] \sim ORP$	1,47	21.27	0.3	3.08E-05	-0.33
$[Cl] \sim ORP$	1,57	12.36	0.16	8.69E-04	-0.37
$[Ca] \sim ORP$	1,57	2.31E-05	-0.018	0.99	0.06
$[Mg] \sim ORP$	1,57	0.39	-0.011	0.54	0.14
$[SO_4] \sim [Fe^{2+}]$	1,57	13.87	0.18	0.28	0.18
$[H_2S] \sim [SO_4]$	1,37	0.16	0.0043	0.69	n.a.
$[HCO_3] \sim [CH_4]$	1,57	0.62	0.011	0.43	n.a.
$[Na] \sim [Cl]$	1,57	36.29	0.39	1.31E-07	n.a.
$[CH_4] \sim DO$	n.a.	n.a.	n.a.	n.a.	-0.53

Table C.4. Various environmental tracers modeled as a function of proximity to ALL hydraulically fractured natural gas wells (permitted after 1980) by linear regression (P, R^2) and logistic regression (P, D).

Dependent variable	DF	F	R^2	P	D
[CH_4]	1,57	n.a.	n.a.	0.22	78.88
[^{222}Rn]	1,57	n.a.	n.a.	0.0037	41.95
ORP	1,57	0.030	5.30E-04	0.86	n.a.
TDS	1,57	1.55	0.026	0.22	n.a.

Table C.5. Various environmental tracers modeled as a function of proximity to ACTIVE hydraulically fractured natural gas wells (permitted between 2011 and 2014) by linear regression (P, R^2) and logistic regression (P, D).

Dependent variable	DF	F	R^2	P	D
[CH_4]	1,57	n.a.	n.a.	0.87	79.71
[^{222}Rn]	1,57	n.a.	n.a.	0.47	49.87
ORP	1,57	1.305	0.022	0.26	n.a.
TDS	1,57	0.19	-0.014	0.67	n.a.

Table C.6. Various environmental tracers modeled as a function of proximity to DEVIATED hydraulically fractured natural gas wells (permitted between 2006 and 2012) by linear regression (P, R^2) and logistic regression (P, D).

Dependent variable	DF	F	R^2	P	D
[CH_4]	1,57	n.a.	n.a.	0.16	77.78
[^{222}Rn]	1,57	n.a.	n.a.	0.11	50.28
ORP	1,57	2.41	0.041	0.13	n.a.
TDS	1,57	1.40	0.024	0.24	n.a.

Table C.7. Moran's I statistic and test for spatial autocorrelation for various spatial relationships and distributions of measured parameters.

Variable/Function	Moran's I	P
Sample distribution	0.35	4.68E-16
$[CH_4]$	0.17	2.05E-05
$[SO_4]$	0.19	6.90E-08
ORP	0.075	1.90E-02
ORP ~ Proximity to gas drilling	0.077	1.80E-02
ORP ~ Proximity to PMTF	-0.044	0.73
ORP ~ Proximity to mining	-0.072	0.89
$[CH_4]$ ~ ORP	0.020	0.21
$[SO_4]$ ~ ORP	0.14	3.20E-04
Prox. to fault ~ Prox. to mining	0.36	2.20E-16
TDS ~ Proximity to mining	0.096	0.62

Table C.8. Various environmental tracers modeled as a function of proximity to the PMTF by non-parametric correlation.

Dependent variable	ρ
$[CH_4]$	-0.2
ORP	0.31
TDS	0.25
$[^{222}Rn]$	-0.17
[Na]	-0.062
[Cl]	-0.02

Table C.9. Various environmental tracers modeled as a function of proximity to surface mining by linear regression (P, R^2), ANOVA (P, F), and non-parametric correlation (ρ).

Dependent variable	DF	F	R^2	P	ρ
ORP (LR)	1,57	4.58	0.074	0.037	n.a.
ORP (ANOVA)	1.57	9.69	n.a.	0.0029	n.a.
TDS	1,57	5.63	0.090	0.021	n.a.
$[CH_4]$	1,57	2.453	0.041	0.12	-0.24
$[^{222}Rn]$	1,4	5.52	0.088	0.022	0.4
$[SO_4]$	1,57	10.33	0.15	0.0022	n.a.
[Na]	1,57	3.99E-05	8.48E-07	0.995	n.a.
[Cl]	1,57	0.029	5.10E-04	0.86	n.a.
$[HCO_3]$	1,57	5.76	0.092	0.20	n.a.

APPENDIX D: DATA TABLES

Table D.1. In situ measurements for groundwater sampled in Letcher County, Kentucky. Measurements not taken for a given site are labeled "n.a."

Site #	Longitude (Dec. °)	Latitude (Dec. °)	Temp. (°C)	Cond. (uS/cm)	TDS (g/L)	DO (mg/L)	pH	ORP (mV)	[HCO_3] (mg/L)	[Fe] Tot. (mg/L)
K001	37.13033	-82.80093	12.54	347	0.23	2.87	7.56	-61.2	244	0.29
K002	37.15470	-82.72815	12.72	591	0.38	0.37	6.82	65.7	152	0.08
K003	37.17365	-82.69747	9.48	813	0.53	6.5	6.87	127.1	204	0.06
K004	37.21292	-82.74359	10.94	543	0.35	2.2	6.69	-72.2	156	12.3
K005	37.21456	-82.74070	10.7	512	0.33	3.38	7.53	-169.1	160	0.62
K006	37.21427	-82.73895	13.57	769	0.5	1.04	7.7	-228.3	284	0.15
K007	37.21394	-82.74209	13.59	460	0.3	0.24	7.59	-210	212	0.15
K008	37.21746	-82.72770	8.86	311	0.2	5.9	7.34	-73.7	124	1.12
K009	37.15781	-82.95034	4.67	329	0.21	5.47	6.44	232.8	76	0.08
K010	37.17240	-82.97812	12.34	670	0.44	4.65	6.89	19.3	368	1.1
K011	37.17293	-82.98975	12.96	1779	1.16	0.46	6.42	-63.1	492	14.9
K012	37.06485	-82.96876	13.45	337	0.22	3.58	7.33	-199.4	152	0.6
K013	37.06536	-82.96756	13.85	373	0.24	5.82	7.64	-112.5	192	0.4
K014	37.02556	-82.96793	14.36	545	0.35	0.21	7.36	-165.2	188	0.32
K015	37.18978	-82.76340	13.27	1031	0.67	4.72	6.83	-71	200	39.27
K016	37.25210	-82.68025	9.8	94	0.06	10.11	6.19	213.9	40	0.09
K017	37.21466	-82.88196	12.9	298	0.19	8.89	6.92	204.1	98	0.07
K018	37.23535	-82.90015	13.53	297	0.19	1.42	7.42	-147.7	176	3.46
K019	37.19375	-82.97082	13.22	847	0.55	3.26	7.33	-103.5	312	2.47
K020	37.13584	-82.93577	14.33	487	0.32	2.82	6.94	-91	228	12.83
K021	37.14624	-82.89180	15.58	539	0.35	0.26	6.84	-42	252	1.38
K022	37.14017	-82.88948	15.42	504	0.33	0.32	7.29	-352.6	208	0.11
K023	37.01682	-82.96759	20.73	374	0.24	7.72	6.91	-34.1	192	0.16
K024	37.03255	-82.97445	18.71	99	0.06	3.58	6.84	-70.6	28	1.28
K025	37.01110	-82.97698	22.06	1396	0.91	0.44	7.63	-215.8	188	0.46
K026	37.01506	-82.96800	15.23	480	0.31	0.61	6.98	-187.5	124	4.88
K027	37.01569	-82.96896	15.94	500	0.32	0.86	7.16	-136.3	180	1.47
K028	37.02495	-82.94913	13.07	246	0.16	0.42	6.79	-164	96	2.81
K029	37.02468	-82.94944	14.22	302	0.2	0.25	6.71	-135.7	128	3.5
K030	37.02558	-82.95134	14.15	337	0.22	0.31	7.03	-189.1	156	1.18
K031	37.11335	-82.90404	16.15	432	0.28	0.87	6.75	-171.3	136	2.35
K032	37.10550	-82.31500	12.87	280	0.18	0.46	7.02	-234.5	140	0.36
K033	37.10888	-82.89693	15.1	362	0.24	0.33	7.3	-241.5	180	0.32
K034	37.10053	-82.89336	13.45	304	0.2	0.42	7.55	-248.1	140	0.59
K035	37.07821	-82.88022	16.46	315	0.21	0.24	7.43	-203.1	168	1.67
K036	37.06377	-82.86654	14.81	440	0.23	0.38	7.27	-165.4	184	0.21
K037	37.05088	-82.88049	15.64	440	0.29	0.63	6.56	-139.6	180	1.57
K038	37.06292	-82.87188	14.27	389	0.25	0.53	7.13	-210.1	208	0.27
K039	37.05055	-82.88165	19.14	506	0.33	0.84	6.81	-232.6	220	1.52
K040	37.06100	-82.86813	13.81	327	0.21	0.88	6.54	-172.4	124	4.58
K041	37.10430	-82.94654	15.76	479	0.31	0.26	7.62	-70.7	160	0.09
K042	37.09689	-82.93413	14.55	466	0.3	0.63	7.08	-88.7	160	0.98
K043	37.09567	-82.92686	19.57	829	0.54	0.27	7.51	-308.4	204	2.28
K044	37.09421	-82.92312	14.8	385	0.25	0.13	7.28	-216.1	140	0.25
K045	37.09293	-82.92224	15.94	401	0.26	0.38	7.31	-212.8	148	0.27
K046	37.09128	-82.92200	17.37	1079	0.7	0.5	7.67	-200.1	232	0.25
K047	37.08987	-82.92191	15.25	431	0.28	0.61	6.94	-147.2	144	0.4
K048	37.09027	-82.92165	15.28	434	0.28	0.54	6.79	-132.2	160	2.16
K049	37.08678	-82.92279	14.36	475	0.31	0.57	7.41	-169.5	200	0.14
K050	37.08783	-82.92335	24.42	421	0.27	0.47	7.5	-186	144	0.98
K051	37.13831	-82.98750	15	188	0.12	1.52	5.75	80.6	68	5.18
K052	37.10041	-83.01608	14.93	570	0.37	0.49	6.78	-194.8	172	4.08
K053	37.10222	-82.00496	15.38	1114	0.72	0.47	8.48	-193	200	0.05
K054	37.09024	-82.99770	15.9	329	0.21	0.34	6.49	-56.7	168	5.56
K055	37.20461	-82.95119	13.93	482	0.31	0.53	6.89	-153	156	4.78
K056	37.20451	-82.95123	15.85	480	0.31	0.72	6.78	-100.3	128	5.3
K057	37.19815	-82.94977	14.32	544	0.35	0.52	6.53	-88.3	152	5.44
K058	37.19853	-82.94739	13.26	578	0.38	0.62	7.27	-160.6	300	0.97
K059	37.20681	-82.95131	14.23	509	0.33	0.71	6.64	-123.8	144	7.52

Table D.2. S Isotope compositions of elemental sulfur and soluble SO_4 in bedrock samples in Letcher County, Kentucky. Presented δ values are in ‰ units with respect to standards specified in **Chapters. 4.2.7**. Measurements below detection limit are labeled "b.d."

Site #	Monosulfide Weight %	$\delta^{34}S$	Polysulfide Weight %	$\delta^{34}S$	Soluble SO_4 Weight %	$\delta^{34}S$
KB01	0.000	b.d.	0.000	b.d.	0.049	0.16
KB02	0.000	b.d.	0.001	0.36	0.001	b.d.
KB03 Sandstone	0.000	b.d.	0.000	b.d.	0.003	b.d.
KB03 Shale	0.000	b.d.	0.013	-23.8	0.007	b.d.
KB04 Red SS	0.000	b.d.	0.001	b.d.	0.001	b.d.
KB04 Shale	0.000	15.04	0.044	3.2	0.002	b.d.
KB05 Coal	0.000	b.d.	0.001	3.4	0.010	-1.94
KB06 Mudstone	0.003	b.d.	0.001	b.d.	0.002	b.d.
KB07 Shale	0.000	b.d.	0.019	-2.5	0.018	-0.77
KB08 Mud	0.000	-0.74	0.004	-1.08	1.296	9.11
KB08 Coal	0.000	4.7	0.150	b.d.	1.919	4.59
KB08 Shale	0.000	b.d.	0.088	-0.5	0.010	3.96
KB08 Sandstone	0.000	b.d.	0.005	25.63	0.015	4.59
KB09 Devonian Shale	0.000	b.d.	0.058	2.17	0.001	b.d.
KB10 Shale	0.000	b.d.	0.019	0.45	0.001	b.d.

Table D.3. Chemical composition of groundwater in Letcher County, Kentucky (first half), including anions, cations, and misc. metals. Presented values are in units of mg/L, excluding ^{222}Rn values, which are in units of pCi/L.

Site #	Water Type	[Ba]	[Ca]	[CH_4]	[Cl]	[Fe]	[K]	[Mg]	[Mn]
K001	1	1.21	19.86	5.97	4.99	< 0.50	2.9	7.78	< 0.50
K002	2	< 0.50	< 0.50	0.11	69.11	< 0.50	< 0.50	< 0.50	< 0.50
K003	2	< 0.50	39.9	< 0.05	1.76	< 0.50	2.13	27.7	< 0.50
K004	2	< 0.50	28.34	0.2	7.98	12.3	1.21	15.72	1
K005	1	1.2	23.43	1.66	57.4	0.62	1.76	9.27	< 0.50
K006	1	0.68	34.53	6.17	46.31	< 0.50	2.02	10.05	< 0.50
K007	1	0.94	28.53	1.7	15.74	< 0.50	1.49	10.9	< 0.50
K008	2	< 0.50	18.09	0.22	1.65	1.12	3.59	7.8	0.55
K009	2	< 0.50	47.25	< 0.05	1.07	< 0.50	1.24	17	< 0.05
K010	1	2.58	87.01	2.05	21.31	1.1	4	31.12	< 0.50
K011	2	< 0.50	406	0.28	6.62	14.9	10.51	143.6	2.41
K012	1	1.72	32.51	1.11	9.6	< 0.50	1.52	10.69	< 0.50
K013	1	2.38	39.45	2.17	14.26	< 0.50	2.68	10.61	< 0.50
K014	1	1.13	33.81	3.18	65.96	< 0.50	2.62	11.71	< 0.50
K015	2	< 0.50	132.5	0.42	24.75	39.27	3.28	61.15	1.77
K016	2	< 0.50	9.53	< 0.05	2.03	< 0.50	1.25	3.85	< 0.05
K017	2	< 0.50	39.26	< 0.05	3.58	< 0.50	1.82	8.54	< 0.05
K018	1	1.19	29.26	2.66	4.35	3.46	2.24	9.07	< 0.50
K019	2	0.72	113	0.39	22.33	2.47	3.76	32.24	< 0.50
K020	2	1.24	74.66	0.05	3.75	12.83	1.95	18.04	0.62
K021	1	1.9	55.57	2.13	5.64	1.17	2.69	19.95	1.06
K022	1	1.73	53.41	7.9	19.07	< 0.50	2.33	19.02	< 0.50
K023	2	1.42	45.31	< 0.05	1.17	< 0.50	2.01	18.42	< 0.05
K024	2	0.54	13.45	0.23	1.74	1.18	1.64	8.47	0.55
K025	1	4.07	40.49	4.56	309.8	0.36	6.61	11.22	< 0.50
K026	1	0.95	45.04	4.78	68.15	13.44	1.84	12.93	0.79
K027	1	0.89	82.6	5.06	47.63	1.94	1.53	20.64	< 0.50
K028	2	0.69	39.08	0.13	2.36	7.11	1.44	13.73	0.68
K029	1	0.68	39.33	1.74	2.88	9.49	2.25	13.87	1.74
K030	1	< 0.50	39.52	5.2	12.97	3.07	2.04	13.18	< 0.50
K031	2	0.58	70.87	0.36	6.16	13.16	1.86	24.59	1.04
K032	1	2.25	42.27	3.44	10.4	0.99	1.75	12.38	< 0.50
K033	1	1.7	29.79	7.26	9.23	0.79	1.92	9.74	< 0.50
K034	1	1.91	22.71	6.38	9.76	1.58	2	6.97	< 0.50
K035	1	1.04	29.58	7.89	5.47	3.74	1.61	8.39	< 0.50
K036	1	2.38	47.17	5.84	35.13	0.68	3.8	13.83	< 0.50
K037	2	< 0.50	77.49	0.33	8.74	< 0.50	2.64	27.05	< 0.50
K038	2	1.98	55.52	0.86	1.83	0.52	2.35	17.01	< 0.50
K039	1	0.66	56.08	5.57	29.73	11.9	1.79	18.66	1.52
K040	2	8.19	60.19	0.23	14.52	3.26	2.78	15.8	< 0.50
K041	1	1.3	11.96	6.42	43.55	< 0.50	2.18	2.98	0.51
K042	1	1.58	22.23	6.08	42.07	1.13	2.29	5.23	0.59
K043	1	< 0.50	< 0.50	4.84	139.12	< 0.50	0.54	< 0.50	0.5
K044	1	1.39	32.35	6.54	23.72	< 0.50	2.47	7.8	0.57
K045	1	1.1	28.79	3.38	24.24	< 0.50	2.01	7.3	0.62
K046	1	2.06	20.32	8.54	209.87	< 0.50	4.01	4.69	0.52
K047	1	2.24	22.79	5.71	211.64	< 0.50	4.57	5.69	0.54
K048	1	1.42	34.87	4.99	34.71	4.49	2.04	8.07	0.63
K049	1	1.19	15.87	7.65	50.17	< 0.50	2.75	3.99	0.52
K050	1	1.17	23.12	6.64	39.47	1.27	2.4	5.99	0.65
K051	2	< 0.50	18.12	0.06	11.87	8.08	1.09	7.52	1.18
K052	1	0.92	31.62	8.54	91.63	10.24	2	8.75	1.36
K053	1	< 0.50	2.43	7.28	225.06	< 0.50	2.07	< 0.50	0.51
K054	2	0.57	35.17	0.37	31.13	7.09	1.28	12.45	0.86
K055	1	0.6	44.5	1.46	19.15	9.45	2.27	11.59	0.88
K056	2	0.64	38.48	0.44	18.36	11.77	2.24	11.19	0.97
K057	2	0.74	47.67	0.08	44.75	17.5	2.42	9.52	1.52
K058	2	1.59	40.97	0.68	8.12	1.04	3	9.13	0.6
K059	2	0.6	40.81	0.63	17.15	14.08	2.6	12.38	1.07

Table D.3. Continued.

Site #	Water Type	[Na]	[Pb]	[^{222}Rn]	[Se]	[Sr]	[P]	[Si]	[SO_4]
K001	1	71.01	< 0.50	56	< 0.50	1.69	0.78	26.31	0.65
K002	2	82.32	< 0.50	40	< 0.50	< 0.50	< 0.50	7.95	21.67
K003	2	21.67	< 0.50	24	< 0.50	2.04	2.13	5.44	200.7
K004	2	18.03	< 0.50	24	< 0.50	0.51	1.25	20.24	111.07
K005	1	34.81	< 0.50	28	< 0.50	1.89	1.07	15.75	1.14
K006	1	116	< 0.50	24	0.5	1.36	0.75	17.16	59.44
K007	1	45.79	< 0.50	40	< 0.50	0.9	1.25	18.97	0.7
K008	2	23.14	< 0.50	24	< 0.50	0.88	0.59	6.2	31.02
K009	2	3.92	< 0.50	304	0.56	< 0.50	0.98	9.08	116.22
K010	1	19.63	< 0.50	24	0.58	2.04	2.24	14.94	5.28
K011	2	30.5	< 0.50	56	0.62	6.82	5.22	27.17	679.15
K012	1	28.14	< 0.50	32	0.7	1.3	1.72	33.48	14.5
K013	1	63.56	< 0.50	40	0.53	2.76	1.65	41.25	0.7
K014	1	121.2	< 0.50	24	< 0.50	1.09	0.96	25.43	1.7
K015	2	123	< 0.50	32	< 0.50	2.47	4.35	25.41	315.4
K016	2	2.9	< 0.50	312	< 0.50	< 0.50	< 0.50	15.9	17.38
K017	2	5.74	< 0.50	195	< 0.50	0.52	0.56	13.2	22.01
K018	1	71.05	< 0.50	40	< 0.50	1.28	2.07	29.31	< 0.50
K019	2	110.2	< 0.50	32	< 0.50	4.72	2.64	36.14	115.43
K020	2	34.76	< 0.50	48	0.68	1.52	2.25	46.22	67.27
K021	1	95.97	< 0.50	80	< 0.50	2.92	1.66	31.1	33.4
K022	1	79.51	< 0.50	64	< 0.50	2.43	1.63	30.76	19.26
K023	2	37.9	< 0.50	72	< 0.50	1.42	1.3	33.13	9.61
K024	2	4.65	< 0.50	40	0.5	< 0.50	0.6	19.85	21.11
K025	1	267.58	< 0.50	40	0.71	4.55	0.93	26.83	2.27
K026	1	74.69	< 0.50	48	< 0.50	0.62	1.67	39.53	1.05
K027	1	48.37	< 0.50	32	< 0.50	0.77	1.96	55.79	16.5
K028	2	9.73	< 0.50	64	< 0.50	0.5	1.29	36.35	16.17
K029	1	34.22	< 0.50	48	< 0.50	0.66	1.33	31.37	11.54
K030	1	56.92	< 0.50	64	< 0.50	0.62	1.2	39.32	0.71
K031	2	30.67	< 0.50	80	< 0.50	1.25	1.91	36.96	80.26
K032	1	38.43	< 0.50	56	< 0.50	1.94	1.29	38.68	0.95
K033	1	92.51	< 0.50	56	0.6	1.45	1.26	37.72	0.68
K034	1	76.74	< 0.50	80	< 0.50	1.81	1.22	37.27	< 0.50
K035	1	75.02	< 0.50	72	< 0.50	0.88	1.77	40.56	1.52
K036	1	115.2	< 0.50	72	< 0.50	3.51	1.13	48.97	0.77
K037	2	39.33	< 0.50	129	< 0.50	0.81	1.94	52.55	48.82
K038	2	57.54	< 0.50	237	< 0.50	1.28	1.15	39.06	5.24
K039	1	16.47	< 0.50	121	< 0.50	< 0.50	1.42	36.72	1.45
K040	2	109	< 0.50	56	0.6	1.3	1.12	53.75	16.54
K041	1	121.35	0.62	40	0.79	1.72	< 0.50	6.79	0.62
K042	1	127.66	0.64	64	0.96	1.72	< 0.50	8.05	0.52
K043	1	144.86	0.58	72	0.77	< 0.50	< 0.50	7.01	< 0.50
K044	1	32.47	0.62	56	0.83	1.5	0.5	8.48	< 0.50
K045	1	28.21	0.61	32	0.77	1.21	< 0.50	6.95	4.53
K046	1	232.44	0.65	97	0.86	2.25	< 0.50	8.29	0.67
K047	1	237.19	0.65	48	0.86	2.07	< 0.50	8.36	2.09
K048	1	22.94	0.62	48	0.82	1.32	0.56	8.56	< 0.50
K049	1	11.79	0.61	72	0.87	1.61	< 0.50	8.53	< 0.50
K050	1	34.84	0.61	40	0.78	1.45	< 0.50	7.51	< 0.50
K051	2	8.4	0.59	97	0.76	< 0.50	< 0.50	10.67	26.73
K052	1	162.17	0.61	129	0.8	0.84	0.52	8.65	1.6
K053	1	216.81	0.58	20	0.81	0.5	< 0.50	5.88	< 0.50
K054	2	12.35	0.59	48	0.85	0.51	0.7	10.13	5.72
K055	1	39.35	0.59	48	0.81	1.51	0.64	7.69	72.86
K056	2	40.27	0.57	56	0.81	1.23	0.69	7.4	75.84
K057	2	44.92	0.61	28	0.83	0.89	0.52	9.03	63.6
K058	2	26.8	0.61	48	0.82	1.63	0.64	10.38	13.78
K059	2	45.96	0.59	40	0.81	1.23	0.73	6.79	93.52

Table D.4. Isotope compositions of the groundwater samples in Letcher County, Kentucky. Presented δ values are in ‰ units with respect to standards specified in **Chapters. 4.2.4** through **4.2.6**. Measurements not taken for a given site are labeled "n.a."

Site #	$\delta^{34}S\text{-}SO_4$	$\delta^{18}O\text{-}SO_4$	$\delta^{2}H\text{-}CH_4$	$\delta^{13}C\text{-}CH_4$	$\delta^{2}H\text{-}H_2O$	$\delta^{18}O\text{-}H_2O$
K001	n.a.	n.a.	-207	-37	-43	-6.9
K002	19	15	n.a.	n.a.	-43	-6.9
K003	-1	-2	n.a.	n.a.	-45	-7.3
K004	9	4	n.a.	n.a.	-43	-7.0
K005	n.a.	n.a.	-224	n.a.	-44	-7.0
K006	24	15	-195	-16	-44	-7.0
K007	n.a.	n.a.	-155	-26	-44	-7.0
K008	31	15	n.a.	n.a.	-44	-7.1
K009	-1	-1	n.a.	n.a.	-40	-6.5
K010	34	10	-171	-48	-44	-7.1
K011	5	5	n.a.	n.a.	-43	-6.8
K012	21	14	-204	-47	-42	-6.6
K013	n.a.	n.a.	-235	-54	-42	-6.6
K014	2	n.a.	-168	-28	-43	-6.7
K015	13	12	n.a.	n.a.	-43	-6.8
K016	4	2	n.a.	n.a.	-49	-7.8
K017	2	1	n.a.	n.a.	-43	-6.8
K018	n.a.	n.a.	-244	-66	-43	-7.0
K019	32	17	n.a.	n.a.	-42	-7.0
K020	13	13	n.a.	n.a.	-44	-7.3
K021	21	14	-86	-31	-41	-6.8
K022	1	14	-153	-51	-39	-6.5
K023	17	14	n.a.	n.a.	-44	-6.9
K024	59	4	n.a.	n.a.	-45	-7.2
K025	n.a.	-2	-220	-36	-42	-6.8
K026	n.a.	n.a.	-220	-54	-42	-6.8
K027	29	n.a.	-221	-44	-42	-6.8
K028	9	13	n.a.	n.a.	-40	-6.6
K029	12	12	-179	-52	-40	-6.7
K030	n.a.	n.a.	-215	-55	-41	-6.6
K031	7	9	n.a.	n.a.	-43	-6.9
K032	n.a.	n.a.	-136	-46	-40	-6.5
K033	n.a.	n.a.	-227	-46	-42	-6.8
K034	n.a.	n.a.	-204	-50	-42	-6.9
K035	n.a.	n.a.	-223	-43	-43	-7.0
K036	n.a.	n.a.	-220	-45	-44	-7.1
K037	1	7	n.a.	n.a.	-47	-7.6
K038	33	13	n.a.	n.a.	-45	-7.2
K039	n.a.	n.a.	-238	-55	-46	-7.5
K040	1	5	-286	-40	-43	-7.0
K041	n.a.	n.a.	-220	-50	-40	-6.6
K042	n.a.	n.a.	-216	-51	-39	-6.6
K043	n.a.	n.a.	-220	-47	-39	-6.6
K044	n.a.	n.a.	-193	-49	-40	-6.5
K045	36	18	-169	-50	-40	-6.4
K046	n.a.	n.a.	-222	-47	-41	-6.6
K047	n.a.	n.a.	-221	-45	-40	-6.6
K048	n.a.	n.a.	-190	-47	-40	-6.5
K049	n.a.	n.a.	-220	-50	-40	-6.9
K050	n.a.	n.a.	-221	-46	-40	-6.7
K051	4	4	n.a.	n.a.	-37	-6.2
K052	n.a.	n.a.	-215	-50	-40	-6.6
K053	n.a.	n.a.	-231	-50	-39	-6.6
K054	26	n.a.	n.a.	n.a.	-38	-6.4
K055	5	5	-165	-53	-41	-6.7
K056	6	7	n.a.	n.a.	-41	-7.2
K057	10	8	n.a.	n.a.	-39	-6.8
K058	8	19	n.a.	n.a.	-42	-7.0
K059	3	5	n.a.	n.a.	-41	-6.7

VITA

St. Thomas Majeau LeDoux was conceived during his parents' second honeymoon in the US Virgin Islands, though his parents do not know wherein, specifically. While with child, his mother, Camille LeDoux, received many joking questions about how "little St. Thomas" was doing; and so, with the encouragement of her reckless husband, and father to St. Thomas, Dik LeDoux, this running joke was eventually decided to be the boy's actual name.

Born in the swamps of Lafayette, Louisiana, St. Thomas was the first of two children in his family, and spent most of his early youth working in the rice fields trapping crawfish and casing boudin alongside his father, who originally worked as a sharecropper and fisherman because his degree in Fine Arts proved economically unfruitful. Though classically trained in opera, St. Thomas's mother eventually found work with an oil and gas company, as is customary for most people hoping to enter the middle class in southern Louisiana. St. Thomas's father soon followed suit, and began work on an offshore oilrig. The economic fortune awarded to the LeDoux family by Dik and Camille's foray into oil and gas afforded them the opportunity to move to the city, where St. Thomas and his sister, Marcelle, were able to finally attend school.

St. Thomas and Marcelle began school are S.J. Montgomery Elementary, where St. Thomas was mistakenly enrolled in classes for the deaf. There he obtained a rudimentary understanding of sign language, but was unable to speak aloud during his first three years of education. Following a flood that destroyed their first home, the LeDoux family relocated to a subdivision alongside a gully, or "coulee" as they are called in Louisiana, down which St. Thomas walked to his new school, Prairie Elementary, where he was finally allowed to enroll in speech courses. Over time, however, St. Thomas began to fall into trouble with juvenile authorities due to delinquent behavior. Citing the absence of a permanent father figure (due to Dik's long stints working offshore), Camille urged the family to relocate to Memphis, Tennessee. There, St. Thomas attended Cordova Middle, where he was first introduced to Memphis rap music and black culture in general. In the coming years, St. Thomas developed a fervent passion for blues music, and joined a working blues band as a bass player upon entry into high school. Despite working late nights playing dive bars around town throughout the week to supplement his family's income, St. Thomas was able to finally excel in school at Houston High, even placing in honors and advanced placement courses by his senior year. His career in blues, however, was cut short following an altercation between himself and the owner of B.B. King's restaurant on Beale St. over a pay dispute. After this incident, St. Thomas began making music with computers and listening exclusively to techno.

Upon graduation from high school, St. Thomas attempted to attend college and many prestigious universities across the country. Though granted admission to Tulane University, New York University, and Boston University, the LeDoux family's lack of savings forced St. Thomas to instead settle for the University of Tennessee, Knoxville, where he was at last awarded the Tennessee Hope Scholarship. At UTK, St. Thomas attempted to major in biomedical engineering, but settled instead for cultural anthropology, in which he graduated with honors. After failing to find gainful employment upon graduation, St. Thomas desperately sought work as a garbage man. Witnessing the routine degradation of his environment by the people who patronized his business, St. Thomas developed a passion for environmental geochemistry, and eventually sought reeducation in the Department of Earth and Planetary Sciences at UTK. Though nearly denied admission due to his lack of prerequisite education in geology, St. Thomas eventually proved to be one of the department's most exemplary students, completing his M.S. in May 2015. He is ironically still pursuing a career in waste management.